Amoxicillin Loaded Mucoadhesive Thiomer Based Nanoparticles for H.pylori Infection Therapy

MPhil Thesis
By

HAJRA ZAFAR

Department of Pharmacy
Faculty of Biological Sciences
Quaid-I-Azam University
Islamabad

2018

Amoxicillin Loaded Mucoadhesive Thiomer Based Nanoparticles for H.pylori Infection Therapy

Submitted by:

HAJRA ZAFAR

Registration # 02331613021

Thesis Submitted to:

Department of Pharmacy

Quaid-I-Azam University, Islamabad

In the partial fulfillment of the requirement for the degree of

Master of Philosophy

In

Pharmacy (Pharmaceutics)

2016-2018

Department of Pharmacy
Faculty of Biological Sciences
Quaid-I-Azam University
Islamabad

2018

DECLARATION

I hereby declare that the thesis titled "**Amoxicillin Loaded Mucoadhesive Thiomer Based Nanoparticles for *H.pylori* Infection Therapy**" submitted at Quaid-I-Azam University Islamabad for the award of degree of **Master of Philosophy** in Pharmacy (Pharmaceutics) is the result of research work carried out by me under the supervision of Dr. Gul Shahnaz, Department of Pharmacy, Faculty of Biological Sciences, Quaid-I-Azam University, Islamabad, during the period of 2016-2018. I further declare that the results present in this thesis have not been submitted for the award of any other degree or fellowship. I am aware of the term of copyright and plagiarism and I shall be responsible for any copyright violation found in work.
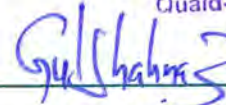
Name: HAJRA ZAFAR

Signature: *Hajra*

Date: 4-10-2018

Approval Certificate

This is certified that the dissertation titled "**Amoxicillin Loaded Mucoadhesive Thiomer Based Nanoparticles for *H.pylori* Infection Therapy**" submitted by **Hajra Zafar** to the Department of Pharmacy, Faculty of Biological Sciences, Quaid-I-Azam University, Islamabad, Pakistan is accepted in its present form as it is satisfying the dissertation requirements for the degree of Master of Philosophy in **Pharmacy (Pharmaceutics).**

Supervisor

Assistant Professor
Department of Pharmacy,
Quaid-i-Azam University
Islamabad

Dr. Gul Shahnaz
Assistant Professor,
Department of Pharmacy
Quaid-I-Azam University,
Islamabad.

External Examiner

Prof. Dr. Azhar Hussain
Dean and Director
Hamdard Institute of
pharmaceutical sciences
Hamdard University,
Islamabad.

CHAIRMAN
Department of Pharmacy
Quaid-i-Azam University
Islamabad

Chairman

Prof. Dr. Gul Majid Khan
Chairman
Department of Pharmacy
Quaid-I-Azam University,
Islamabad.

Dated: 4-10-2018

Table of Contents

Acknowledgment

List of Tables

List of Figures

List of Abbreviations

% w/v	Percent weight by volume
μg	Microgram
μl	Microliter
μmol	Micromoles
AM	Amoxicillin
AM-PCP	Amoxicillin loaded polycarbophil nanoparticles
AM-PCP-Cys	Amoxicillin loaded thiolated polycarbophil nanoparticles
AM-PCP-PAP	Amoxicillin loaded papain modified polycarbophil nanoparticles
AM-PCP-Cys-PAP	Amoxicillin loaded papain modified thiolated polycarbophil nanoparticles
Bid	Twice a day
CaCl2	Calcium chloride
CCD	Central composite design
CMC	Carboxy-methyl cellulose
Conc	Concentration
EDAC	Ethyl dimethyl aminopropyl carbodiimide
EE	Entrapment efficiency
FDA	Fluorescein diacetate
FTIR	Fourier transform infrared analysis
G	Gram
GERD	Gastroesophageal reflux disease
GIT	Gastrointestinal tract
H.pylori	Helicobacter pylori
H_2 receptors	Histamine receptors
HCl	Hydrochloric acid
HPC	hydroxyl-propyl cellulose
Hr	Hour

M	Molar
Mg	Milligram
MIC	Minimum inhibitory concentration
Ml	Milliliter
mM	Millimolar
Mm	Millimeter
N	Normal
NaBH$_4$	Sodium borohydride
NaCl	Sodium chloride
NaCMC	Sodium carboxy-methyl cellulose
NaOH	Sodium hydroxide
NHS	N-hydroxysuccimide
Nm	Nanometer
NSAIDS	Non-steroidal anti-inflammatory drugs
OD	optical density
P value	Probability
Pa.s	Pascal second
PAP	Papain
PB	Phosphate buffer
PCP	Polycarbophil
PCP-Cys	Thiolated polycarbophil
PCP-PAP	Polycarbophil papain conjugate
PDI	Polydispersity index
PLGA	Polylactic co glycolic acid
PPI	Proton pump inhibitors
PVA	Polyvinyl alcohol
R-value	Regression coefficient
rpm	Rotation per minute
RSM	Response surface methodology

SD	Standard deviation
SEM	Scanning electron microscopy
Tid	Three times a day
UV-VIS	Ultraviolet visible
VacA	Vacuolating cytotoxin

Abstract

The aim of research project was to prepare mucoadhesive and mucopermeating carrier system based on thiomer (thiolated polycarbophil) nanoparticles incorporating amoxicillin and improve the drug stability and prolong retention in H.pylori infection. Amoxicillin (AM) loaded unmodified polycarbophil, thiolated polycarbophil and papain modified thiolated polycarbophil nanoparticles were synthesized by ionic gelation method and characterized for entrapment efficiency, particle size, polydispersity index, zeta potential, *in-vitro* drug release and mucopermeation. The sizes of all nanoparticles were in range of 111 nm to 288 nm. SEM analysis confirmed the spherical shape of amoxicillin loaded papain modified thiolated polycarbophil (AM-PCP-Cys-PAP) nanoparticles with average particle size less than 400 nm. Zeta potential and entrapment efficiency of AM-PCP-Cys-PAP nanoparticles were found to be − 13.4 mV and 78 ± 7.2 % respectively. The mucoadhesive property was evaluated by rheological investigation of nanoparticles. Due to presence of thiol groups in polymer backbone, thiolated polycarbophil nanoparticles displayed 2 fold higher mucoadhesive properties. Amoxicillin loaded papain modified thiolated polycarbophil (AM-PCP-Cys-PAP) nanoparticles displayed sustained drug release up to 48 hours. For *ex-vivo* diffusion/ mucopermeation study, nanoparticles were loaded with fluorescence diacetate and silicon tube method was adopted to determine percent mucopermeation. Fluorescence diacetate is a lipophilic dye that retain in nanoparticles through temporary attachment. Papain modified nanoparticles showed deepest permeation into the mucus by cleavage of mucoglycoproteins as compared to unmodified nanoparticles. The *in-vitro H.pylori* growth inhibition activity of amoxicillin loaded papain modified thiolated polycarbophil (AM-PCP-Cys-PAP) nanoparticles and pure amoxicillin suspension was evaluated. AM-PCP-Cys-PAP nanoparticles were found to have better *in-vitro* efficacy based on high stability, prolong drug release and complete eradication of bacteria as compared to pure amoxicillin. Thus, from the results it is evident that amoxicillin loaded papain modified thiolated polycarbophil (PCP-Cys-PAP) nanoparticles can be an effective nanocarrier for H.pylori infection because of enhanced mucopermeation and mucoadhesion property with better stability and prolong drug release.

Key Words: Amoxicillin, polycarbophil, papain, mucopermeation, H. pylori

CHAPTER 1

INTRODUCTION

1. INTRODUCTION

Helicobacter pylori (*H.pylori*) has become one of the most common and widespread pathogens, affecting 50 % of the world population (Cai J *et al.*, 2015). *H.pylori* is a gram-negative, spiral-shaped bacterium that lives in the deep gastric mucosal layer. Due to its unique features it survives in the human gastrointestinal environment. Two scientists Warren and Marshall cultured this bacterium in 1982. They took biopsy samples from 11 patients with gastritis and discovered a strong connection between the presence of bacteria and development of peptic ulcer and chronic inflammation (A El-Zahaby S *et al.*, 2014). It resides throughout the life of individual. Most of the time the presence of this bacterium is harmless but in 5-10 percent individuals it causes peptic ulcer and other chronic diseases. The pathogen is associated with high mortality and morbidity. It is the main etiological factor that plays important role in the development of several diseases i.e. gastritis, ulcer of stomach or duodenum and gastro carcinoma (Yamamoto Y *et al.*, 2015). World health organization stated *H.pylori* as class 1 carcinogen for gastroduodenal cancer (Lin Y-H *et al.*, 2014). It is considered to be the most usual cause of cancer. The pathogenic factors produced by this microbe cause damage to the cell layer of epithelium and help in bacterium survival in the deep mucosa (Lin Y-H *et al.*, 2012). This bacterium along with hydrochloric acid damages stomach and duodenal tissues thus, causing severe inflammation. Presence of *H. pylori* is also linked with cardiovascular, immune, skin, respiratory, growth and neurological anomalies (Tsang KW and Lam SK, 1999). Therefore, eradication of this bacteria is necessary to reduce the risk for development of gastroduodenal ulcer. Several diagnostic procedures are used for detection of *H. pylori* with high sensitivity and specificity. Once pathogenic factor is identified, then wide range of therapeutic strategies can be applied to eradicate bacteria.

1.1. Gastrointestinal Mucus Layer and Its Physiology

The gastrointestinal (GI) wall has a viscous, elastic and sticky gel lining known as mucus. The width of mucus layer is reported to be 50-600 micrometers in stomach and 15-450 micrometers in intestine (Cu Y and Saltzman WM, 2009).

1.1.1. Composition

Healthy mucus is composed of following components:

- Aqueous component (95%)

- Mucus glycoproteins
- Minerals
- Electrolytes.

The mucus glycoproteins are responsible for the mass properties of viscous mucus gel (Lehr C-M, 2000). Mucus is structurally composed of peptide chain which has glyosidic bond with various polysaccharides. These polysaccharides include

- Galactosamine
- Glucosamine
- Fucose
- Sialic acid
- Galactose.

These glucoside regions protect the underlying parts from bacterial and enzymatic attack (Lamont JT, 1992).

1.1.2. Physiology of mucus lining

The mucus layer performs several physiological functions. The most important of these functions include the defense properties (McColl KE, 2012). Stomach lining comprises various cells that produce several substances which perform different roles **Table 1.1.** The mucus layer provides an obstacle to acid (hydrochloric acid) produced by parietal or oxyntic cells by releasing carbonates continuously. These bicarbonates neutralize the acid and damage to underlying epithelial cells is inhibited. The buffering property of mucus layer is important for the protection of gastrointestinal wall. A pH gradient as shown in **Figure 1.1** (low at the lumen side and high towards epithelial side) is created in mucosa which serves as barrier to entry of exogenous substances. There is also maintenance of balance between the continuous production and loss of mucus which plays an important role to keep the gastrointestinal layer intact. The mucus lining prevents the self-digestion of GIT wall by inhibiting enzymatic substances such as pepsin toward the wall. Mucus layer helps in the passage of food through the GI wall (Kharia AA and Singhai AK, 2013).

In terms of drug absorption, mucus layer serves as a major obstacle for diffusion across GI wall. Due to viscoelastic nature, mucus possesses the properties of both liquids and

solid with respect to flow and elasticity. Both properties of mucus help in the protection of cell wall by preventing breakage and passage of toxic agents.
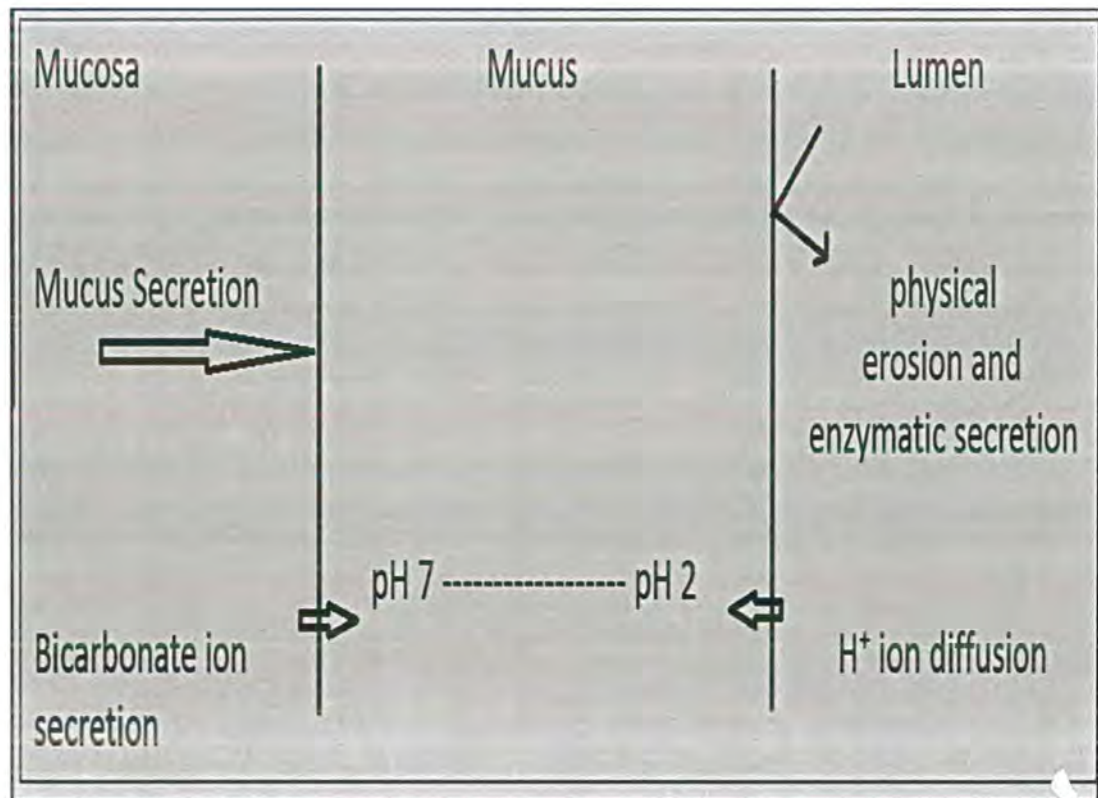
Figure 1.1. Mucosal barrier protective mechanism (MacAdam A, 1993).

1.2. Peptic Ulcer

Damage of stomach and duodenum epithelial cells line that leads to inflammation and ulceration. Peptic ulcer is known as main clinical burden that affects half of the world population (Proctor MJ and Deans C, 2014). Ulcer located in stomach is called gastric ulcer while located in duodenum is called duodenal ulcer. Most of patients with peptic ulcer do not show any symptoms. While in some cases symptoms are quite uncomfortable. Common symptoms include pain, heartburn, reflux disorder, bloating, swallowing difficulty, fever, loss of appetite and nausea (Ohta T *et al.*, 2001).

There may be breakage of blood capillaries which leads to other complications such as bleeding, abdominal cramps, anemic attacks, and melena. In most cases peptic ulcer is also associated with development of gastroesophageal reflux disease (GERD). Other chronic complications include blockage at stomach and duodenum junction, severe bleeding that can be life-threatening and fissures in gastrointestinal wall.

Table 1.1. Cells of stomach lining and their functions (A El-Zahaby S *et al.*, 2014)

Stomach Cells	Secretion	Release trigger	Function
Mucus cells	Mucus	Toxin	Barrier property
	Carbonates	Mucus	Neutralize acid secreted by parietal cells
Chief cells	Lipase enzyme and pepsin	ACh*, HCl**	Pepsin digests proteins and lipase helps in digestion of lipids
Parietal cells	Hydrochloric acid and substance that activates pepsin	ACh, Gastrin and histamine	Killing of microbes by acid and pepsin activation
Chromaffin cell	Histamine	ACh	Promot gastric acid s retion
G cells	Gastrin	Amino acids and ACh	Helps in secretion of HCl from parietal cells
D cells	Somatostatin	HCl	Antagonizing effect at acid cells that stops further secretion of hydrochloric acid

* ACh: Acetylcholine, ** HCl: Hydrochloric acid

1.3. Etiology of Peptic Ulcer

In most of the cases, peptic ulcer is caused by one of these two factors:

- Helicobacter pylori (*H. pylori*)
- Non-steroidal anti-inflammatory drugs (NSAIDS)

People with both of these factors are at high risk of development of gastrointestinal ulcers (McNulty CA *et al.*, 2011).

Other factors that are linked to peptic ulcer are shown in **Table 1.2**

Table 1.2. Causative factors linked with the development of gastrointestinal ulcer

Drugs	Lifestyle	Diseases	Therapies	Malignancy
Clopidogrel, acetaminophen, cocaine, methamphetamine	Stress, alcohol intake and smoking	Crohn's disease, sarcoidosis, Zollinger-Elison disease, viral diseases	Chemotherapy and radiotherapy procedures	Lymphomas, carcinomas

1.3.1. Helicobacter pylori (*H. pylori*)

H. pylori, previously known as *Campylobacter pylori* are gram-negative spiral bacteria. It was discovered in 1982 by Warren and Marshall. This bacterium is most commonly present in human stomach and small intestine. Presence of *H.*pylori pathogen in human gastro-intestinal environment is silent in majority of population. But in some cases, it triggers inflammation and ulceration of stomach or duodenum mucosal lining (Suerbaum S and Michetti P, 2002). It generates several physiological changes that needs to be critically assessed. Therefore, bacteria should be properly diagnosed and timely eradicated to prevent chronic ulcer.

1.3.1.1. Structure components of H.pylori

H.pylori is microaerophilic in nature and requires very low amount of oxygen for its survival. It generates several enzymes including urease, oxidase, and catalase which serve as energy sources. The bacterial structure is 3 micrometer in length that is a helical rod with several flagella **Figure 1.2** (Josenhans C *et al.*, 2000). Presence of flagella gives high motility to bacteria due to which it burrows deep in mucus membrane. A very thin wall surrounds the bacterial body. It is composed of inner membrane and outer membrane. The outer membrane has small porins for transfer of nutrients. Between outer and inner membrane, a very delicate peptidoglycan layer composed of saccharides and amino acids is present. Saccharides includes N-acetylglucosamine and N-acetylmuramic acid. Peptides are present in these saccharides chains and crosslink the sugars via glycosidic bonding. Due to this layer the bacterial wall remains intact and protects the bacteria from outer environment (Tsang KW and Lam SK, 1999).
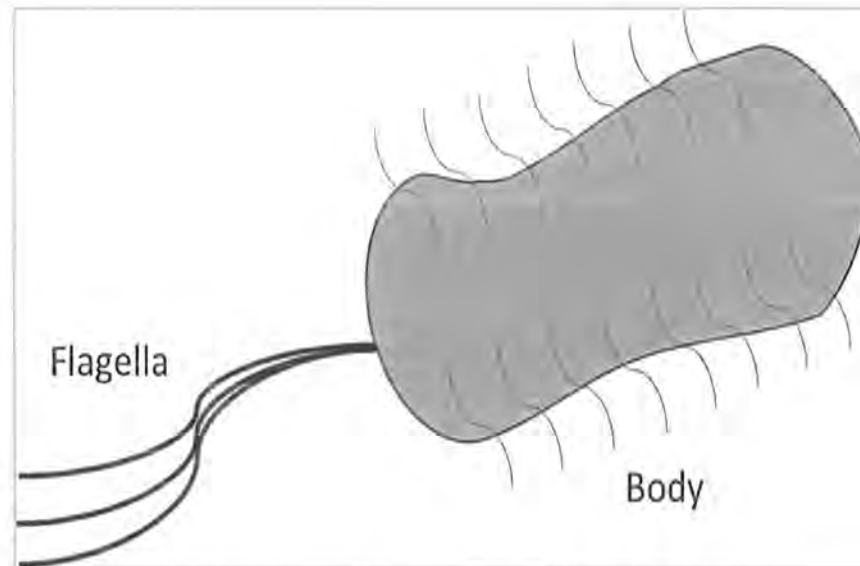
Figure 1.2. Structure of *H. pylori* (Tsang KW and Lam SK, 1999).

1.3.2. Non-steroidal anti-inflammatory drugs (NSAIDs)

The excessive use of NSAIDs is also known to cause severe gastro-duodenal ulceration. These drugs include aspirin, naproxen, brufen, diclofenac etc. Their mechanism of action involve inhibition of cyclo-oxygenase enzymes that produce prostaglandins (Sostres C *et al.*, 2010). Prostaglandins have protective effects over gastro-duodenal wall and prevent harm to the cells. It helps in mucus secretion and provide barrier properties. Reduce production of prostaglandins by NSAIDs thus, cause injury to mucosal tissues that may progress to ulcer (A El-Zahaby S *et al.*, 2014).

1.4. Prevalence and Spread of *H.pylori* Bacteria

$2/3^{rd}$ of world population is known to be affected by *H.pylori*. The affected population comprises of 80 percent adults in developing countries and 20 percent individuals in developed countries. The prevalence is highly associated with social and economic condition, age, regional factors and ethnicity. Poor social and economic conditions are thought to be important factors for high prevalence of infection. Higher risks are reported with poor sanitation, overcrowding, un-hygienic diet, contaminated water and food sources (Hunt R *et al.*, 2011). It affects individuals by birth and reported to remain throughout life if not eradicated in time (Otero Regino W *et al.*, 2009). The risk of infection increases with older age. Oral fecal route is considered to be the main transmittance route for pathogen.

1.5. Diagnosis of Peptic Ulcer and *H.pylori* Infection

Diagnosis of peptic ulcer has two major goals:

1. To determine exact location of ulcer

2. To identify the cause of ulcer

Following are methods usually employed to diagnose peptic ulcer.

1.5.1. Physical examination

From physical examination and symptoms of patients, the clinician can confirm the existence of ulcer. These include examination of stomach and symptoms like bloating, tender area, and burps (Umamaheshwari R *et al.*, 2004).

1.5.2. Gastrointestinal endoscopy with biopsy

Endoscopy of gastro intestine is a standard procedure to determine the exact location of ulcer (McNulty CA *et al.*, 2011). The visualization process covers esophagus, whole stomach and half of small intestine which makes the diagnosis easier. In this procedure, a soft elastic tube with a terminal scope (for imaging) is passed through esophagus and foresee the upper gastrointestinal tract (GIT) directly. It is a quick and easy procedure with high accuracy. Medication for pain and sedation are usually given before the procedure.

Radiotherapy, therapeutic endoscopy and surgery is done for the management of complications of ulcer (bleeding, perforations and blockage). The endoscopy procedure also allows clinicians to take biopsy samples for *H.pylori* detection. The biopsy samples are tested for histological, morphological examination and detection of *H.pylori* (Engstrand L *et al.*, 1997). Histologic investigation is done with hematoxylin and eosin stain for best examination of bacteria.

1.5.3. Rapid Urease test with biopsy

Rapid urease test is another standard method for detection of *H.pylori*. It is a quick and cost-effective test with high specificity and sensitivity (Arora S *et al.*, 2011). This method is based on conversion of urea into ammonium ions and carbon dioxide by the bacterial urease enzyme. Biopsy sample is added to mixture of urea and phenol. If the color changes to red, the test is positive and indicates the presence of bacteria.

1.5.4. Urea breath test

Urea breath test is also an important method for diagnosis of *H.pylori* (McNulty CA *et al.*, 2011). In urea breath test, labelled urea is inhaled by the patient. If pathogen is

present, it will convert urea into labelled carbon dioxide which can be detected in exhaled air. This test takes short time for completion and gives accurate results.

1.5.5. Blood test/stool antigen-antibody test

Blood test and stool test based on detection of antigen antibodies is also a common method for diagnosis of peptic ulcer and its cause. These are non-invasive methods with high sensitivity and specificity (Otero Regino W *et al.*, 2009).

1.5.6. Gastrointestinal X-rays

Gastrointestinal X-ray studies are also reported for diagnosis of peptic ulcers. Barium is swallowed by patient and the contrast produced is used to diagnose peptic ulcer. However, this procedure is time consuming, less accurate and do not detect *H.pylori* pathogen due to which it is not often used. This method has also chances of false positive and false negative results. Therefore, endoscopy is most preferred method for diagnosis of ulcer.

1.6. *H.pylori* Infection and Adaptation in Humans

The discovery of *H.pylori* in connection to presence of ulcer in 1982 has made this bacteria as a major etiological factor in development of gastric and duodenal ulcer, inflammation, severe gastritis and cancer of stomach/small intestine (Proctor MJ and Deans C, 2014). *H.pylori* infection results in 95 percent of stomach ulcer and 70 percent of small intestinal ulcer. *H.pylori* has several distinctive features. The bacterium is curling and rod-shaped that makes it highly motile through thick mucus membrane of gastric or duodenal mucosa (Marshall B and Warren JR, 1984). The gastroduodenal lining is usually well secured against most of microbes and other toxic factors. The acidic condition of gastric environment, narrow range of nutrients and persistent emptying prevents most of pathogenic microbes from harboring mucosal wall (Persson C, 2009). *H.pylori* with special array of features is highly adaptable to human gastrointestinal environment. It occupies the antral portion of stomach and upper small intestine (duodenum) where it causes infection and inflammation. By using its unique features including high motility and structural alignment, *H.pylori* settles deep in mucosal region and attaches to epithelial cells (Suerbaum S and Michetti P, 2002). Bacteria produces special kind of proteinaceous substances that help in bacterial adhesion to epithelial cells of gastrointestinal wall. These include receptins and adhesins. The adhesins are proteins and glycolipids while receptins are proteins in

nature. In the beginning of colonization, bacterium uses adhesins to interact with epithelial surface receptors including peptides, lipids, glycoproteins and glycolipids. Receptins, on other hand helps in final binding to cells (Dubreuil JD *et al.*, 2002).

1.7. Pathophysiology of *H.pylori* Infection

H.pylori exploits various mechanisms to cross the several stomach barriers that allows its attachment to deep mucosal tissues. Once the bacteria invades stomach, it encounters highly acidic environment. Immediately it produces an enzyme called urease that converts urea present in stomach to ammonium ions and carbon dioxide. Due to presence of ammonium ions, the surrounding pH increases and high pH aids in survival of pathogen (Ohta T *et al.*, 2001). Bacteria then moves easily through thick mucus where it colonizes and initiate infection. Increase in pH is reported to inhibit somatostatin release from D cells and enhance gastrin secretion by G cells. The inhibitory mechanism of somatostatin also in turn increases gastrin production that causes imbalance of gastrin secretion, leading to parietal cells dysplasia and increased gastric acid secretions (McColl KE, 2012) **Figure 1.3**. The production of ammonium ions also disrupts the cohesiveness of mucus layer. *H. pylori* also produces a toxic substance called vacuolating cytotoxin (VacA) that disrupts tight junctions and harm the cytoskeleton (Fedwick JP *et al.*, 2005). This toxin is also reported to be linked with high pathogenicity. *H. pylori* infection is also known to impair neural pathway. Neural pathway is considered to be responsible for controlling acid production. Thus, an increase acid secretion results due to disruption of inhibitory reflex. High acid secretion is responsible for gastric cells hyperplasia and reduction of pH in duodenum which further promotes colonization of bacteria in small intestine. High motility of bacteria due to its helical shape and presence of flagella, allows it to reside in deep layer of thick mucus. All these physiological changes cause impairment of gastroduodenal mucosal defense and thus cause damage to GI lining. Upon interaction of pathogen with phagocytes, mast cells are activated that may lead to acute or chronic inflammation (Konturek J, 2003). A local breakage of mucosal barrier is induced which leads to chronic ulceration of stomach and duodenum.

1.8. Current Treatment Strategies for *H.pylori* Eradication

Various treatment strategies have been adopted for eradication of *H.pylori* from mucosal epithelium. These strategies involve use of various antibiotics as shown in **Table 1.3** (A El-Zahaby S *et al.*, 2014). Other drugs include proton pump inhibitors,

bismuth salicylate and metronidazole. Bismuth salicylate coats inflamed regions in ulcer and help in healing. H_2 (histamine) receptor blockers are also available for suppression of acid in stomach. These agents block histamine receptors on surface of parietal cells that are involved in production of acid. Drugs included are cimetidine and ranitidine. Similarly, proton pump inhibitors (PPI) are used to reduce acid secretion. They are superior to H_2 blockers and widely used now-a-days. PPI block K/H^+ ATPase that is an enzymatic pump involved in regulation of final step in acid secretion. These drugs include omeprazole, esomeprazole, rabeprazole etc.
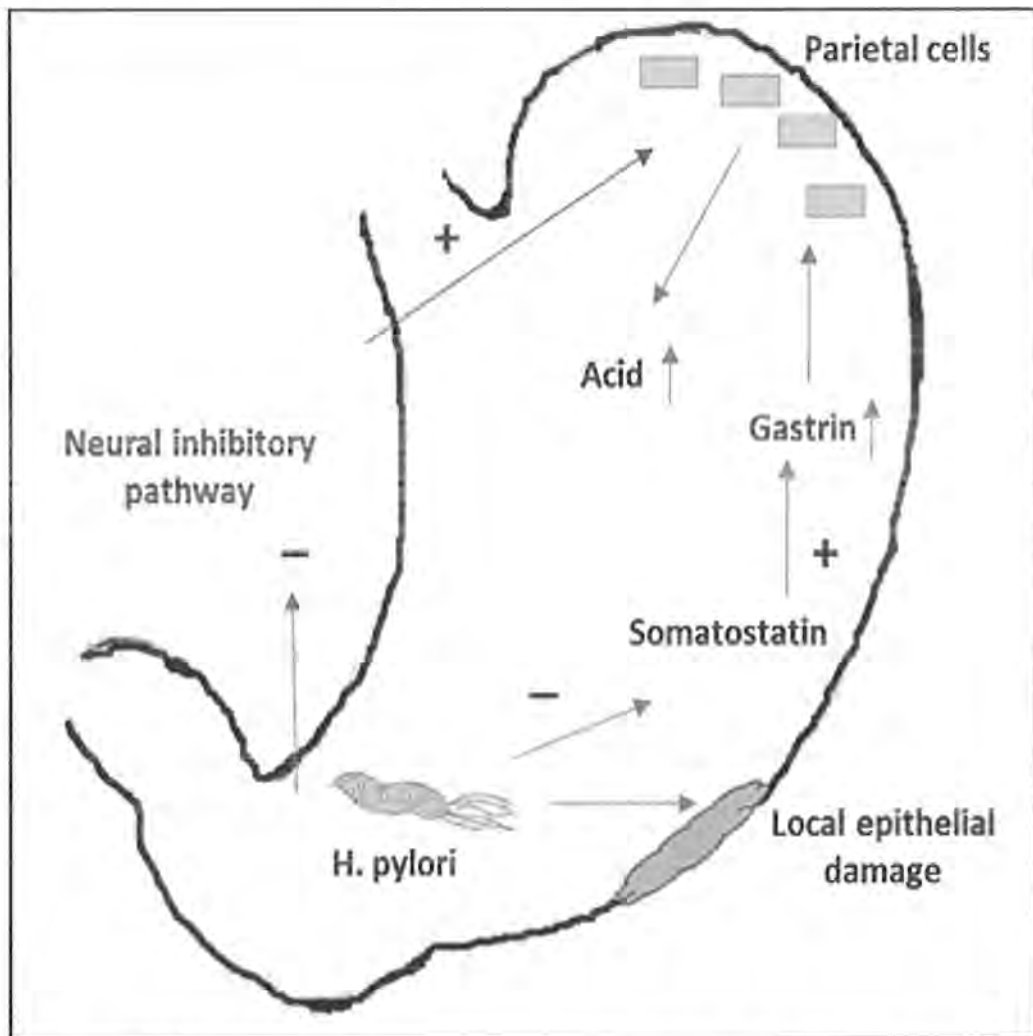
Figure 1.3. Pathophysiology of H.pylori infection (Proctor MJ and Deans C, 2014).

As a standard, triple therapy has been used for years for eradication of *H. pylori* and cure of infection **Table 1.4.** The standard triple therapy is a combination of antibiotic including amoxicillin/clarithromycin/metronidazole and an acid suppressing agent. These therapeutic regimens vary in different regions and result in high cure rates.

Table 1.3. Drugs available for H.pylori infection

Drugs available for H.pylori infection	
Class	**Drugs**
Antibiotics	Amoxicillin, clarithromycin, tetracycline (minocycline), nitrofurans (furazolidone), quinolones (finafloxacin) and rifabutin
Proton pump inhibitors	Omeprazole, esomeprazole, rabeprazole, lansoprazole
H2 blockers	Cimetidine and ranitidine
Other	Bismuth salicylates, metronidazole

Table 1.4. Course for *H.pylori* eradication

Standard triple therapy course for seven to fourteen days			
Antibiotic medication			Antacids
Amoxicillin	**Clarithromycin**	**Metronidazole**	
1 gram bid	500 mg bid	--	Proton pump inhibitors like omeprazole, rabeprazole, esomeprazole bid
--	250 mg bid	400 mg bid	
1 gram bid; 500 mg tid with PPI	--	400 mg bid; 400 mg tid with PPI	

1.8.1. Clarithromycin

Clarithromycin is a macrolide antibacterial that has broad spectrum of activity. It has wide range of applications in various infections. These include skin, ear, throat, respiratory and H.pylori infections. It works by inhibiting protein synthesis by binding to 50S subunit of ribosome. Its acid stability is less than amoxicillin. It is quickly absorbed with high bioavailability. Major side effects include diarrhea, vomiting, skin

allergies, headache and liver abnormalities. It is mostly taken orally. In gastro duodenal ulcer associated with *H.pylori*, it is used in combination with another antibiotic and acid reducing agent (Wu H *et al.*, 2000).

1.8.2. Amoxicillin

Amoxicillin (AM) belongs to beta lactam class of antibiotics. It has a broad *in vitro* spectrum of activity against many gram + and gram − bacteria. It works by inhibiting transpeptidase enzyme that cross-links amino acids to sugars in bacterial cell wall (Patel P *et al.*, 2014). Amoxicillin exists in the form of hydrates among which trihydrate form is most stable. It has large volume of distribution and is quickly diffused in many tissues. It has alpha amino group attached to carbonyl group as shown in the **Figure 1.4** due to which it is acid stable and orally advantageous. It is used in number of infections including skin, respiratory, ear, dental, nose, throat and urinary tract infections. It is most useful drug in *H.pylori* eradication therapy. It has been used in combination with other antibacterial agents and antacids. Common side effects include diarrhea, rashes and hypersensitivity reaction (Umamaheshwari R *et al.*, 2004).
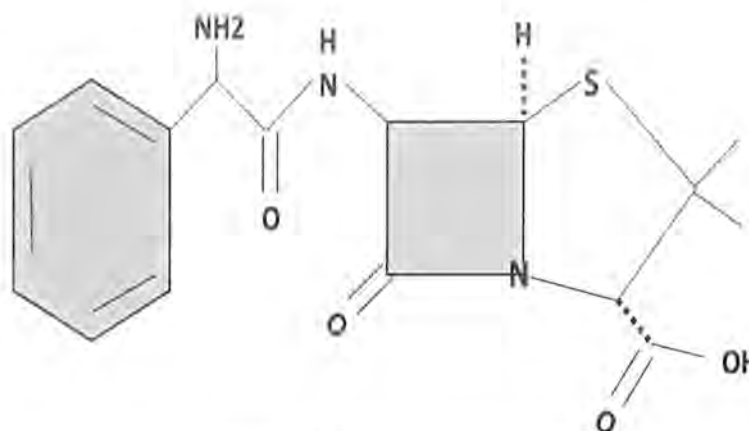
Figure 1.4. Amoxicillin structure.

1.9. Drawbacks of Conventional Treatment Strategies

Although conventional treatments for H.pylori eradication are well effective but they are still associated with the high bacterial resistance (Wu H *et al.*, 2000). Current treatment strategies have come across high failure rates due to their poor stability, short retention time and bacterial resistance (Cammarota G *et al.*, 2012). Moreover, a film is produced by bacterium around itself that inhibit the access of antibiotics both from the lumen side and blood side (Pan-In P *et al.*, 2014). H. pylori is sensitive to many antibacterials in *in-vitro* analysis but difficult to eliminate *in-vivo* (Umamaheshwari R

et al., 2004). Patient compliance problems are also associated with conventional therapies due to repeated dosing in single day. Therefore, more effective and simple treatment is required to eliminate the bacteria that has high stability and prolong retention time.

1.10. Mucoadhesive Drug Delivery System

1.10.1. Mucoadhesion

Mucoadhesion is the state in which the drug delivery system adhere to the mucosal surfaces including epithelial cells (Bernkop-Schnürch A *et al.*, 2003). The adhesion occurs for prolong time due to development of various forces between mucosa and drug delivery material. These forces include interfacial energy, chemical bonds and hydrophobic interactions etc.

1.10.2. Theories of Mucoadhesion Mechanism

Mucoadhesion is based on basic seven theories which are as follows:

1.10.2.1. Wetting theory

This theory is based on spreading of mucoadhesive dosage form over mucus layer. Upon contact, they take up liquid from mucus site and sprea over the surface. Their affinity toward liquid determine the strength of mucoadhesion. More the affinity of mucoadhesive material for liquid, stronger will be the mucoadhesive strength.

1.10.2.2. Electronic theory

This theory explains the formation of oppositely charged layer between the bioadhesive and mucus. When the mucoadhesive material comes in contact with the mucus layer, there is transfer of electrons and electrostatic forces are established between the two surfaces which help in mucoadhesion (Chowdary K *et al.*, 2001).

1.10.2.3. Adsorption theory

Adsorption theory of mucoadhesion explains the formation of primary and secondary forces between mucoadhesive material and mucus layers (Asija R, 2014). These chemical interactions include:

- Hydrophobic interactions
- Van der Waal forces
- Hydrogen bonding

- Covalent bonding
- Non-covalent interactions
- Electrostatic forces

1.10.2.4. Diffusion theory

Diffusion theory mainly concerns with the physical linkage of mucoadhesive drug delivery system and mucus membrane. After the initial contact, the mucoadhesive material gets entangled within in the mucus inner network and strengthen the mucoadhesive force (Netsomboon K and Bernkop-Schnürch A, 2016).

1.10.2.5. Fracture theory

Fracture theory explains the phenomenon that determine the force of separation of mucoadhesive material from the mucus layer. It also measures the strength of mucoadhesive bonding (Callens C et al., 2003).

1.10.2.6. Mechanical theory

This theory is based on the physical nature of mucus layer surface. The mucus lining has rough surface parts. The roughness of mucus layer increase the surface area and interfacial tension. By applying a liquid-based mucoadhesive drug delivery system, the spaces in rough surface are filled by the liquid thus provide strong mucoadhesion.

1.10.2.7. Dehydration theory

According to this theory, those mucoadhesive material which become gel in presence of aqueous environment when comes in contact with mucus, they dehydrate due to difference in osmotic pressure between the mucus layer and mucoadhesive substance. This dehydration leads to gel formation and strengthening of mucoadhesion.

1.10.3. Stages of Mucoadhesion

Mucoadhesion has two main stages (Lele B and Hoffman A, 2000):

1. Contact stage
2. Consolidation stage

1.10.3.1. Contact stage

In contact stage as shown in **Figure 1.5.** , the mucoadhesive material comes in close contact to the mucus layer. Different types of attractive and repulsive forces exists between mucus surface and mucoadhesive drug delivery system. The repulsive forces include osmotic pressure and electrostatic repulsive forces while the attractive forces

include hydrogen bonding and electrical opposite charges and van der Waal forces. To achieve strong mucoadhesion, the mucoadhesive devices must have ability to overcome the repulsive forces (Chowdary K *et al.*, 2001).
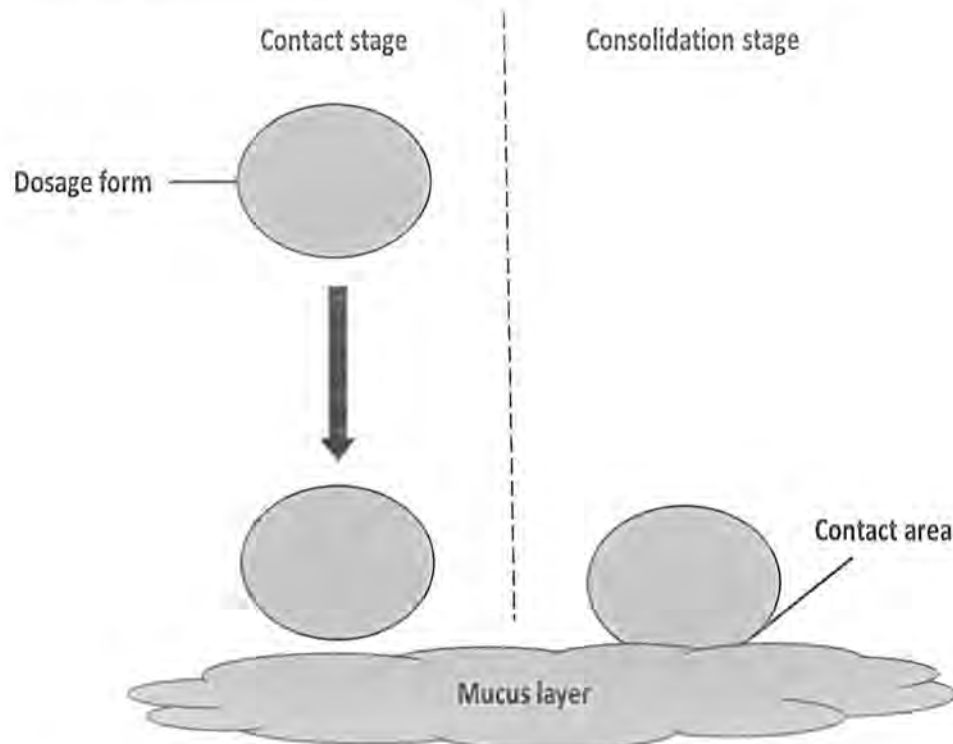
Figure 1.5. Stages of mucoadhesion (Bernkop-Schnürch A *et al.*, 2000).

1.10.3.2. Consolidation stage

Consolidation stage takes place after initial contact. The mucoadhesive substances absorb moisture at mucus site and get plasticized **Figure 1.5.** Thereby they built electrostatic and chemical interactions with the mucus and increases the mucoadhesive force. This stage follows both diffusion and dehydration theory.

1.10.4. Mucoadhesive drug delivery system

Mucoadhesive drug delivery system are drug devices that are directed towards mucosal surface where they adhere and release the drug for prolong period of time (Perioli L *et al.*, 2011). These are used for various purposes.

The purpose of mucoadhesive dosage forms is to provide localized or systemic delivery of drugs. Mucoadhesive drug delivery systems control the release of drugs in such a way that bioavailability is optimized. It remain in contact to the mucosal surface and continuously deliver the drug to the target site. Mucoadhesive drug delivery system can developed in variety of dosage forms for the ease of administration. They can also be delivered via different routes.

1.10.4.1. Mucoadhesive dosage forms

Mucoadhesive drug delivery systems are prepared in variety of dosage forms as indicated in **Table 1.5**. (Sayın B *et al.*, 2008) including powders, suspensions, tablets, gels, patches, films, semisolids

1.10.4.2. Delivery routes

Mucoadhesive drug delivery system can be administered by different routes **Table 1.5**. for specified purposes (Chowdary K *et al.*, 2001).

Table 1.5. Mucoadhesive drug delivery routes and dosage forms

Mucoadhesive drug delivery routes and dosage forms	
Routes	**Dosage forms**
Ocular	Solutions, particulates (liposomes, microspheres, nanoparticles), hydrogels, inserts
Nasal	Gels, nanocarriers, sprays
Oral	Micro and nanoparticles, granules, discs, tablets
Buccal	Patch, gels, tablets, films, ointments
Rectal/ vaginal	Suppositories, semisolids, hydrogels
Topical	Transdermal patches, powders, semisolids

1.10.4.3. Benefits of mucoadhesive drug delivery system

Mucoadhesive drug delivery systems have a wide range of benefits over conventional devices (Lele B and Hoffman A, 2000). These benefits include:

- Prolong drug delivery
- Controlled/sustained drug release
- Lower side effects
- Enhance patient compliance
- Fewer doses
- Increase bioavailability
- Cost-effectiveness

- Increase retention and stability

1.10.5. Mucoadhesive polymers

Mucoadhesive polymers are continuously discovered and investigated for the use in mucoadhesive drug delivery systems. These polymers can be used to prepare array of dosage forms where it performs several functions (Netsomboon K and Bernkop-Schnürch A, 2016). These functions include:

1. Retard the drug release
2. Provide stability to the drugs
3. Response to certain stimuli for drug release like pH, temperature, enzymes and chemical stimulus
4. Protect the drug from external environment
5. Increase the solubility of poorly soluble drugs

1.10.5.1. Types of mucoadhesive polymers

Mucoadhesive polymers can be natural, synthetic and semisynthetic. These polymers are listed in **Table 1.6.** The natural source of polymer include animals and plants. These are preferred polymers because of several properties like biocompatibility, biodegradability and safety. On the other hand synthetic polymers and semi-synthetic are derived from natural origin or prepared by various chemical reactions. They are macromolecules having various functional groups in polymer network (Viji Chandran S *et al.*, 2015).

1.10.5.2. Thiolated polymers

Thiolated polymers are class of highly mucoadhesive polymers that have thiol groups on polymeric backbone (Bernkop-Schnürch A, 2005). Till now various polymers have been thiolated. These include chitosan, polyacrylic acids and its derivatives and sodium alginate etc.

1.10.6. Interaction of mucoadhesive polymeric devices with mucus layer

The gastro-intestinal wall is lined with a continuous mucus layer with a thickness of 15-600 micrometers (Sigurdsson HH *et al.*, 2013). It is complex aqueous gel composed of glycoproteins that provide barrier properties to the underlying membranes. First and second generation non-thiolated mucoadhesive polymers have several functional groups like carboxylic groups, amino groups and hydroxyl groups that render theses polymers negative or positively charged (Samaridou E *et al.*, 2014).

Table 1.6. Types of mucoadhesive polymers (Chowdary K *et al.*, 2001)

Natural	Semisynthetic	Synthetic	Others
Starch, polysaccharides, pectin, xanthan, guar, sodium alginate, carrageenan, gellan	Chitosan, gelatin, hyaluronic acid	Cellulose derivatives including hydroxyl-propyl cellulose (HPC), hydroxyl-propyl methyl cellulose, Carboxy-methyl cellulose (CMC), methyl and ethyl cellulose, carbopol, polyacrylates, methacrylic acids, Polyacrylic acid, polycarbophil, poly-ethylene glycol	poly-vinyl alcohol (PVA), poloxamers, Methacrylamide polymers, thiolated polymer, polyoxyethylene, poly-vinyl pyrrolidone

These non-thiolated polymers can be formulated into variety of drug delivery systems including gels, micro and nanoparticles, nanospheres, liposomes, transferosomes, beads, films and patches (Bernkop-Schnürch A, 2005).

These polymers interact with mucus layer through hydrogen bonding, ionic interaction, Vander Waal forces, hydrophobic and electrostatic interactions. These non-covalent interactions are weak and do not retain for longer times. These problems were eliminated third generation thiolated polymers. These include thiolated polymers form covalent bond with the mucus layer. Mucus layer is composed of cysteine domains with thiol bridging. Thiolated polymer forms covalent linkage by exchange of disulfide bond with thiol bridging in mucus layer as shown in **Figure 1.6.** These covalent bonds increase mucoadhesion to greater extent and the delivery systems remain in contact for prolong time to the mucus membrane (Rathee P *et al.*, 2011). Thiolated polymers are used extensively for controlled or sustained drug delivery to the target site.
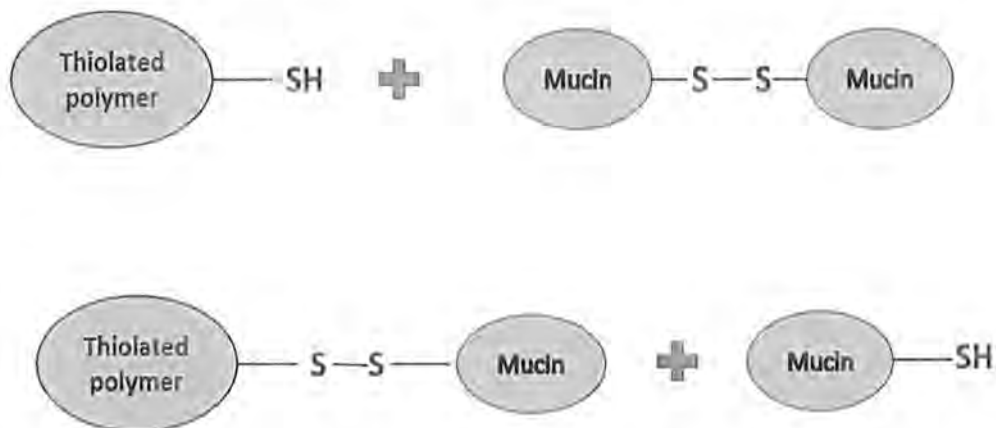
Figure 1.6. Thiomer interaction with the mucus layer (Cevher E *et al.*, 2008).

1.11. Nanotechnology

Nanotechnology concerns with study of molecules and atoms at dimensions of less than 100 nanometers. It has wide range of applications including forensic, textile, agriculture and medical therapeutics (Kumari A *et al.*, 2010). In medical field the idea was given by Paul Ehrlich who called these nanocarriers as "magic bullets" because of their targeted delivery to the infection site. These nanocarriers include polymeric nanoparticles, liposomes, nanospheres and niosomes. Nanocarriers for drugs provides several advantages including high bioavailability, high solubility, reduced degradation, targeted delivery, increase efficacy and cost-effectiveness. Nanocarriers tend to release the drugs in controlled manner thus reducing the toxicity and improve patient compliance.

1.11.1 Polymeric nanoparticulate drug delivery system for oral administration

Oral is the most widely used pathway of medicine administration for most of the drugs because of lower side effects and best patient compliance (De Sousa IP *et al.*, 2015). Mucosal surface is quickly accessible and are easy target for the delivery of orally administered drugs (Prego C *et al.*, 2005). These mucosal dosage forms are used for both the systemic and local delivery of drugs. The use of oral nanoparticulate drug delivery systems is becoming common to diminish all the problems linked with the conventional drug delivery systems (Zazo H *et al.*, 2016). The nanocarrier based systems for mucosal delivery are able to cross the barriers and maintain the therapeutic concentration of drugs for longer period with minimum side effects. Variety of polymers are used in such nanoparticulate systems to make mucosal dosage forms with size less than 1 micrometer. These polymers can be natural or synthetic. Nanoparticles made of natural polymers including albumin, gelatin and chitosan have high solubility,

biocompatibility and reduced cost. They also have various drawbacks like impurities, incompatibility with lipophilic drugs and limited loading of drugs. Synthetic polymers for nanoparticulate drug delivery are extensively used that are non-toxic, biocompatible, and biodegradable. Synthetic polyacrylic derivatives such as carbopol, polycarbophil, poly acrylates and methacrylic acids are used in nanoparticulate drug devices with several advantages like biocompatibility, controlled drug release and safety (Samaridou E *et al.*, 2014).

1.11.2. Thiolated polycarbophil (PCP) nanoparticles

In order to improve the efficacy of polymeric nanoparticles, there is a need to prolong the residence time and increase the stability at the mucosal site. The nanoparticles based on thiomers is a new method that prolongs the residence time at gastro-intestinal (GI) mucosal layer and ensuring optimal bioavailability of drugs (Bernkop-Schnürch A, 2005). These thiomer nanoparticles provide strong mucoadhesion by disulfide exchange reaction with the cysteine-rich parts of GI mucus layer. Polycarbophil (PCP) is a highly mucoadhesive, anionic and hydrophilic polymer (Asija R, 2014) that can be easily modified by carbodiimide chemistry thus facilitating its permeation through highly densely negatively charged mucus layer because of sulfonic and sialic acid groups (Crater JS and Carrier RL, 2010). Thiolation of PCP with cysteine render this polymer more mucoadhesive that can control the release of drugs for prolong time. PCP is compatible with large number of drugs. Its thiolated nanoparticles are usually prepared by ionic gelation method. Cationic crosslinkers like calcium chloride (CaCl2) are used to link these polymers to the drugs.

1.11.3. Mucopenetrating nanoparticulate drug delivery system for H.pylori infection therapy

The mucus layer is a thick viscous layer (Sigurdsson HH *et al.*, 2013), that is complex aqueous gel composed of glycoproteins that provide barrier properties to the underlying membranes (Cone RA, 2009). These properties together with the high mucus turnover rate, usually clear the nanoparticles from mucosa before the therapeutic concentration could reach the deep tissues where H.pylori resides (Arora S *et al.*, 2011). Therefore the targeting strategies for nanoparticulate drug delivery systems has shifted to enhanced mucopenetration effect. The drug delivery system needs to be capable of being mucopenetrating as well as mucoadhesive. Mucoadhesion effect can be improved by thiolation. But these thiomer nanoparticles must have the ability to penetrate the

mucus and eradicate the bacteria from the target site (Dünnhaupt S *et al.*, 2011). The most promising technique is to use protease enzymes in the nanoparticulate system to cleave glycoproteins of mucus layer (Müller C *et al.*, 2013).

(Samaridou E *et al.*, 2014) functionalized trypsin, papain, bromelain and chymotrypsin over PLGA nanoparticles and reported high permeability in mucosa. Among these enzymes, papain has been found to significantly reduce the viscosity of mucus. In recent years papain has been linked to a polymeric particulate system with the ability to selectively cleave and penetrate the mucus layer.

1.11.3.1. Papain functionalization on polymeric nanoparticles

Papain is a protease enzymes that is used in polymeric drug delivery systems to enhance the mucopenetration effect. It can be easily grafted on Poly (lactide-co-glycolide) and poly acrylic acid polymers through covalent bond formation. Papain has superior mucolytic properties over other proteases. Papain is reported to be safe, non-toxic and biocompatible enzyme for drug delivery systems. Papain is also known to have antioxidant, anti-inflammatory, antiviral, anti-bacterial effect (Mamboya EAF, 2012).

1.11.4. Synthesis of amoxicillin loaded papain modified thiomer nanoparticles

Amoxicillin is synthetic, orally absorbed antibacterial with improved spectrum against gram-negative bacteria (Rossi A *et al.*, 2016). It has worldwide use in standard therapy against *H.pylori* eradication combined with another antibiotic and an antacid. It is a water soluble drug that can be easily incorporated in nanoparticles. Its lower efficacy is due to short residence time and poor stability. These properties can be improved by thiomer nanoparticulate drug delivery system. Therefore amoxicillin loaded thiolated polycarbophil (PCP) nanoparticles were prepared by ionic gelation method using calcium chloride as cross linker.

PCP is an anionic biocompatible, biodegradable polymer with high safety profile. Thiolation of PCP is done to increase its mucoadhesive and controlled release properties. For enhancing mucopenetration effect, papain was immobilized on polymer. Papain cleave the mucoglycoproteins bonds and facilitate transport of drug to deeper tissues where it retains for longer times. PCP is also found to retain the mucolytic properties of papain. (Metin AÜ and Alver E, 2016). The proposed nanoparticulate system will have the advantage of ease of administration (being oral liquid), stability and prolong retention. The particles will first overcome mucus layer owing to its

mucolytic activity, then due to mucoadhesive properties, it will increase the residence time.

1.12. Aim and Objectives

Aim

- The aim of project was to prepare mucopermeative & mucosal adhesive papain modified thiolated polycarbophil nanoparticles incorporating amoxicillin with the ability to use in anti *H.pylori* therapy.

Objectives

- To evaluate the stability, prolong retention and prolong drug release of nanoparticulate system.

- To assess nano formulation through exvivo studies

- To evaluate the formulation for invitro studies.

CHAPTER 2

MATERIALS AND METHODS

2. MATERIAL AND METHODS

2.1. Material

2.1.1. Reagents

Amoxicillin trihydrate (active drug) was obtained from Global pharmaceuticals. Polycarbophil (PCP), N-hydroxysuccimide (NHS) (obtained from Sigma Aldrich, Germany). L-cysteine hydrochloride (purchased from Daejung China). Mannitol, calcium chloride ($CaCl_2$) (Scharlau, Germany). Bradford reagent (Coomassie brilliant blue) Ellman's reagent (Di thio-bis nitro benzoic acid Alfa Aesar), Papain was obtained from Merck Germany. EDAC (Ethyl dimethyl aminopropyl carbodiimide, Penicon), Casein powder (Science Home, Pakistan), Fluorescein diacetate (FDA) were purchased from Avonchem United Kingdom. Hydrochloric acid (Riedel-De-haen, RDH, Labor chemikalein, GmBh & Co), Sodium chloride (Merck, Scharlau, Hohenbrunn, Germany), potassium dihydrogen phosphate (Scharlau, Germany), sodium dihydrogen phosphate (Scharlau, Germany), dipotassium hydrogen phosphate (Scharlau, Germany), Sodium hydroxide (Merck, Scharlau, Hohenbrunn, Germany), Acetone, Nutrient Broth (Merck, Germany), Chocolate agar (Sigma Aldrich, Germany), Distilled water was used from Pharmaceutics lab (Department of Pharmacy, QAU, Islamabad)

2.1.2. Apparatus and equipment

Weighing balance (Ohaus corporation, US), Multi hot plate stirrer (Magik, UK), Lyophilizer (Alpha 1-2 LD plus, Christ, Germany, Centrifuge machine (Hermle Labortechnik, Z-206A, Germany), Sonicator (Elma E-60 H Elmasonic, USA), FTIR spectrophotometer (Bruker Alph-P, USA), Dialysis membrane (Cell Sep®, T4 Series, Texas, USA), Pharmaceutical Refrigerator (MPR-161D H, Panasonic, Japan), Freezer (Panasonic, Japan), pH Meter (Bante Instruments, PHS-25CW, Chicago, USA), UV visible double beam spectrophotometer (Dynamica Halo DB-20, UK), Conical flasks, Funnel, Petri plates, Beakers, Micro Pipette, Micro filters, Syringes, Eppendorf tubes, Glass slides, Graduated cylinder, volumetric flasks, Magnetic stirrer, Micro titration plate reader (Perkin Elmer), Water bath and Shaker (Memmert, WNB-7, Germany, Oven (Memmert, Germany), Zetasizer (Malvern, Vσ.7.12, USA), Incubator, Laminar flow hood, Autoclave Machine, Scanning electron microscope (FEI Nova NanoSEM 450, USA). Silicone tubes, Rheometer, Single punch tablet machine (Single punch tablet press CSP12 Liaoyang Pharma Machinery, Germany).

2.2. Methods

2.2.1. Preparation of solutions

2.2.1.1. 0.4 % polycarbophil solution

For the preparation of 0.4 % polycarbophil solution, 0.4 gram or 400 mg of polymer was weighed and dissolved in small amount of distilled water. Then volume up to 100 ml was obtained with distilled water (Müller C *et al.*, 2014).

2.2.1.2. 0.1 % polycarbophil solution

To prepare 0.1 % of polycarbophil solution, we weighed accurately 0.1 gram or 100 mg of polymer. It was added in a small amount of distilled water and dissolved completely while stirring. The final volume was made up to 100 ml with more distilled water.

2.2.1.3. 1 Molar NaOH solution

The preparation of 1 Molar NaOH required 4 grams of sodium hydroxide that was dissolved in sufficient amount of distilled water. Volume was adjusted to 100 ml.

2.2.1.4. 5 Molar NaOH solution

For the preparation of 5 M NaOH solution, 20 grams of sodium hydroxide was weighed accurately and dissolved in sufficient amount of distilled water. The volume was made up to 100 ml (Bernkop-Schnürch A and Steininger S, 2000).

2.2.1.5. 50 mM EDAC solution

To prepare 50 mM EDAC, 0.96 grams or 960 mg of EDAC was dissolved in distilled water. Stirred well until completely dissolved. Volume was adjusted to 100 ml with distilled water.

2.2.1.6. 1 % NaCl solution

For the preparation of 1 % NaCl solution, 1 gram of sodium chloride was added to 10 ml distilled water and dissolved completely by stirring. More distilled water was added to make the volume up to 100 ml.

2.2.1.7. 1 Molar HCl solution

To prepare 1 Molar HCl solution, 8.3 ml of concentrated hydrochloric acid was added to a small amount of distilled water and stirred well. More distilled water was added to obtain 100 ml of final volume.

2.2.1.8. 1 mM HCl solution

415 µl of concentrated hydrochloric acid was added in small amount of distilled water and stirred well. More distilled water was added to obtain 5 L of final volume.

2.2.1.9. 0.5 mM HCl

To prepare 5 L of 0.5 mM HCl solution, 207 µl of concentrated hydrochloric acid was added in small quantity of distilled water and stirred well. The final volume was adjusted to 5 Liter with distilled water (Dünnhaupt S et al., 2011).

2.2.1.10. 4 % NaBH₄ solution

For the preparation of 4 % $NaBH_4$, 4 grams of sodium borohydride was weighed accurately and dissolved completely in sufficient amount of distilled water. After complete dissolution, the final volume up was adjusted to 100 ml with distilled water.

2.2.1.11. 0.2 % papain solution

For the preparation of 0.2 % papain solution, 0.2 grams or 200 mg of papain was weighed accurately and dissolved in sufficient amount of distilled water. After complete dissolution, final volume up to 100 ml with distilled water was obtained.

2.2.1.12. 0.1 % CaCl₂ solution

For the preparation of 0.1 % $CaCl_2$ solution, 0.1 gram or 100 mg of calcium chloride was added in 10 to 15 ml distilled water and dissolved completely by stirring. More distilled water was added to make the volume up to 100 ml.

2.2.1.13. 0.5 % CaCl₂ solution

For the preparation of 0.5 % CaCl2 solution, 0.5 grams or 500 mg of calcium chloride was added in small quantity of distilled water and dissolved while stirring. After complete dissolution, final volume up to 100 ml with distilled water was obtained.

2.2.1.14. 0.1 % Fluorescein Diacetate (FDA) solution

To prepare 0.1 % FDA solution, 0.1 gram or 100 mg of fluorescein diacetate was dissolved it completely in sufficient quantity of acetone. After complete dissolution, acetone was added to obtain a final volume up to 100 ml.

2.2.1.15. 0.1 N HCl solution

To obtain 0.1 N HCl solution, 830 µl of concentrated hydrochloric acid was added to sufficient amount of distilled water and stirred well. Then more distilled water was added to make up the final volume up to 100 ml.

2.2.1.16. 5 % artificial mucin dispersion

For the preparation of 5 % artificial mucin dispersion, 5 gram of artificial mucin was dispersed in small amount of phosphate buffer (pH 6.8). Then final volume up to 100 ml with additional phosphate buffer (pH 6.8) was obtained.

2.2.1.17. 12 mM L-cysteine solution

To prepare 12 mM L-cysteine solution, 145.3 mg of L-cysteine was added in sufficient amount of distilled water and dissolve it completely. After complete dissolution, final volume was adjusted to 100 ml with distilled water.

2.2.1.18. Phosphate buffer PBS (pH 8)

For the preparation of phosphate buffer (pH 8), 2.88 grams of disodium hydrogen phosphate and 1.154 grams of potassium dihydrogen phosphate were dissolved in sufficient amount of distilled. The final volume up to 100 ml with additional distilled water was obtained. Then pH was adjusted with 1 M NaOH.

2.2.1.19. Phosphate buffer PBS (pH 6.8)

To prepare phosphate buffer (pH 6.8), 6.8 grams of potassium dihydrogen phosphate was added in a volumetric flask containing 300 ml of distilled water. Then 0.9 grams of sodium hydroxide was added to previous mixture. It was shaken well to get a homogenous solution. After complete dissolution, the volume was made up to 1000 ml with distilled water and pH was adjusted.

2.2.1.20. 0.1 M NaCl solution

To prepare 0.1 M NaCl, 585 mg of sodium chloride was added in a beaker and dissolved in sufficient amount of distilled water. It was put on continuous stirring until completely dissolved. After complete dissolution more distilled water was added to make up the volume up to 100 ml.

2.2.1.21. 0.1 % amoxicillin solution

For the preparation of 0.1 % amoxicillin trihydrate solution, 0.1 gram or 100 mg of amoxicillin trihydrate was weighed in a flask. Drug was dissolved in small quantity of distilled water completely. The final volume was adjusted to 100 ml with addition of more distilled water.

2.2.1.22. 0.5 % amoxicillin solution

For the preparation of 0.5 % amoxicillin trihydrate solution, 0.5 grams or 500 mg of papain was weighed accurately and dissolved in sufficient amount of distilled water with

continuous stirring. After complete dissolution final volume up to 100 ml with distilled water was obtained.

2.2.2. Synthetic procedure

2.2.2.1. Synthesis of polycarbophil-cys conjugate (PCP-Cys)

PCP-Cys conjugate was prepared according to the previous method (Bernkop-Schnürch A *et al.*, 2000) in which there is covalent attachment of L-cysteine to polycarbophil and an amide bonding between COOH groups of polymer and NH_2 moieties of L-cysteine. As shown in **Figure 2.1**, a solution of polycarbophil was made by dissolving 1000 mg in 250 ml of distilled water and the polymer solution was neutralized with NaOH (1 M). For the activation of carboxylic acid groups of hydrated polycarbophil, 50 mM EDAC (ethyl dimethylaminopropyl carbodiimide) was added. Thereafter 2 grams L-cysteine hydrochloride was slowly added to the reaction blend. pH was adjusted to 6 with NaOH (5 M) in order to increase the amount cysteine groups attached covalently to the polymer backbone (Clausen AE and Bernkop-Schnürch A, 2000). Then for 3 hours, the prepared reaction mixture was incubated at room temperature with continuous stirring. To purify the thiolated polymer and remove the unbound material, the conjugate was dialyzed four times in tubing (12-14 kDa molecular weight) at 10 °C. First dialysis was carried out against HCl (1 mM), the second and third against HCl (1 mM) with 1% NaCl and finally dialyzed against HCl (0.5 mM). After dialysis, the pH of PCP-Cys conjugate was adjusted to 5. Afterward, the dialyzed polymer was dried by lyophilization and stored at 4 °C until further use.

2.2.2.2. Synthesis of polycarbophil-papain (PCP-PAP) conjugate

Covalent attachment of papain to the polymer resulted in the formation of PCP-PAP conjugate (Köllner S *et al.*, 2015). Briefly, 0.1 % solution of polcarbophil was prepared in distilled water **Figure 2.2**. pH value of the polymer solution was adjusted to 6 with NaOH (5 M). Then aqueous solution of EDAC (500 mg) and of N-hydroxysuccimide (NHS) (300 mg) was added slowly to the solution. Under continuous stirring, incubation of the mixture was done for 2 hours. After incubation, papain solution (100 mg in 50 ml water) was slowly added to the polymer solution. The blend was kept under agitation for 12 hours at 10 °C. For next two days, dialysis was carried out for the resultant conjugate against deionized water at 10 °C in dark. The resultant product was lyophilized and stored at 4 °C until further use. The prepared polycarbophil papain conjugate was also checked for color, odor and aqueous solubility

Polycarbophil Solution +
EDAC + Cysteine

Stirred
3 hrs

pH adjusted to 6

Dialysis

pH adjusted to 5

Lyophilized Polycarbophil-Cys
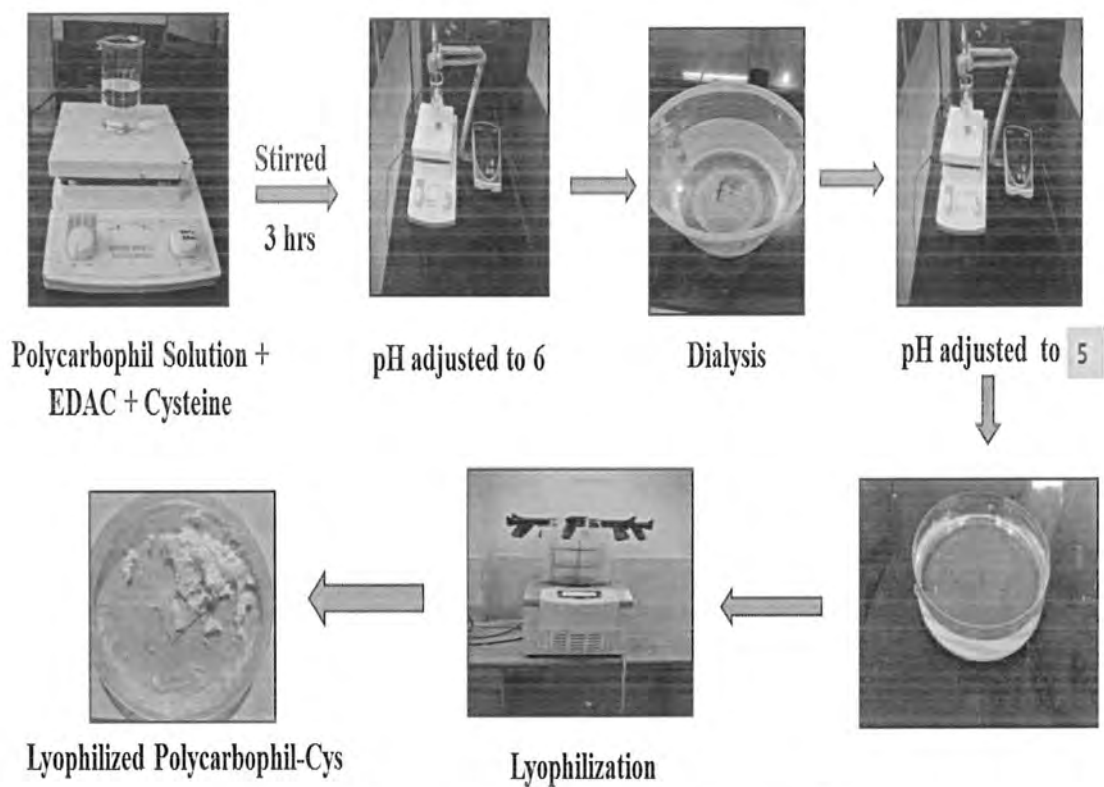
Lyophilization

Figure 2.1. Procedure for thiolation of polycarbophil.

0.1 % Polycarbophil Solution
+ EDAC NHS

pH adjusted to 6

Stirred
2 hrs

Addition of papain
solution

Stirred
12 hrs

Dialysis

Lyophilized PCP-PAP Conjugate
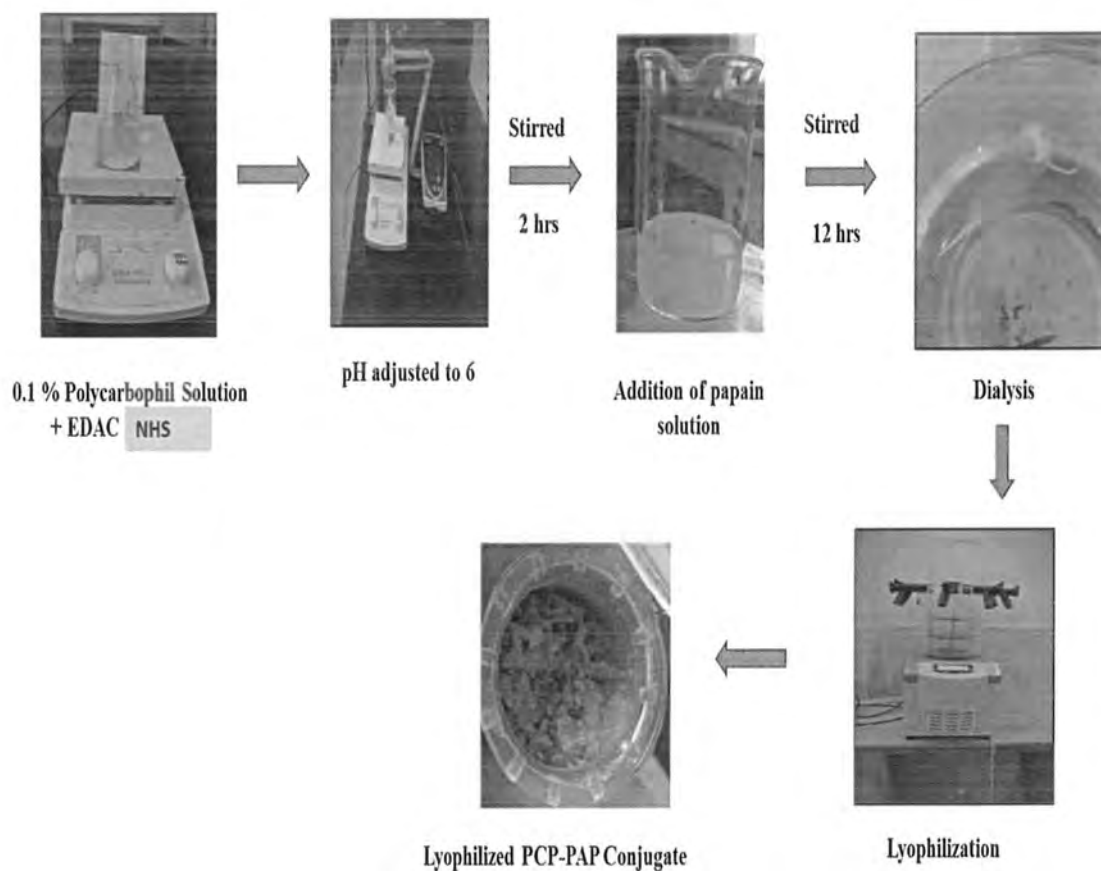
Lyophilization

Figure 2.2. Synthesis of polycarbophil-papain conjugate.

2.2.2.3. Preparation of tablets

30 mg of the lyophilized conjugates i.e. PCP-Cys and PCP-PAP and control polymer (PCP) were compressed by single punch tablet press (CPS12 Pharma Test, Germany) in a flat disc-shaped tablets of 5 mm diameter. A constant compression force was used for the preparation of all discs/tablets.

2.2.2.4. Experimental design

Several factors such as polymer concentration, crosslinker amount and reaction time were found to affect the physicochemical characteristics of nanoparticles. Therefore, the concentration and ratios of various factors for the synthesis of polycarbophil (PCP) and thiolated polycarbophil (PCP-Cys) nanoparticles were optimized using central composite design (CCD) of Design Expert software version 7.0. Response surface methodology (RSM) was utilized to optimize the concentration of independent variables i.e. PCP, PCP-Cys and $CaCl_2$. Nanoparticles were optimized for % entrapment efficiency (EE), particle size, and polydispersity index (PDI) as dependent/response variables. Formulations were prepared according to the runs generated by the software. The results of response variables (dependent) were fed into the software and analyzed for statistical significance.

Table 2.1. Runs developed by design expert software

Runs	Factor 1 A: PCP concentration (%)	Factor 2 B: CaCl₂ concentration (%)
1	0.10	0.30
2	0.08	0.50
3	0.10	0.50
4	0.05	0.30
5	0.08	0.10
6	0.05	0.10
7	0.1	0.10
8	0.08	0.30
9	0.05	0.50

AM: Amoxicillin, PCP: Polycarbophil

The model was considered significant at p-value < 0.05. The best-fitted model for each response was selected on the basis of noise ratio, probability, adequate precision, adjusted R-squared value and predicted R-squared. Concentration of polymer was 0.05 % to 0.1 % while concentration range of calcium chloride was 0.1 % to 0.5 %. The ratio of polymer to enzyme conjugate and polymer to the drug was kept constant as 1:2 and 1:1. **Table 2.1** indicates different runs of design expert software.

2.2.2.5. Preparation of amoxicillin loaded polycarbophil (AM-PCP) and thiolated polycarbophil (AM-PCP-Cys) nanoparticles

Nanoparticles were prepared by ionic gelation method (Arora S *et al.*, 2011) using calcium chloride (CaCl$_2$) as a crosslinker. The concentrations of polymer and cross linker generated by the design expert software were used in the development of nanoparticles. To obtain amoxicillin loaded polycarbophil (AM-PCP) and thiolated polycarbophil (AM-PCP-Cys) nanoparticles, the non-thiolated and thiolated polymers in a concentration of 0.05 - 0.1 % (w/v) were hydrated in demineralized water. It was put on continuous agitation till completely dissolved. After complete dissolution, amoxicillin trihydrate (0.05 - 0.1 % w/v) was added to the polymer solution. The pH of samples was adjusted to 8 with NaOH (1 M) solution and a solution of calcium chloride (0.1 - 0.5 % w/v) was added dropwise to the mixture until turbidity was observed. Turbidity indicated the final fabrication of nanoparticles. The samples were centrifuged (for purification) three times at 6000 rpm for 20 minutes with mannitol (1 % w/v) to prevent aggregation. After completion of centrifugation, the pellet was redispersed in distilled water. The mixtures were freeze-dried and kept at 4 °C. Schematic representation for preparation of amoxicillin loaded polcarbophil nanoparticles is shown in **Figure 2.3**.

2.2.2.6. Preparation of amoxicillin loaded papain modified polycarbophil (AM-PCP-PAP) and thiolated polycarbophil (AM-PCP-Cys-PAP) nanoparticles

A similar ionic gelation method was used for the preparation of amoxicillin loaded papain modified polycarbophil nanoparticles. The concentrations of polymer and cross linker obtained from the design expert software was used for the preparation of amoxicillin loaded papain modified polycarbophil nanoparticles. Whereas the ratio of polymer to enzyme conjugate was kept constant that is 1:2. Schematic diagram of papain modified nanoparticles is shown in **Figure 2.4**. First the non-thiolated and thiolated polymer was dissolved in distilled water according to values given in **Table**

2.1. Then drug in ratio of 1:1 to polymer was added. The mixture was completely dissolved. After dissolution, papain conjugate was added to this mixture in ratio of 2:1 to polymer. Again agitation was done to obtain a homogenous mixture. The pH of samples was adjusted to 8 with 1 M NaOH solution and a solution of calcium chloride (0.1 - 0.5 % w/v) was added dropwise to the mixture until turbidity was observed. Turbidity indicated the final fabrication of nanoparticles. The samples were centrifuged (for purification) three times at 6000 rpm for 20 minutes with mannitol (1 % w/v) to prevent aggregation. After completion of centrifugation, the pellet was redispersed in distilled water. The mixtures were freeze-dried and kept at 4 °C.

2.2.2.7. Fluorescein diacetate (FDA) labeling of nanoparticles

For diffusion and permeation procedures, fluorescein diacetate (FDA) marker was incorporated into the AM-PCP, AM-PCP-Cys, AM-PCP-PAP and AM-PCP-Cys-PAP nanoparticles according to previous method (Müller C *et al.*, 2014). Solutions of drug and polymer/polymer conjugates were made and mixed with FDA (0.1 % w/v) solution in acetone. The solutions were incubated with protection from light for 20 minutes. Then calcium chloride was used as a crosslinker to prepare nanoparticles. The nanoparticle suspensions were stirred for 2 hours under light protection at 15 °C. The labeled nanoparticles were centrifuged, redispersed in deionized water and lyophilized with mannitol (1 %) as cryoprotectant.
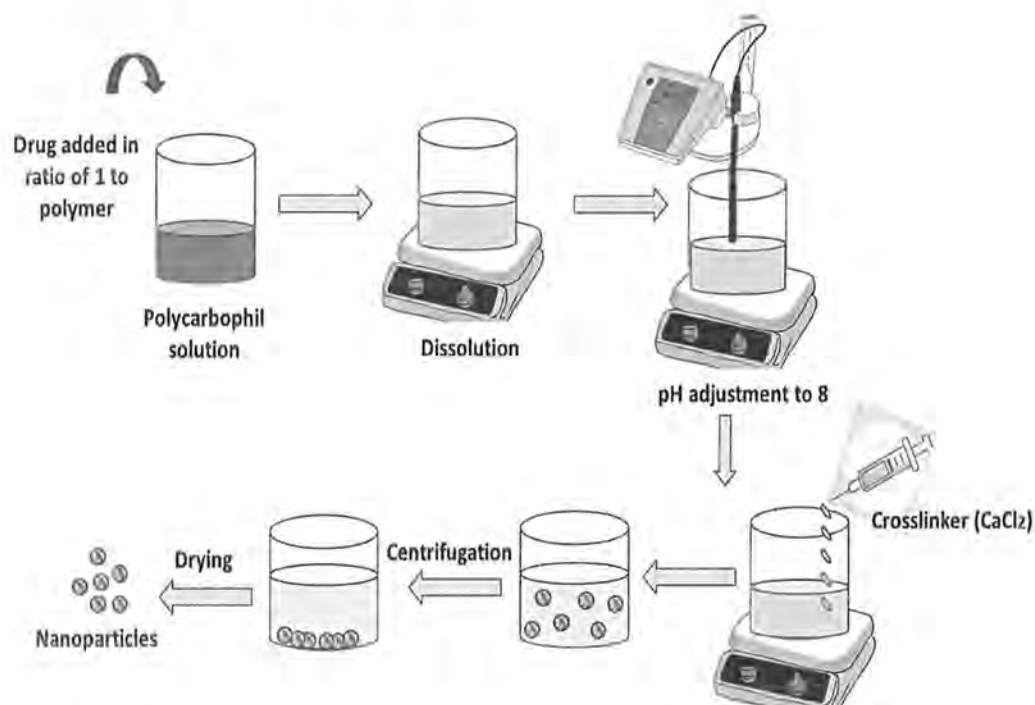
Figure 2.3. Ionic gelation method for the preparation of amoxicillin loaded polycarbophil nanoparticles.
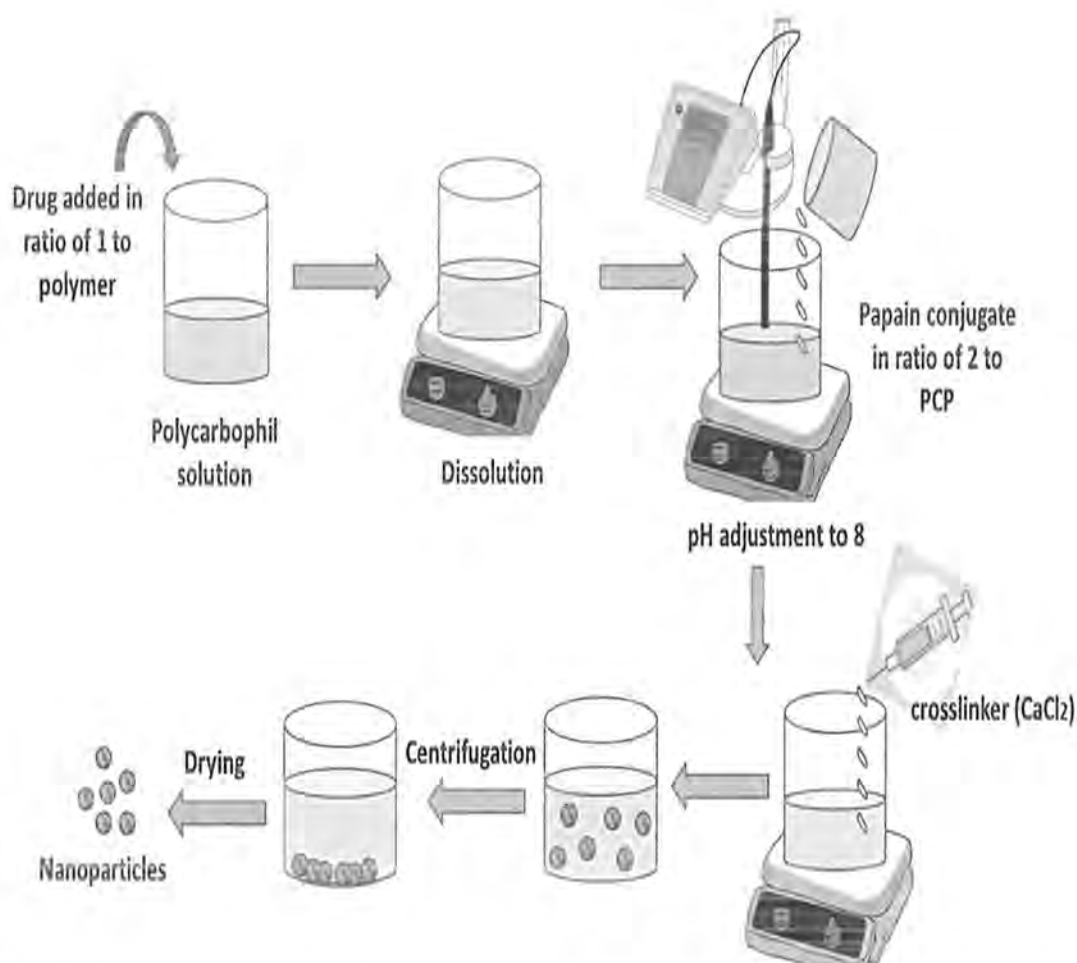
Figure 2.4. Schematic diagram of ionic gelation method for the preparation of amoxicillin loaded papain modified polycarbophil nanoparticles.

2.2.3. Characterization methods

2.2.3.1. Degree of conjugation

The degree of conjugation that refers to thiol groups number on the polymer backbone was calculated spectrophotometrically by Ellman reaction as described previously (Bernkop-Schnürch A and Steininger S, 2000 ; Köllner S *et al.*, 2015). In brief polymer solution was prepared by dissolving 0.5 mg of PCP-Cys in 250 µl of demineralized water and then 250 µl of phosphate buffer (0.5 M, pH 8.0) was added. Afterward, 0.5 ml of Ellman's reagent (3 mg dissolved in 10 ml of phosphate buffer; 0.5 M, pH 8.0) was added. Incubation of samples was done for 2 hours under complete protection from light and centrifuged. The supernatant was added to 96 well plate to determine absorbance at 450 wavelength utilizing microplate tester (Perkin Elmer). A standard curve of L-cysteine hydrochloride was used to calculate the number of thiol groups immobilized on the polymer.

2.2.3.2. Disulfide bond formation

The degree of disulfide bond formation was determined by Ellman's test after reduction with sodium borohydride (NaBH$_4$) (Dünnhaupt S et al., 2011 ; Iqbal J et al., 2012). 0.5 mg Polymer conjugate was hydrated in 350 µl demineralized water. To this mixture, 650 µl of phosphate buffer (0.05 M, pH 6.8) was added. The sample was kept under continuous stirring at 37 °C. After 30 minutes of shaking, 1 ml of 4 % (w/v) NaBH$_4$ was added and left for 1 hour stirring at 37.5 °C. To remove the unused sodium borohydride, 200 µl of HCl (5 M) was added and mixed. Neutralization of the sample was done with 1 ml phosphate buffer (0.5 M, pH 8) and 0.1 ml of Ellman's reagent (0.4 % in phosphate buffer; 0.5 M, pH 8) was added. The mixture was again incubated for 1 hour at room temperature. The absorbance of samples was measured by microplate reader (Perkin Elmer). The concentration of attached cysteine was determined by the calibration curve. Subtraction of free thiol groups from total thiol groups resulted in amount/degree of disulfide bonds.

2.2.3.3. Evaluation of swelling behavior

The swelling behavior of control polymer and conjugates i.e. PCP, PCP-Cys, PCP-PAP was investigated by using gravimetric method (Shahnaz G et al., 2010). The discs/ tablets prepared before were attached to the needle of a syringe and placed in a beaker containing phosphate buffer (pH 6.8) at 37 °C. At regular time intervals, the discs were removed from the buffer medium and accurately weighed. The amount of buffer absorbed was calculated as a function of time by using the equation:

$$Swelling\ index\ (\%) = \frac{W_t - W_0}{W_0} \times 100$$

Here W_0 is the initial weight of the disc in dry state and W_t presents the wet weight of the swollen disc at time t.

2.2.3.4. Calibration curve of amoxicillin trihydrate

To develop standard calibration curve of amoxicillin trihydrate, stock solution of drug was made by dissolving 10 mg of amoxicillin trihydrate in sufficient quantity of distilled water. After complete dissolution more distilled water added to make up the volume up to 10 ml. From this solution 1 ml was taken in a beaker containing 99 ml of distilled water. The beaker was labeled as stock with a concentration of 10 µg/ml. A standard solution was prepared from this stock by taking 5 ml from the same and diluted up to 50 ml with distilled water. The standard had concentration of 1 µg/ml. From the

standard a number of dilutions were prepared with different concentrations from 0.1 to 0.6 micrograms per ml. First dilution was made by taking 1 ml from the standard solution and diluted up to 10 ml with distilled water. Similarly further dilutions were prepared and labeled. Spectrophotometric analysis was performed on these solutions. Standard was scanned for λmax that was found to be 210 nm. Afterward, absorbance of each dilution was determined at wavelength of 210 nm against blank. Simple distilled was used as blank. A graph was plotted between absorbance and concentrations of all dilutions with absorbance on y-axis and concentration on x-axis using Microsoft Excel 2013.

2.2.3.5. Entrapment efficiency (%)

The percent drug entrapment of nanoparticles was calculated as follows:

The % entrapment efficiency (EE) was determined by first separating the nanoparticles from the aqueous medium by ultracentrifugation (Saha P *et al.*, 2010). The amount of unbound drug in the supernatant was measured spectrophotometrically. The pelleted nanoparticles were added to phosphate buffer pH 6.8 and subjected to overnight stirring so that bound drug comes off the nanoparticles. Centrifugation was performed for the samples were at 7000 rotations per min at room temperature. Amoxicillin amount loaded in nanoparticles was found spectrophotometrically at 210 lambda max. % entrapment efficiency determined by the following **Equation 1**:

$$\text{Entrapment efficiency } \% = \frac{Amount\ of\ drug\ in\ nanoparticles}{Total\ Amount\ of\ drug\ added} \times 100$$

2.2.3.6. Particle size, polydispersity index, zeta potential and morphology

Size of nanoparticles, zeta potential & PDI (polydispersity index) were determined using Malvern zetasizer Vσ.7.12. Values were reported as the ± standard deviation of at least 3 samples. The nanoparticles were subjected to scanning electron microscopy (SEM) (FEI Nova NanoSEM 450, USA) in order to confirm size, shape and morphology of formed nanoparticles.

2.2.3.7. Fourier transform infrared analysis

Fourier Transform Infrared (FTIR) analysis (Bruker alph-P, USA) were performed on drug, polymer, enzyme, polymer/enzyme conjugates, and nanoparticles.

2.2.3.8. Procedure for in-vitro drug release

a. preparation of phosphate buffer (pH 6.8)

To prepare phosphate buffer (pH 6.8), 6.8 grams of potassium dihydrogen phosphate was added in a volumetric flask containing 300 ml of distilled water. Then 0.9 grams of sodium hydroxide was added to previous mixture. It was shaken well to get a homogenous solution. After complete dissolution, the volume was made up to 1000 ml with distilled water and pH was adjusted.

b. Standard calibration curve of amoxicillin trihydrate in phosphate buffer (pH 6.8)

A calibration curve of amoxicillin trihydrate was made in phosphate buffer (PB) (pH 6.8) to quantify the amount of drug in the release medium. For this, a 10 mg of drug was dissolved completely in 1 ml of distilled water and diluted up to 10 ml with phosphate buffer (pH 6.8). From this 1 ml was taken in a volumetric flask a more PB (pH 6.8) was added to make up the volume up to 100 ml. The solution was labeled as stock with concentration of 10 µg/ml. From the stock solution further dilutions were prepared ranging in concentration from 2 µg/ml to 10 µg/ml. First dilution was prepared by taking 2 ml from the stock and diluted up to 10 ml with phosphate buffer (pH 6.8). Similarly all the dilutions were prepared in labeled. The first dilution was scanned for λmax that was found to be 240 nm. Afterward absorbance of each dilution was determined at wavelength of 240 nm against blank. Phosphate buffer (pH 6.8) was used as blank. A graph was plotted between absorbance and concentrations of all dilutions with absorbance on y-axis and concentration on x-axis using Microsoft Excel 2013 and checked for linearity.

c. Drug release of nanoparticles

Amoxicillin *in vitro* release from amoxicillin suspension, AM-PCP, AM-PCP-Cys, AM-PCP-PAP and AM-PCP-Cys-PAP nanoparticles was determined by dialysis tube method (Novelli F *et al.*, 2017) at pH 6.8 for 48 hours. Known quantity of amoxicillin loaded modified and un-modified polycarbophil nanoparticles were redispersed in small quantity of phosphate buffer (pH 6.8) after separation by ultracentrifugation. Afterward, these nanosuspensions were transferred to dialysis tube, tied at both ends and suspended in phosphate buffer (pH 6.8) in beakers. The beakers were then placed in bath shaker and temperature was maintained at 37 ± 0.5 °C. At pre specified points of time, small volume was withdrawn & equal volume from freshly prepared phosphate buffer (pH 6.8) was replaced in release medium to maintain sink conditions for whole experimental period. Samples were analyzed for drug release. Drug content was

determined spectrophotometrically at 240 nm. Different kinetic models were applied to determine the mechanism of release from prepared nanoparticles.

2.2.3.9. Stability in 0.1 N HCl (pH 1.2)

Stability of amoxicillin and final formulation i.e. amoxicillin loaded papain modified thiolated polycarbophil (AM-PCP-Cys-PAP) nanoparticles was evaluated in 0.1 N HCl (pH 1.2) according to previously used method (Arora S *et al.*, 2011). Briefly, 5 mg pure amoxicillin and nanoparticles equivalent to 5 mg amoxicillin were dispersed in 25 ml 0.1 Normal Hydrochloric acid in a beaker & left at 37 ± 0.5 °C with continuous agitation. At specific points of time, samples were taken & analyzed for drug content spectrophotometrically. Percent degradation of amoxicillin was determined from the UV analysis.

2.2.3.10. Mucoadhesive behavior via rheological study

The viscoelastic properties of nanoparticles-mucus mixtures were determined by using cone-plate viscometer according to previous study (Sohail MF *et al.*, 2016). Briefly, 5 % (w/v) of artificial mucin dispersion was made in phosphate buffer (0.1 M; pH 6.8). Then 1 ml of each nanoparticle suspension was added to 5 ml mucin dispersion. Incubation of the mixture was done at 37 ± 0.5 °C for 6 hours. Pure mucin dispersion was taken as reference. At time interval of 1, 2, 4 and 6 hours, 400 µl of each nanoparticle suspension was added to cone-plate viscometer and rheological parameter was determined at share rate of $50 \ s^{-1}$ by using the formula:

$$\Delta \eta = \eta_{mix} - \eta_{muc}$$

Where η_{mix} is the apparent viscosity of nanoparticle-mucin mixture in Pa.s (Pascal second) and η_{muc} is viscosity of reference mucus dispersion.

2.2.3.11. Method for ex-vivo study

a. Mucus separation and purification

Mucus was separated and purified according to a previous method described by (Müller C *et al.*, 2013). Firstly a small portion of goat upper small intestine was excised and collected from slaughtered house. It was immediately transferred to icebox. The intestine was washed thoroughly with normal saline to remove the debris material. Afterward, the intestine was everted to open the mucosal side **Figure 2.5**. The mucosal side was rinsed with normal saline. Mucus was collected in a jar by scraping off with a

sharp object. The collected mucus was purified with NaCl (0.1 M). For 1 gram of mucus, a 5 ml of NaCl (0.1 M) was added and put on continuous stirring for 1 hour with a temperature of 4 °C. After completion of specified time, 1 hour centrifugation was done at 1000 rotation per minute. The procedure was repeated again using 2.5 ml of NaCl (0.1 M) for 1 gram mucus this time. Supernatant was removed and the purified mucus was stored at − 20 °C till use.

b. Fluorescein diacetate (FDA) calibration curve

Calibration curve of fluorescein diacetate (FDA) was developed to quantify the amount of FDA in labeled nanoparticles and % permeated through the mucus. Briefly a stock solution of FDA was prepared by dissolving 10 mg of FDA dye in 10 ml of acetone in a flask. The stock was diluted up to 50 ml with NaOH (5 M) to obtain a concentration of 0.2mg/ml. The solution was labeled as stock. From the stock solution five dilutions were prepared ranging in concentration from 0.6 µg/ml to 14 µg/ml. The first dilution was developed by taking 0.15 ml from the stock solution and diluted up to 50 ml with NaOH (5 M). For the second dilution, 0.5 ml of stock solution was diluted up to 50 ml with NaOH (5 M). For the third, fourth and fifth dilutions, 1.5 ml, 2.5 ml and 3.5 ml respective stock solutions were diluted up to 50 ml with NaOH (5 M). To each dilution, 2 ml of acetone was added to stop further hydrolysis of dye. The absorbance of each dilution was determined at wavelength of 490 nm against blank. NaOH (5 M) was used as blank. A graph was plotted between absorbance and concentrations of all dilutions with absorbance on y-axis and concentration on x-axis using Microsoft Excel 2013 and checked for linearity.

Figure 2.5. Procedure for mucus isolation.

c. Quantification of FDA in nanoparticles

Alkaline test (Bernkop-Schnürch A *et al.*, 2006) was used to calculate the amount of fluorescent dye loaded in AM-PCP, AM-PCP-Cys, AM-PCP-PAP and AM-PCP-Cys-PAP nanoparticles with little modification. Freeze dried nanoparticles were completely dissolved in NaOH (5 M, pH 9). The solutions were kept under constant stirring at 37 °C for 1 hour. Afterward, the mixtures were centrifuged and the supernatant was analyzed. As shown in **Figure 2.6** the colorless FDA compound will be hydrolyzed to colored sodium fluorescein that absorbs strongly in the visible range at 490 nm wavelength and can be detected by UV-VIS spectrophotometry (Adam G and Duncan H, 2001). The quantity of FDA loaded in nanoparticles were determined by calibration curve as described previously.

Figure. 2.6. Quantification of fluorescein diacetate (FDA) in nanoparticles by alkaline treatment.

d. *Ex-vivo* permeation study using silicon tube method

The rotating mucus filled silicon tube method as described by (Köllner S *et al.*, 2015) with small modification was used to analyze the penetration of particles in natural intestinal mucus layer. Silicon tubes (34 mm) were filled with 400 µl mucus and sealed at one end. Thereafter 60 µl of each FDA labeled AM-PCP, AM-PCP-Cys, AM-PCP-PAP and AM-PCP-Cys-PAP nanoparticles redispersed in phosphate buffer (pH 6.8) were added to the open end of silicon tubes and sealed at the same end. 400 µl of fresh mucus was used as a blank. All the tubes were kept at 37 °C in an incubator under horizontal stirring. After 4 hours, tubes were frozen at -25 °C for minimum 12 hours. Then 16 slices of 2 mm were made of each frozen tubing. To hydrolyze FDA to sodium

fluorescein, a 500 µl of NaOH (5 M) solution was added to each slice and incubated at 37 °C. Afterward, ultrasonification was done for 30 minutes and the resultant sodium fluorescein was measured spectrophotometrically. The percent nanoparticle penetration in each slice was calculated from the spectrophotometric analysis of sodium fluorescein. **Figure 2.7** shows the procedure of silicon tube method.

Silicone tube filled with mucus

FDA labeled nanoparticles added

Horizontal agitation at 37 °C

FDA quantification

Alkaline treatment and sonication

Frozen tubes cut in 2 mm slices
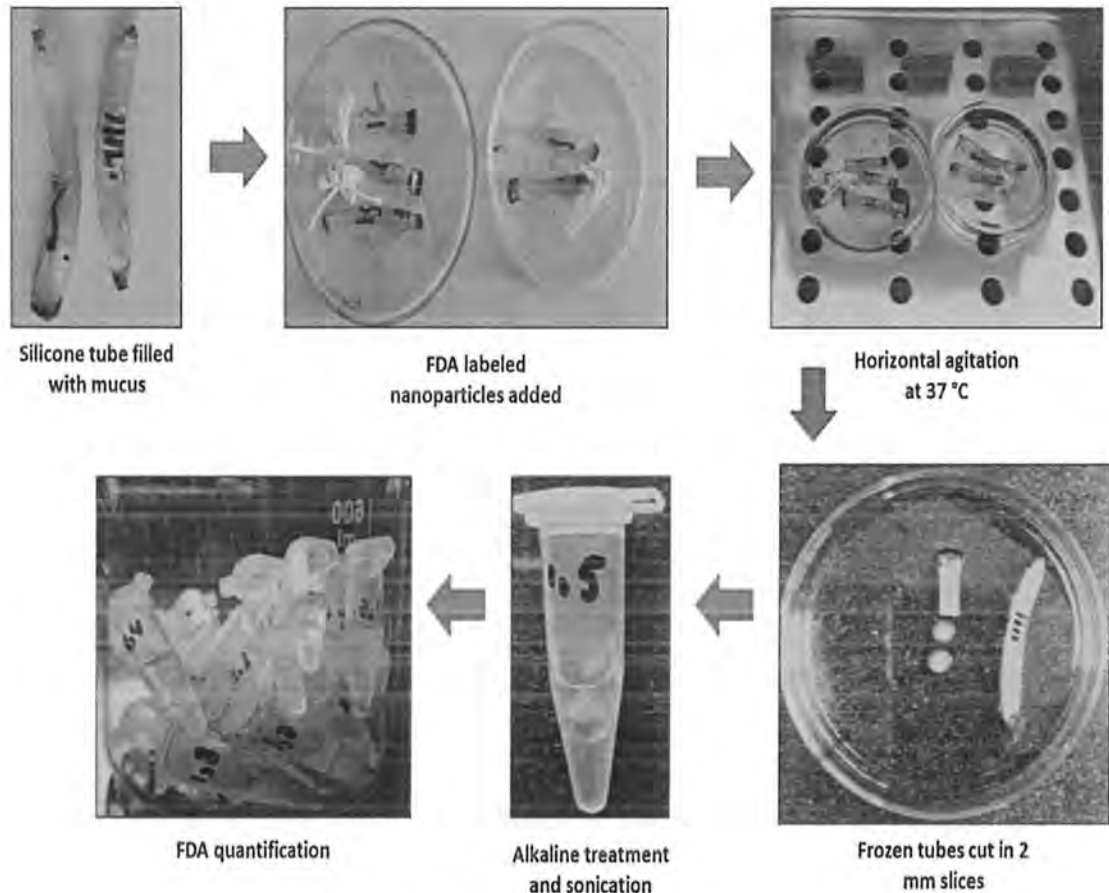
Figure 2.7. Silicon tube method.

2.2.3.12. In-vitro growth inhibition study

The *in-vitro* growth inhibition study was conducted according to the previously defined method. (Narkar M *et al.*, 2010). For this purpose, clinical isolates of *H.pylori* were selected and biopsy samples were taken. Immediately homogenization of biopsy sample was done in brucella broth. Under microaerophilic conditions (5 % oxygen, 10 % carbon dioxide, 85 % nitrogen) at 37 ± 0.5 °C, *H.pylori* strains were grown in 5 days on chocolate agar medium. By spectrophotometric analysis at a wavelength of 600 nm, the growth of *H.pylori* was determined using optical density (OD) as measuring parameter. 1 OD is reported to be equal to 108 colony forming units in one ml broth. The bacterial species were subjected to identification tests including morphological

examination. Afterward, the *in-vitro* growth inhibition test was performed by preparing test tubes each containing a full loop of strain and 5 ml of nutrient broth. Then AM-PCP-Cys-PAP nanoparticle suspension and pure amoxicillin suspension containing double the minimum inhibitory concentration (MIC) value (4 µg/ml) of drug were added to the above mixtures. Tube containing pure culture served as reference. The tubes were kept in incubator under continues shaking and microaerophilic environment at 37 ± 0.5 °C. From these tubes, a sample of 50 µl was taken at different time intervals and placed on skirrow's medium containing petri plates. Incubation of 4 hours was carried out for all the plates at 37 ± 0.5 °C in microaerophilic conditions. Upon completion of incubation, the plated were removed and colonies were counted on each agar plate. The percent inhibition was calculated by using the formula:

$$\text{Percent inhibition (\%)} = \frac{Number\ of\ colonies\ of\ given\ mixture}{Number\ of\ colonies\ of\ pure\ strain} \times 100$$

Statistical Data Analysis

All the results of AM, amoxicillin loaded PCP, amoxicillin loaded PCP-Cys, amoxicillin loaded PCP-PAP and amoxicillin loaded PCP-Cys-PAP nanoparticles were compared using analysis of variance (ANOVA) and simple t-test to check the significance. Significance was assigned to p value less than 0.05. The outcomes were displayed as means $\pm$ standard deviation (n = 3).

CHAPTER 3

RESULTS

3. RESULTS

3.1. Synthesis of Polycarbophil-cys and Polycarbophil-papain Conjugates

Thiomer (PCP-Cys) was synthesized successfully by conjugating the carboxyl functional groups of polycarbophil to the amino moieties of L-cysteine covalently. Carboxyl moieties of polymer were activated by EDAC to achieve the formation of an amide bond between polycarbophil and L-cysteine based on carbodiimide chemistry. The conjugation resulted in the attachment of cysteine to the polymer backbone as shown in **Figure 3.1 (A)**. The amount of thiol groups immobilized on the polymer backbone were 334 ± 24 µmol per gram of thiolated polymer while the number of disulfide bonds formed was calculated to be 152 ± 15 µmol per gram of the polymer. These results confirmed the successful thiolation of polycarbophil. After freeze-drying, a white, fibrous and odorless thiomer was obtained with improved water solubility. A similar synthesis shown in the second step of **Figure 3.1 (A)** was carried out for the preparation of polycarbophil papain (PCP-PAP) conjugate. The carbodiimide based coupling reaction leads to amide bonding among the NH_2 groups of papain & COOH of polycarbophil. Immobilization rate of papain was increased by the addition of NHS during the reaction. PCP-PAP conjugate also appeared to be fibrous, odorless and brownish powder after lyophilization.

3.2. Swelling Behavior of Polycarbophil (PCP) Conjugates

Swelling behavior of polycarbophil and its conjugates i.e. PCP, PCP-Cys and PCP-PAP was evaluated by immersion of thin flat discs of these physical mixtures in phosphate buffer (pH 6.8). The results are shown in **Figure 3.2**. The water uptake behavior showed a rapid swelling and disintegration of polycarbophil (PCP). PCP tablet was eroded within 60 minutes. Whereas the disc made of thiomer (PCP-Cys) mixture displayed an abrupt water uptake and swelling in first 15 minutes. The swelling then gradually increased as compared to the non-thiolated polymer and the water uptake was retained constant for around 90 minutes which is necessary for prolong mucoadhesion. pH of thiolated polycarbophil plays an important role in the improvement of swelling behavior. The pH of PCP-Cys was 5. At pH above 3, H^+ ion concentration decreased and the amount of cysteine groups immobilize on polymer increases. This in turn significantly ($p < 0.01$) improved the swelling behavior of thiolated polymer. Papain modified polymer showed less swelling as compared to thiolated polymer due to the absence of thiol moiety. In comparison to PCP, PCP-PAP tablets had improved

swelling behavior and would have a better influence over prolong retention and stability.
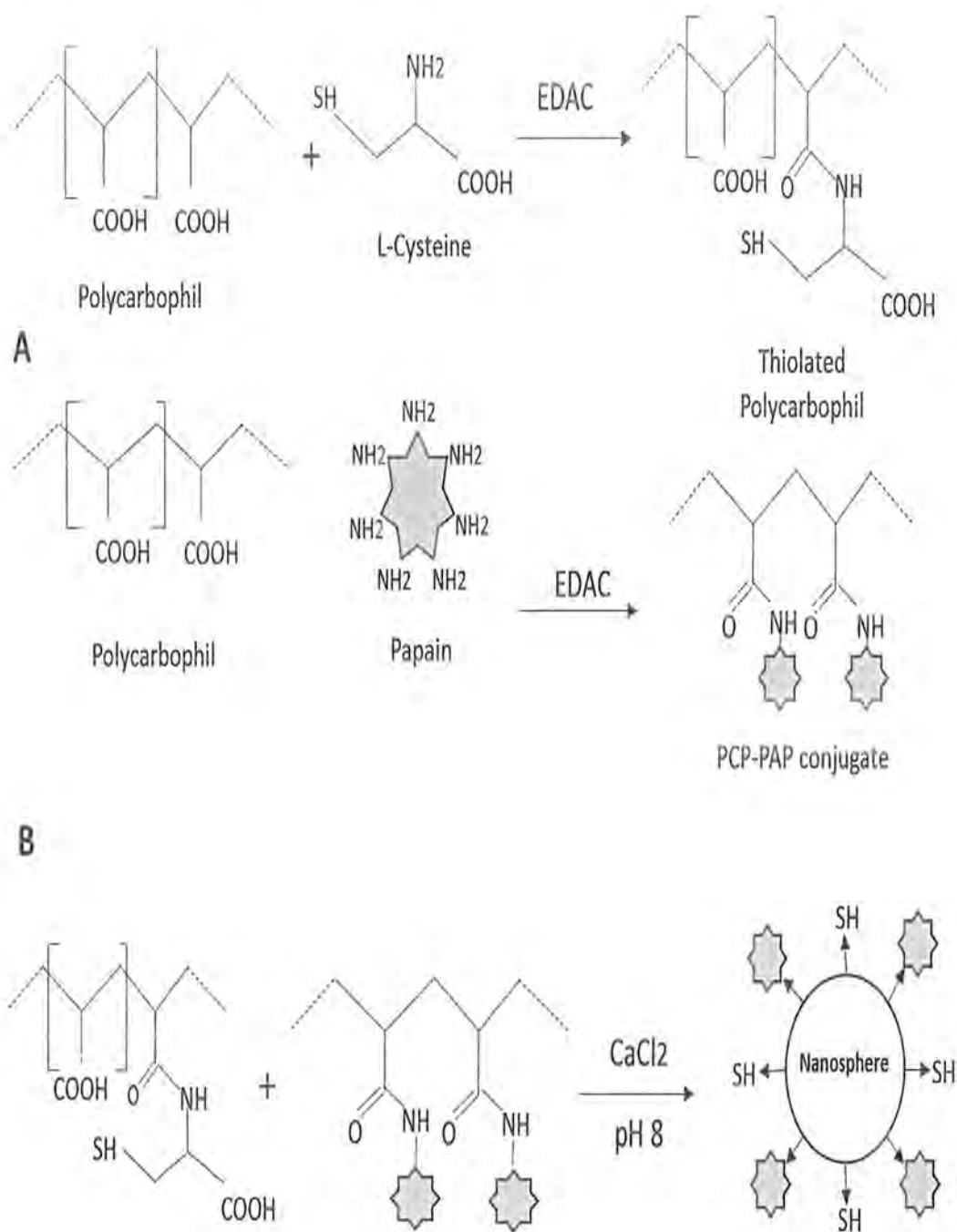
Figure 3.1. Synthetic pathway for the preparation of polymer conjugates and nanoparticles.

Step A represents the synthesis of PCP-Cys conjugate based on covalent attachment of ʟ-cysteine to the backbone of polycarbophil in which amide bond is formed joining COOH of polymer & NH_2 of ʟ-cysteine. A step also presents amide bonding among amino moieties of papain & carboxylic groups of polycarbophil to form PCP-PAP conjugate. Step B refers to the preparation of nanospheres using $CaCl_2$ as crosslinker.
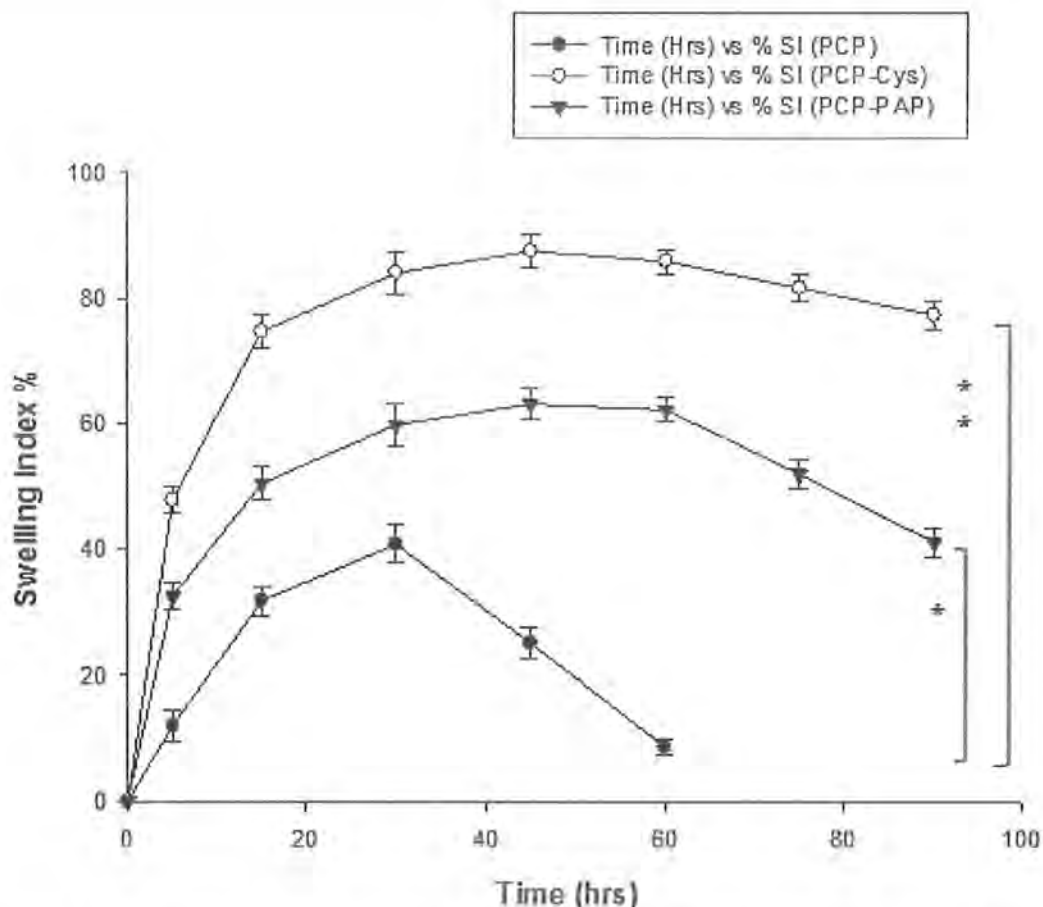
Figure 3.2. Swelling behavior of physical mixtures of polycarbophil conjugates. Listed values are ± standard deviation of means (n = 3).

PCP: Polycarbophil, PCP-Cys: Thiolated polycarbophil, PCP-PAP: Polycarbophil papain conjugate
* $p < 0.05$, ** $p < 0.01$

3.3. Entrapment Efficiency

For the % entrapment efficiency, a standard calibration curve was developed using dilutions as discussed in section 2. Absorbance was determined at 210 nm. Values are given in **Table 3.1**. By using Microsoft Excel 2013, graph was plotted between concentrations and dilutions. The standard calibration curve shown in **Figure 3.3** was utilized to calculate % entrapment efficiency.

3.4. Optimization of Nanoparticles by Design Expert Software

Different variables like polycarbophil (PCP) concentration and concentration of crosslinker ($CaCl_2$) were found to have a significant effect on response variables including entrapment efficiency (% EE), particle size and polydispersity index (PDI) as shown in **Table 3.2**. Actual formulations **Figure 3.4** were prepared according to the runs given by the software. Optimization of nanoparticle formulation was done using

Design Expert Software to select most suitable concentrations of independent variables by central composite design (CCD).

Table 3.1. Concentrations of amoxicillin dilutions and their absorbance

Dilutions	Concentration (µg/ml)	Absorbance
1	0.1	0.0755
2	0.2	0.0865
3	0.3	0.0975
4	0.4	0.1145
5	0.5	0.1225
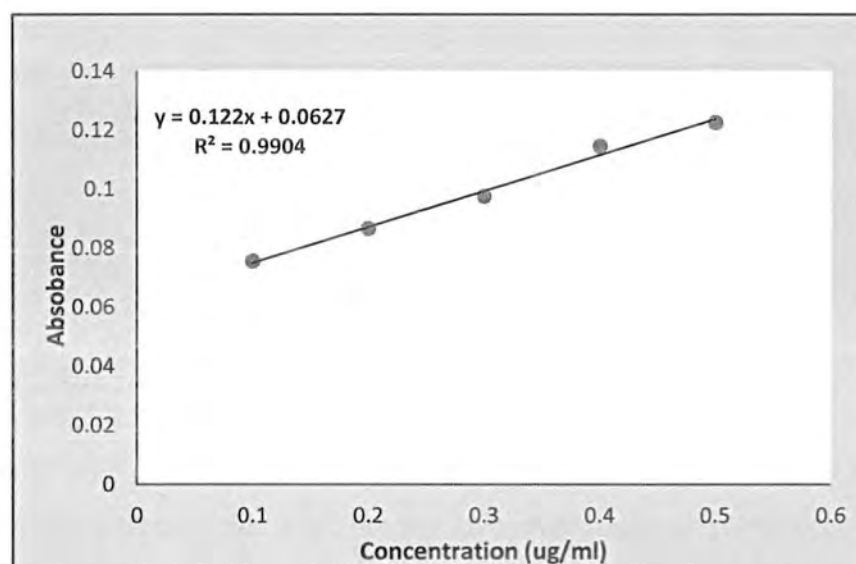
Figure 3.3. Calibration curve of amoxicillin.

Figure 3.4. Actual formulations prepared according to design expert software.

Based on ANOVA, numerical optimization and predictive analysis were done for several formulations that were produced by the software. To confirm the prediction, these formulations were reproduced in given concentrations. Based on the impact of response variables, a point at optimal area was chosen where % entrapment efficiency was maximum and particle size and polydispersity index were minimum. This formulation was considered to be an optimized formulation used for further studies.

Table 3.2. Entrapment Efficiency, particle size and PDI of 9 runs given by software

Runs	Response 1 EE (%)	Response 2 Particle size (nm)	Response 3 PDI
1	85.8	182	0.15
2	83.2	153	0.078
3	88	192	0.17
4	76	99	0.05
5	73.99	135	0.099
6	70	95	0.087
7	86	179	0.18
8	77.89	143	0.070
9	84	111	0.043

EE: Entrapment efficiency, PDI: Polydispersity index

3.4.1. Effect of independent variables on entrapment efficiency (EE)

The results for entrapment efficiency (EE) are given in **Table. 3.2**. The values lies in range of 70 % to 88 %. The values represents the effect of independent factors on percent entrapment efficiency. The graphical representation of influence of individual factor on entrapment efficiency is given in **Figure 3.5.** Whereas the 3D response surface plots are shown in **Figure 3.6.** The quadratic model explains the relation of independent variables and EE response which is:

EE = + 77.71+4.97 * A + 4.20 * B -3.00* A * B + 3.27* A2 + 0.97* B2

The positive sign in polynomial equation shows positive impact of independent variables on response factor. While negative sign indicates negative impact on response

variable. F value is 329.31 and p values is 0.0003. The model was found significant in terms of p-value < 0.01. The "Pred- R" Squared value 0.9798 is close to Adj R-Squared value that is 0.9982. The "Adeq precision" which measures signal to noise ratio is 51.4 greater than 4 implies its desirability. Thus the model can be used to navigate design space.

The polynomial equation clearly shows positive impact of independent variables on response factor. By increasing the concentration of variable: A that is polymer, the % EE increases. Similarly, positive sign with the independent variable: B i.e. $CaCl_2$ also shows positive impact on response factor. That means, by increasing the crosslinker concentration, the % EE increases. Direct association was found between independent variables and response factor (% EE)

Polymer impact on % EE   CaCl2 impact on % EE

Figure 3.5. Effect of individual variable on entrapment efficiency.
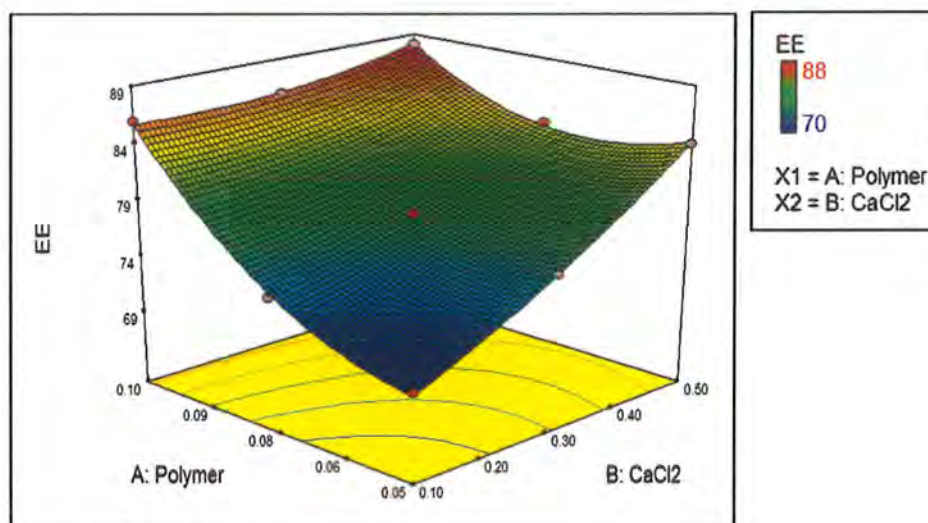
Figure 3.6. Three dimensional response surface plot for impact of independent variable on EE.

45

3.4.2. Effect of independent variables on particle size

The results for particle size are given in **Table. 3.2.** The values lies in range of 95 nm to 182 nm representing the significant effect of independent factors on particle size. The graphical representation of impact of individual factor on particle size is given in **Figure 3.7.** While the 3D response surface plot is shown in **Figure 3.8.** The linear model is used to explain the association of independent factors and response variable which is as follows:

Particle size = + 143.22 + 41.33 * A + 7.83 * B

The positive sign in polynomial equation shows direct association between independent variables and particles. The model F value of 1192.14 and p value < 0.0001 that is less than 0.05 implies the model is significant. The "Pred- R" Squared value 0.9942 is in good agreement with the Adj R-Squared value that is 0.9967. The "Adeq precision" which measures signal to noise ratio is 80.70 that is greater than 4. Thus it indicates sufficient signal due to which model can be used to navigate design space.

The polynomial equation indicates positive sign with experimental parameters showing positive impact on response factor. By increasing the concentration of variable: A that is polymer, the particle size increases. Similarly, positive sign with the independent variable: B i.e. $CaCl_2$ also shows a positive impact on response factor. That means, by increasing the crosslinker concentration, the particles increases but to a mild extent. Direct association was found between independent variables and particle size.

Polymer impact on nanoparticle size
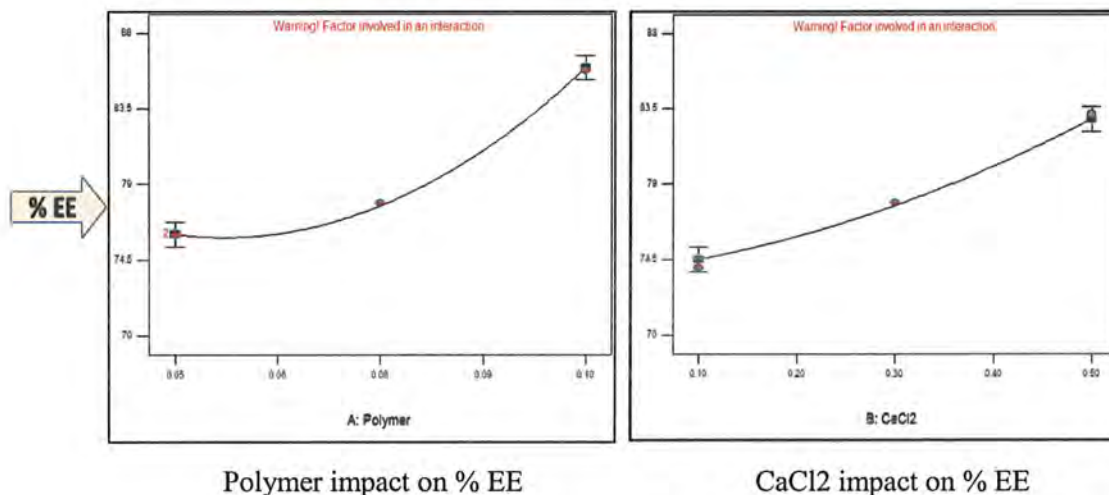
CaCl2 impact on particle size
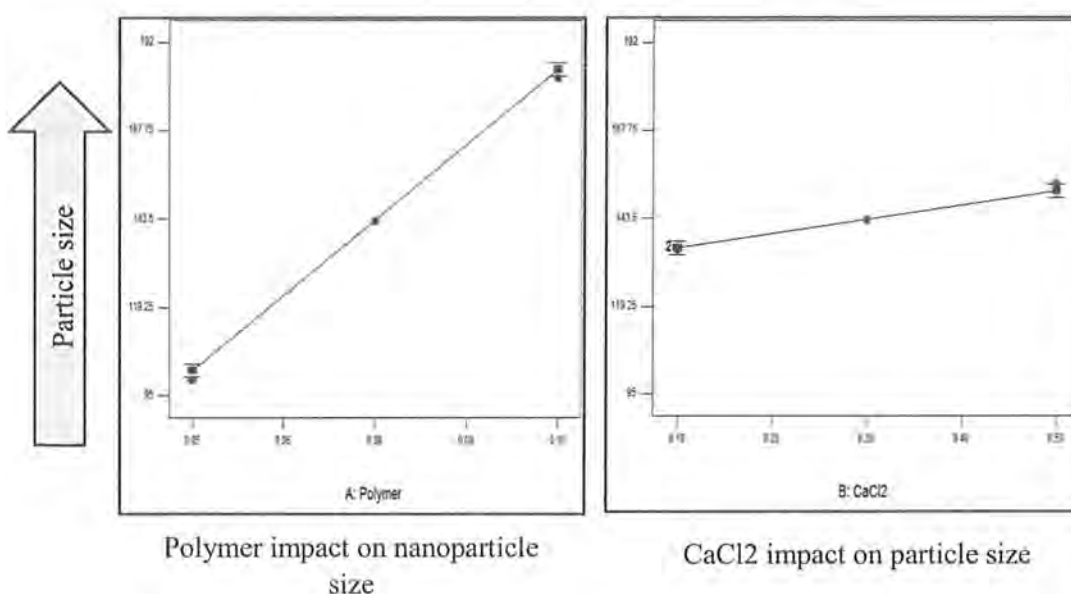
Figure 3.7. Effect if individual variable on particle size.
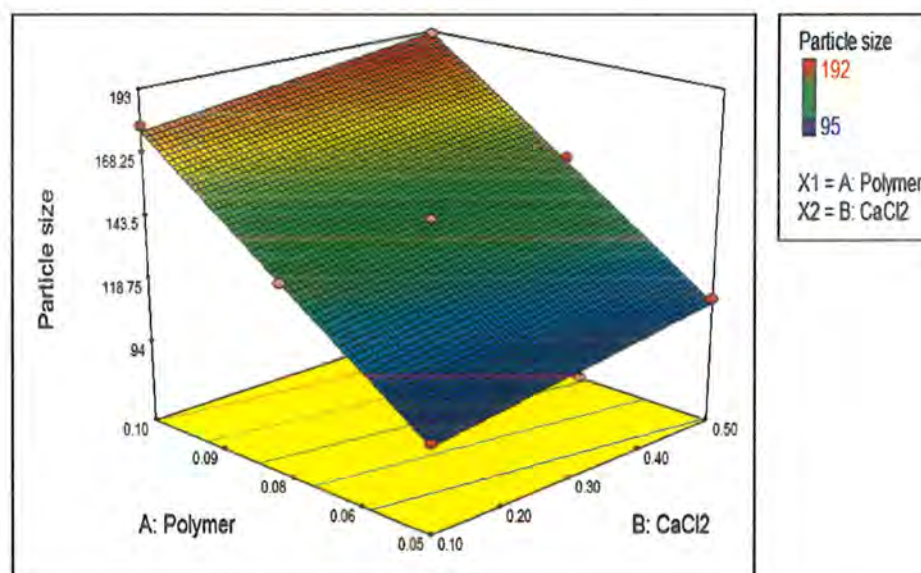
Figure 3.8. Three dimension response surface plot for the impact of independent variable on particle size.

3.4.3. Effect of independent variables on polydispersity index

The results for polydispersity index (PDI) are given in **Table. 3.2**. The values lie in range of 0.043 to 0.18 representing the influence of independent variables on PDI. **Figure 3.9** shows the graphical representation of impact of individual variable on PDI. While the 3D response surface plots are shown in **Figure 3.10**. The quadratic model demonstrates the association of independent factors and response variable as follows:

$$PDI = + 0.069 + 0.053 * A - 0.013 * B + 8.500E{\text -}003 * A * B + 0.031 * A2 + 0.020 * B2$$

The positive sign in polynomial equation shows a synergistic effect between independent variables and PDI while the negative sign indicates a negative impact on response. The model was observed to be significant in term of F value 271.63 and p-value < 0.0004 which is less than 0.05. The "Pred- R" Squared value 0.9734 is in good correspondence with the Adj R-Squared value that is 0.9941. The Adequate precision ratio is 41.0333 (>4) which illustrated an adequate signal to noise ratio. For this reason, model can be used to navigate design space.

The polynomial equation indicates positive sign with variable A and negative with variable B showing a direct and inverse association between independent parameters and PDI. By increasing the concentration of variable: A that is a polymer, the PDI increases. While on the other hand when the concentration of independent variable: B i.e. CaCl$_2$, increases, the PDI decreases. Thus direct relation was observed between

47

polymer concentration and PDI, while inverse association was found between crosslinker concentration and PDI.

Polymer impact on PDI   CaCl₂ impact on % PDI
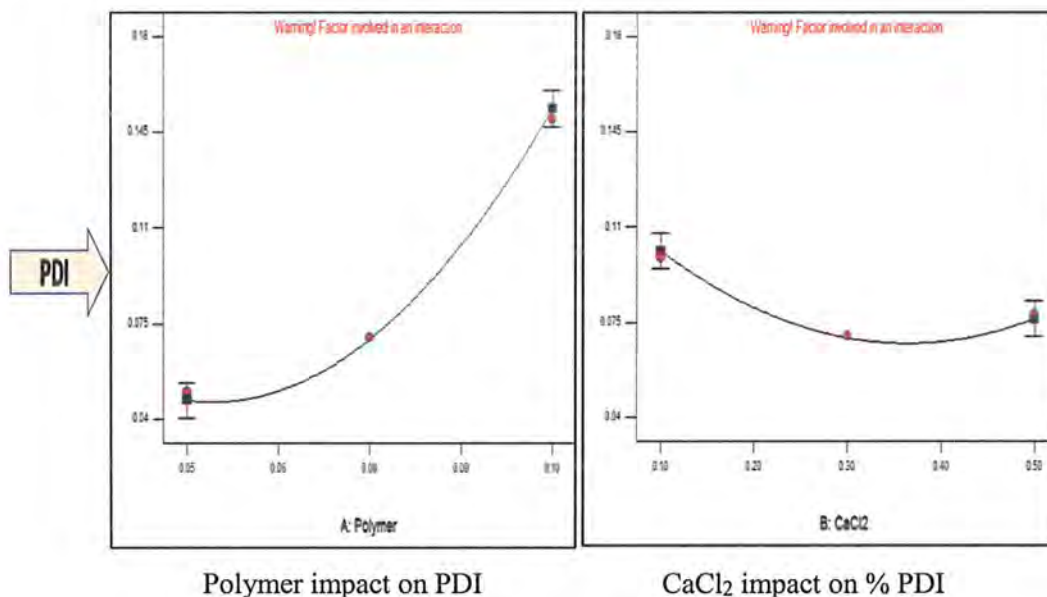
Figure 3.9. Effect if individual variable on polydispersity index.
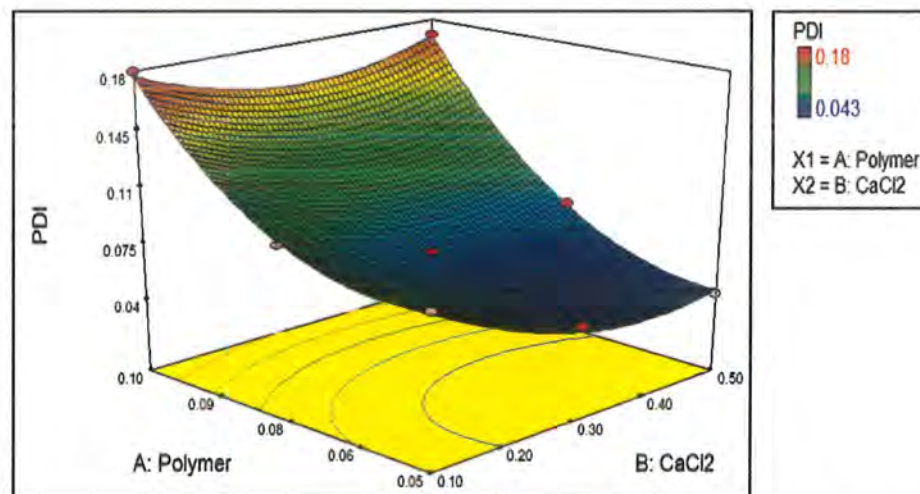
Figure 3.10. Three dimensional response surface plot for the impact of independent variable on Polydispersity index.

3.4.4. Optimization

Numerical optimization and predictive analysis were performed for several formulations that were produced by the software. Based on the impact of response variables, a point at optimal area was chosen where % entrapment efficiency was maximum and particle size and polydispersity index were minimum. Then optimized parameters were predicted on the basis of desirability factor (0.87). These were A: 0.05 % (polymer), B: 0.5 % (CaCl2) with predicted response values of 84 %, 109 nm and

0.045 for % entrapment efficiency, particle size and polydispersity index respectively **Figure 3.11**. The selected optimized formulation was again developed and compared with the predicted results **Table 3.3**. The results indicated that both experimental analysis and predicted values were close to each other, thus favoring the predictability of CCD generated model at nano level.
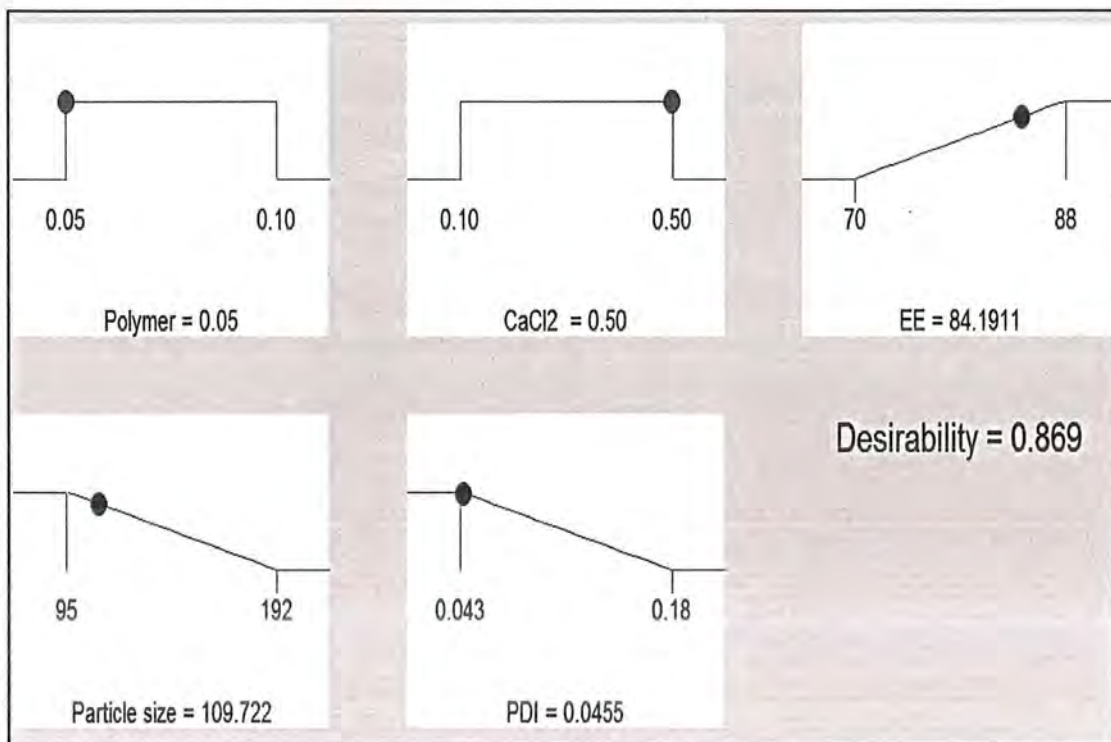
Figure 3.11. Optimized parameters by design expert software.

Table 3.3. Comparison of observed and predicted response values for optimized nanoparticle formulation

Response	Predicted values	Observed values
EE (%)	84	82
Particle size (nm)	109.72	111
PDI	0.045	0.05

EE: Entrapment efficiency, PDI: Polydispersity index

3.5. Development of Optimized Amoxicillin Loaded Polycarbophil Nanoparticles

Amoxicillin loaded Polycarbophil (AM-PCP) nanoparticles were successfully prepared by ionic gelation method based on the optimized values of concentrations for independent variables generated by Design Expert software. The nanoparticles were

developed at a polymer concentration of 0.05 % with crosslinker concentration 0.5 %. Whereas the drug to polymer ratio was fixed at 1:1.

3.6. Synthesis of Optimized Amoxicillin Loaded thiolated and Papain modified Polycarbophil Nanoparticles

After optimization of AM-PCP nanoparticles at nanoscale, amoxicillin loaded PCP-Cys, PCP-PAP and PCP-Cys-PAP nanoparticles, were produced by the same ionic gelation procedure. To obtain the lowest size AM-PCP-PAP and AM-PCP-Cys-PAP nanoparticles **Figure 3.1 (B)** a ratio of 1:2 was used for polymer to papain. The thiol and papain modifications were confirmed by FTIR results and physicochemical properties. The zeta sizer analysis of optimized AM-PCP, AM loaded PCP-Cys, PCP-PAP and PCP-Cys-PAP nanoparticles are given in the following figures:

AM-PCP Nanoparticles	
Size	111.9 nm
PDI	0.275
Zeta potential	-17.2

Figure 3.12 Zeta sizer results of amoxicillin loaded polycarbophil (AM-PCP) nanoparticles.

Figure 3.13 (a). Zeta sizer results of amoxicillin loaded thiolated polycarbophil (AM-PCP-Cys) nanoparticles showing average size and PDI.

Results

			Mean (mV)	Area (%)	St Dev (mV)
Zeta Potential (mV):	-16.2	Peak 1:	-16.2	100.0	5.78
Zeta Deviation (mV):	5.78	Peak 2:	0.00	0.0	0.00
Conductivity (mS/cm):	0.367	Peak 3:	0.00	0.0	0.00

Zeta Potential Distribution
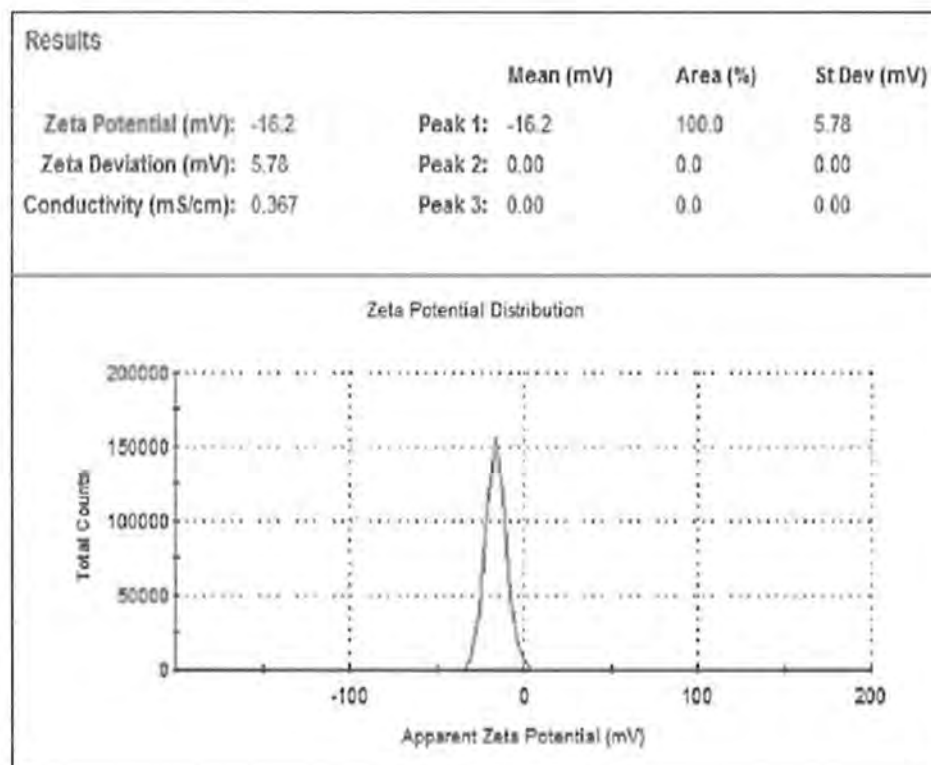
Figure 3.13 (b). Zeta sizer results of amoxicillin loaded thiolated polycarbophil (AM-PCP-Cys) nanoparticles showing zeta potential.

Results

			Size (d.nm):	% Intensity:	St Dev (d.n...
Z-Average (d.nm):	274.8	Peak 1:	350.0	100.0	129.8
PdI:	0.207	Peak 2:	0.000	0.0	0.000
Intercept:	0.944	Peak 3:	0.000	0.0	0.000

Size Distribution by Intensity
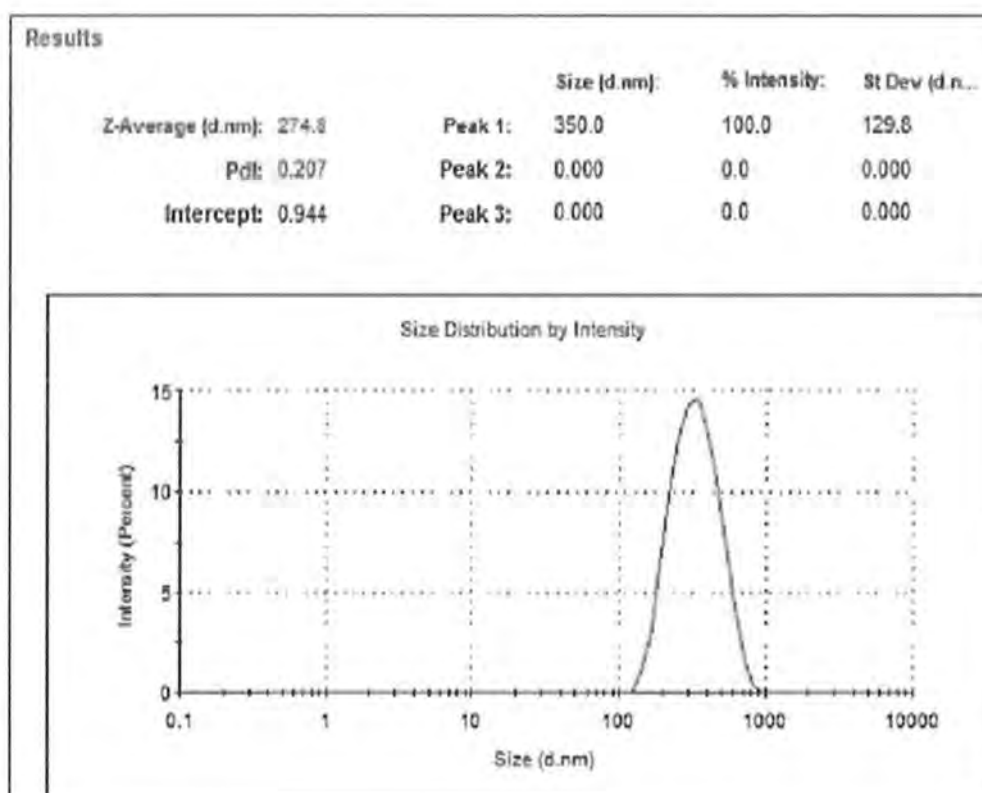
Figure 3.14 (a). Zeta sizer results of amoxicillin loaded papain modified polycarbophil (AM-PCP-PAP) nanoparticles showing average size and PDI.

Results

	Mean (mV)	Area (%)	St Dev (mV)
Zeta Potential (mV): -14.0	Peak 1: -14.0	100.0	5.43
Zeta Deviation (mV): 5.43	Peak 2: 0.00	0.0	0.00
Conductivity (mS/cm): 0.655	Peak 3: 0.00	0.0	0.00

Zeta Potential Distribution
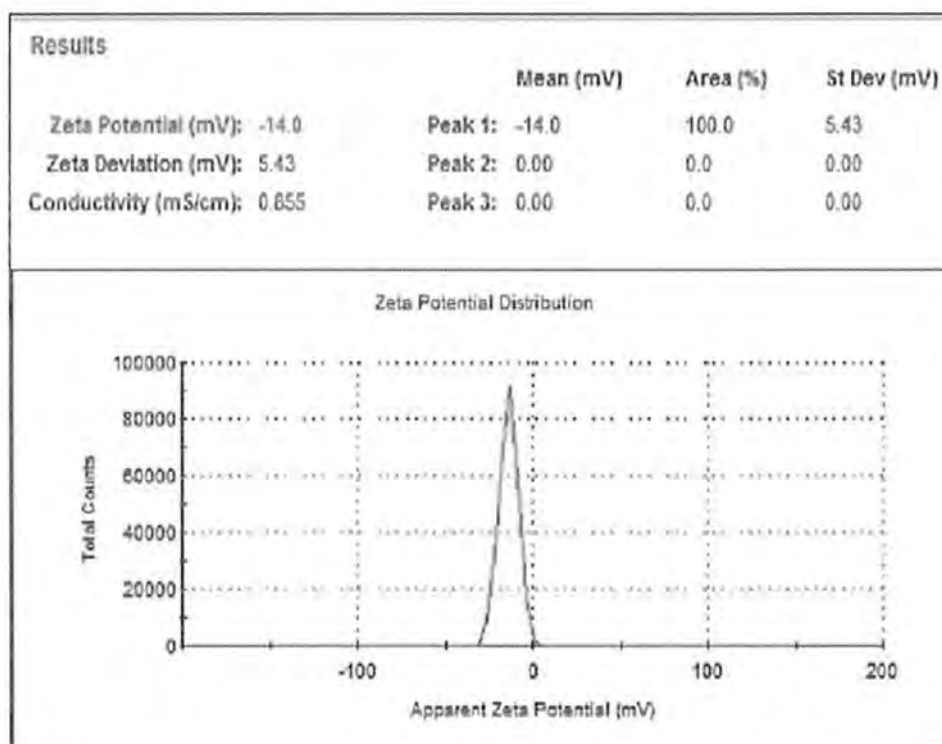
Figure 3.14 (b). Zeta sizer results of amoxicillin loaded papain modified polycarbophil (AM-PCP-PAP) nanoparticles showing zeta potential.

Results

	Size (d.nm):	% Intensity:	St Dev (d.n...
Z-Average (d.nm): 288.8	Peak 1: 394.0	86.4	162.3
Pdi: 0.409	Peak 2: 64.15	10.5	13.79
Intercept: 0.921	Peak 3: 5202	3.1	474.2

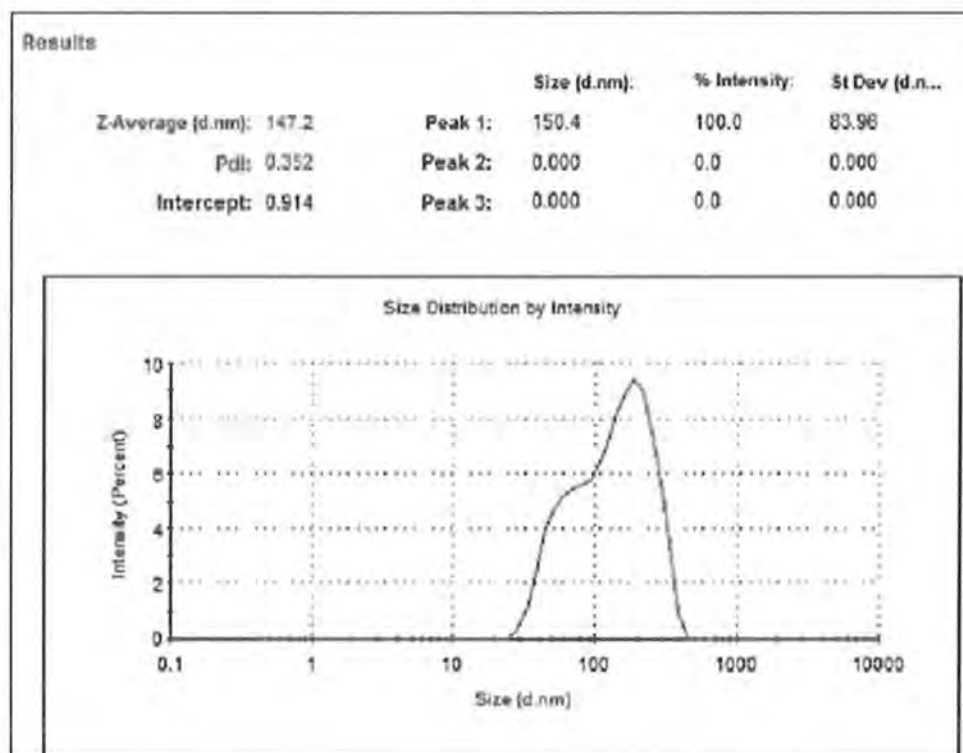Size Distribution by Intensity
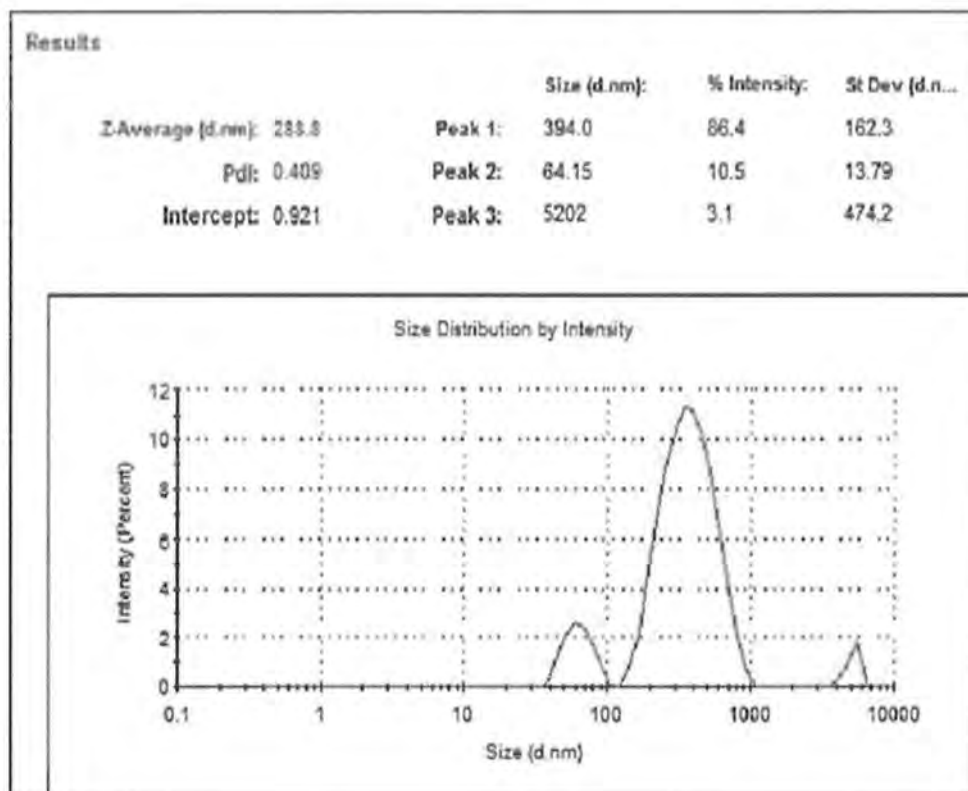
Figure 3.15 (a). Zeta sizer results of amoxicillin loaded papain modified thiolated polycarbophil (AM-PCP-Cys-PAP) nanoparticles showing average size and PDI.

Results

		Mean (mV)	Area (%)	St Dev (mV)
Zeta Potential (mV): -13.2	Peak 1: -13.2	100.0	5.78
Zeta Deviation (mV): 5.78	Peak 2: 0.00	0.0	0.00
Conductivity (mS/cm): 0.837	Peak 3: 0.00	0.0	0.00

Zeta Potential Distribution
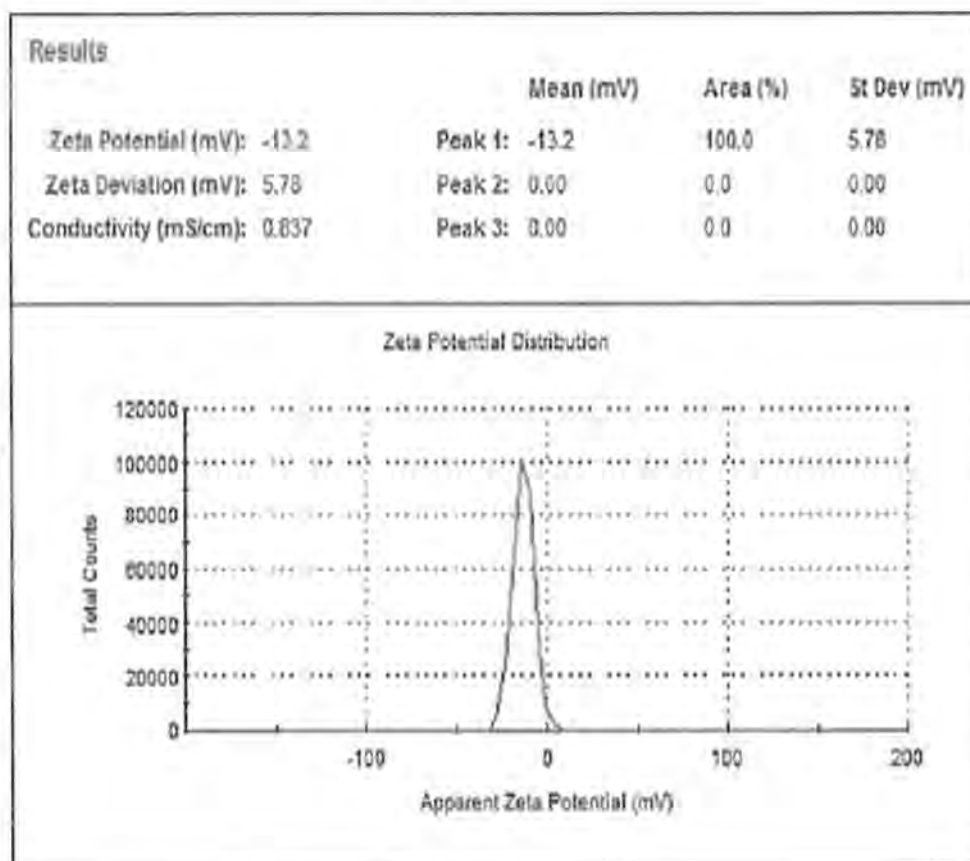
Figure 3.15 (b). Zeta sizer results of amoxicillin loaded papain modified thiolated polycarbophil (AM-PCP-Cys-PAP) nanoparticles showing zeta potential.

3.7. Physicochemical Properties and Morphology of Nanoparticles

Physicochemical properties of nanoparticles including particle size, encapsulation efficiency, polydispersity index and zeta potential are listed in **Table 3.4**. All the formulations showed particle size in the range of 111 nm to 288 nm with negative zeta potential due to carboxylic groups of polycarbophil. Unmodified nanoparticles displayed lowest particle size and highest negative zeta potential. Whereas thiolated and papain modified nanoparticles resulted in increased particle size. Also, the negative zeta potential was reduced with thiolation and papain modification. All the nanoparticles had uniform size distribution as the PDI was determined to be less than 0.45. The % entrapment efficiency (EE) also did not decrease to a greater extent with enzyme modification. Scanning electron microscopic (SEM) analysis was performed to confirm the shape and size of nanoparticle formulation. As shown in **Figure 3.16**, the nanoparticle formulations of modified and un-modified polymer displayed spherical shape and particle size < 400 nm. Particle size increased due to attachment of thiol groups to the polymer backbone. The size further increased when modified with papain.

53

Table 3.4. Physicochemical characterization including particle size, encapsulation efficiency, polydispersity index and zeta potential of optimized amoxicillin loaded polycarbophil nanoparticles.

Amoxicillin loaded Formulations	Particle size (nm)	EE (%)	PDI	Zeta potential (mV)
AM-PCP	111.9	82.9 ± 11.68	0.27	-17.2
AM-PCP-Cys	147	80.7 ± 6.27	0.35	-16.2
AM-PCP-PAP	274	84.33 ± 9.39	0.207	-14
AM-PCP-Cys-PAP	288	78.76 ± 7.68	0.40	-13.2

EE: Entrapment efficiency, PDI: Polydispersity index

AM: Amoxicillin, AM-PCP: Amoxicillin loaded polycarbophil nanoparticles, AM-PCP-Cys: Amoxicillin loaded thiolated polycarbophil nanoparticles, AM-PCP-PAP: Amoxicillin loaded papain modified polycarbophil nanoparticles, AM-PCP-Cys-PAP: Amoxicillin loaded papain modified thiolated polycarbophil nanoparticles.

Figure 3.16. Scanning electron micrographs of amoxicillin loaded **(A)** polycarbophil **(B)** polycarbophil-cys **(C)** polycarbophil-papain and **(D)** polycarbophil-cys-papain nanoparticles.

3.8. FTIR Results

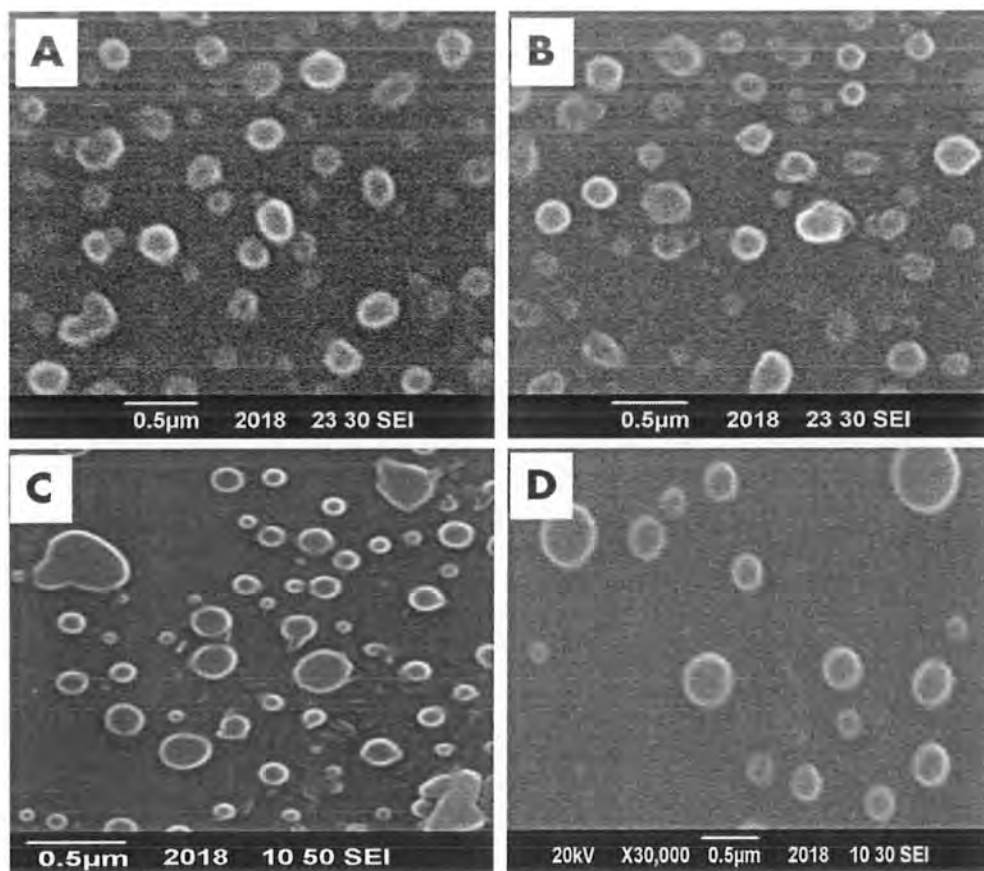FTIR analysis of drug, polymer, enzyme, polymer conjugates and amoxicillin loaded papain modified thiolated polycarbophil (AM-PCP-Cys-PAP) nanoparticle formulation was performed and the results are shown in **Figure 3.17.** The conjugation of cysteine group and papain on polycarbophil backbone was confirmed by FTIR analysis as shown. The pure polycarbophil showed an intense peak at 1709 cm^{-1} which confirmed the presence of carboxylic groups in the structure of polymer. CH vibrations were present at 1414 cm^{-1}. In case of PCP-Cys, the stretching peaks at 2889 cm^{-1} represent the SH groups of cysteine on polymer backbone. Amide band stretching peak at 1636 cm^{-1} and amide band incline at 1557 cm^{-1} was found in the spectrum of PCP-Cys conjugate that confirms the formation of amide bond in thiomer structure. In case of papain spectrum, the peak at 3276 cm^{-1} and 1632 cm^{-1} refer to NH stretch and C=O stretch of the enzyme. The additional peaks in the spectrum of PCP-PAP conjugate at 1537 and 1452 cm^{-1} were assigned to the amide bond which clearly indicates that papain was successfully fixed on polymeric backbone.

The IR spectra of pure drug and final nanoparticle formulation is shown in **Figure 3.17.** Pure amoxicillin shows C=O stretching peak at 1575 cm^{-1} while the peaks at 3031 cm^{-1} and 2967 cm^{-1} represent NH and OH. The bands at 650-1100 cm^{-1} refer to CH aromatic ring. These characteristics peaks of drug were observed in IR spectrum of final nanoparticle formulation (AM-PCP-Cys-PAP) indicating the successful entrapment of drug. Characteristics peaks of PCP-Cys and papain were present in final nanoparticle formulation. No interaction was found between drug and polymer conjugates.

3.9. *In-vitro* Drug Release Studies

3.9.1. Calibration curve of amoxicillin in phosphate buffer (pH 6.8)

Calibration curve of amoxicillin was developed using different concentrations of amoxicillin in phosphate buffer (pH 6.8). The descriptive procedure is given in section 2. **Table 3.5** shows the concentrations of different dilutions and their respective absorbance. Calibration curve of amoxicillin in phosphate buffer (pH 6.8) is shown in **Figure 3.18**.

The calibration curve shows the linearity, accuracy and precision of the validation method. Concentration values are displayed on x-axis while values at y-axis shows their respective absorbance. Absorbance was determined at 240 nm wavelength.
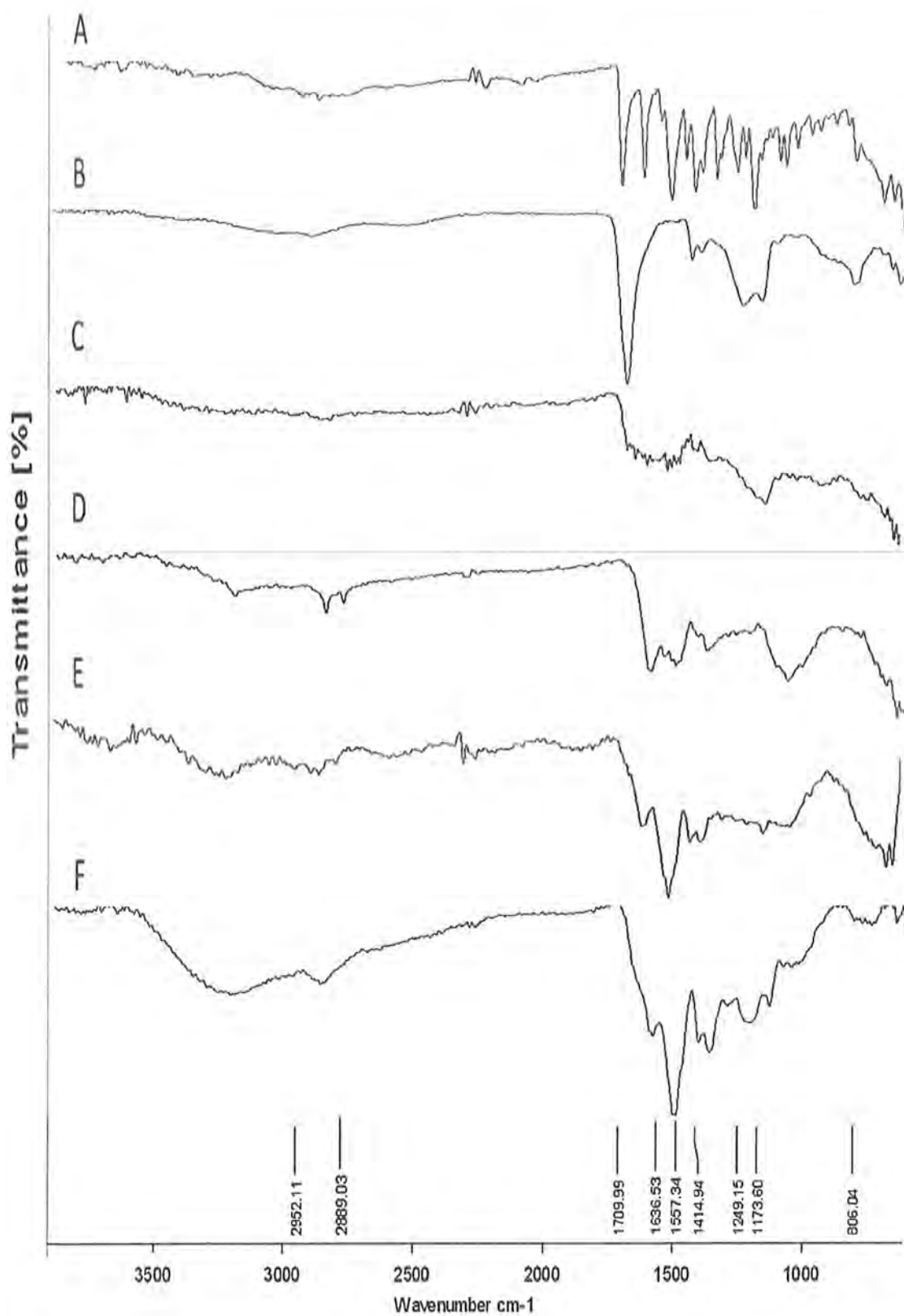
Figure 3.17. FTIR spectra of amoxicillin (A), polycarbophil (B), thiolated polycarbophil (C), papain (D), polycarbophil-papain conjugate (E) and amoxicillin loaded polycarbophil-cys-papain nanoparticles.

Table 3.5. Concentrations and absorbance of amoxicillin dilutions in phosphate buffer pH 6.8

Dilutions	Concentration (µg/ml)	Absorbance
1	2	0.21
2	4	0.42
3	6	0.58
4	8	0.76
5	10	0.966
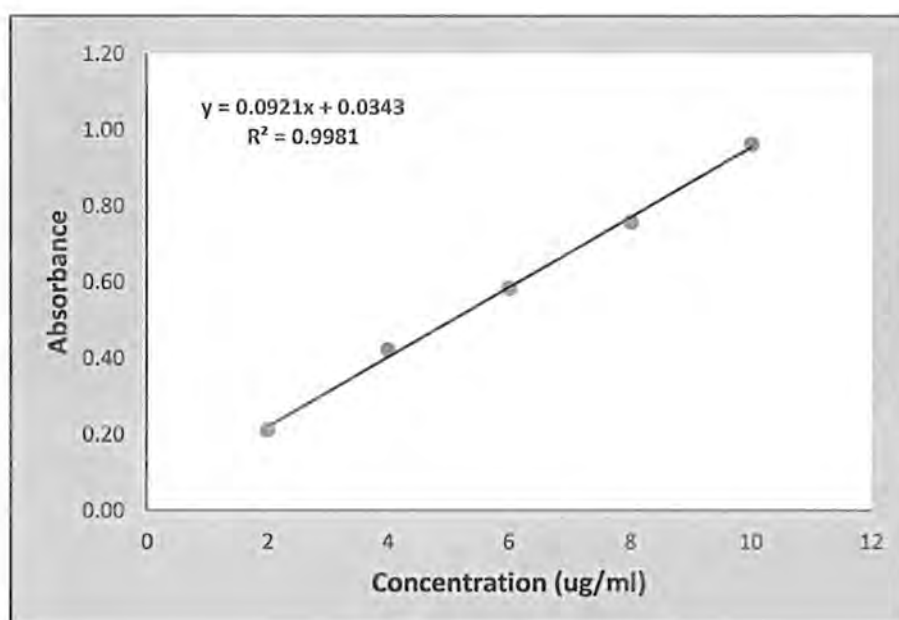
Figure 3.18. Calibration curve of amoxicillin in phosphate buffer (pH 6.8).

3.9.2. Drug release profile

Amoxicillin *in vitro* release from amoxicillin suspension and AM-PCP, AM-PCP-Cys, AM-PCP-PAP, AM-PCP-Cys-PAP nanoparticles was evaluated for 48 hours at pH 6.8 by sink condition dialysis membrane method. Percent release of amoxicillin from various formulations was determined in time-dependent manner **Figure 3.19**. The nanoformulation indicated two phase release behavior. There was a little outburst in first phase followed by a sustained release pattern. AM-PCP showed higher release rate with burst release of 35 % in first 2 hours in comparison to thiomer and papain modified nanoparticles. The reason for this can be the weak interaction of polymer to the drug. The cumulative release for AM-PCP was found to be 94 % within 24 hours. While AM-PCP-Cys, AM-PCP-PAP, and AM-PCP-Cys-PAP nanoparticles showed cumulative release of 63 % 87 % and 70 % respectively in 48 hours.

Various release kinetic models were applied to AM release data from AM suspension, AM-PCP, AM-PCP-Cys, AM-PCP-PAP, AM-PCP-Cys-PAP nanoparticles. Models of kinetic included first and zero order, korsmeyer peppas, higuchi & hixson-crowell. The results for these models are shown in **Table 3.6.** In case of AM-PCP nanoparticles, the release followed First-order kinetics behavior on the basis of R^2 value while AM-PCP-Cys, AM-PCP-PAP and AM-PCP-Cys-PAP showed Higuchi model suggesting matrix diffusion controlled mechanism.
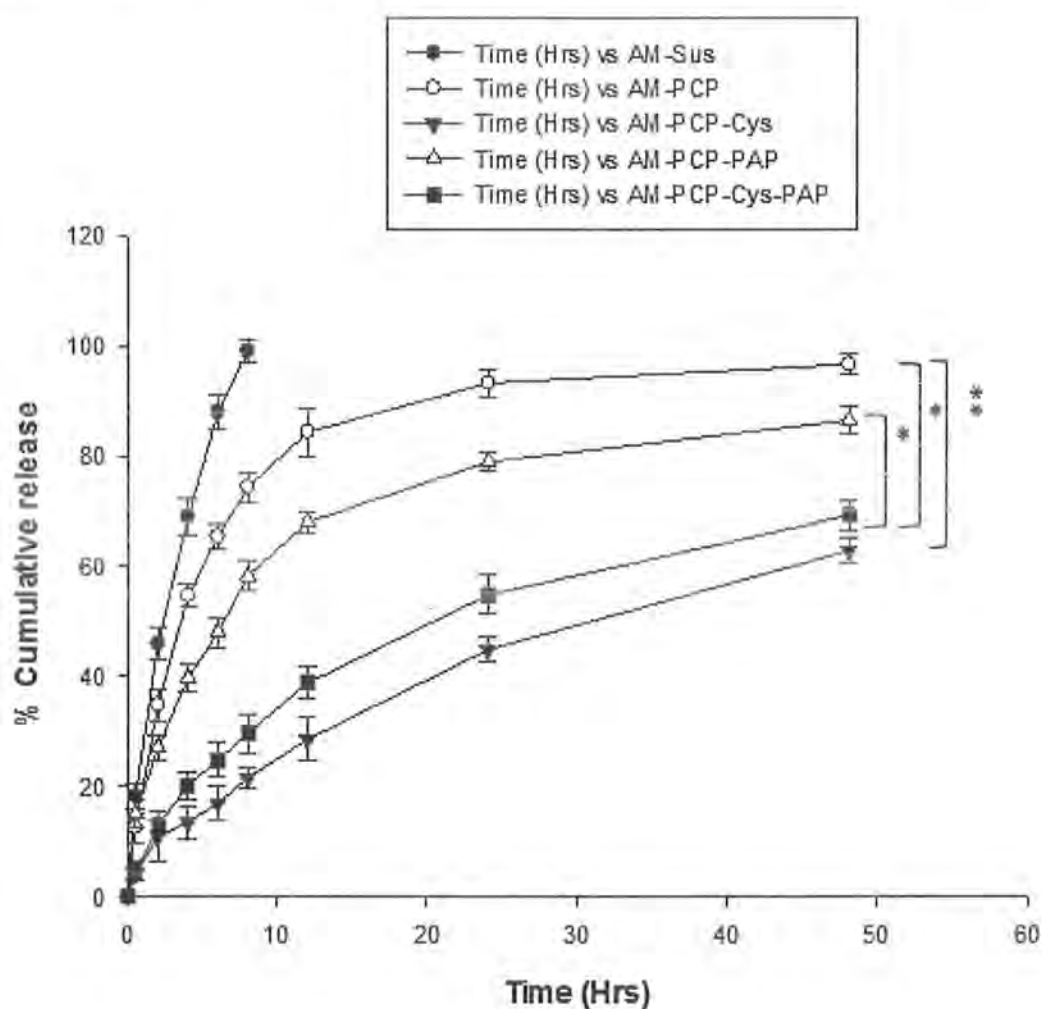
Figure 3.19. Amoxicillin in vitro release from pure suspension, from amoxicillin loaded unmodified and modified polycarbophil nanoparticles by dialysis tube method in phosphate buffer (pH 6.8) for 48 hours. The values are listed as ± standard deviation of means (n = 3).

AM: Amoxicillin, AM-PCP: Amoxicillin loaded polycarbophil nanoparticles, AM-PCP-Cys: Amoxicillin loaded thiolated polycarbophil nanoparticles, AM-PCP-PAP: Amoxicillin loaded papain modified polycarbophil nanoparticles, AM-PCP-Cys-PAP: Amoxicillin loaded papain modified thiolated polycarbophil nanoparticles.

* $p < 0.05$, ** $p < 0.01$

Table 3.6. Amoxicillin kinetic models to determine the mechanism of drug release from nanoparticles at pH 6.8

Amoxicillin loaded Formulations	Zero order	First order	Higuchi	Kors' Peppas	Hixson Croswell
AM-PCP-Cys-PAP	0.9572	0.9812	0.9904	0.7123	0.9742
AM-PCP-Cys	0.9558	0.972	0.9837	0.7008	0.967
AM-PCP-PAP	0.9149	0.9811	0.9978	0.5043	0.9644
AM-PCP	0.8814	0.9895	0.9883	0.5639	0.9637

AM: Amoxicillin, AM-PCP: Amoxicillin loaded polycarbophil nanoparticles, AM-PCP-Cys: Amoxicillin loaded thiolated polycarbophil nanoparticles, AM-PCP-PAP: Amoxicillin loaded papain modified polycarbophil nanoparticles, AM-PCP-Cys-PAP: Amoxicillin loaded papain modified thiolated polycarbophil nanoparticles.

3.10. Stability in 0.1 N HCl (pH 1.2)

Stability of pure amoxicillin and newly developed amoxicillin loaded papain modified thiolated polycarbophil (PCP-Cys-PAP) nanoparticles was evaluated in 0.1 N HCl with a pH of 1.2. This medium is used for drug release from delivery systems without enteric coating. Results are shown in **Figure 3.20**. Pure amoxicillin showed 36 ± 3 % degradation within 6 hours in acidic medium. On the other hand, when amoxicillin was loaded in newly developed papain modified thiolated polycarbophil nanoparticles, the stability was significantly ($p < 0.01$) improved. AM-PCP-Cys-PAP nanoparticles displayed 6.7 ± 2 %, 7.9 ± 1.05 % and 8.2 ± 1.05 % degradation in 2, 4 and 6 hours respectively.

3.11. Mucoadhesion Study via Rheological Investigation

To determine the mucoadhesion behavior of nanoparticles, rheological study was carried out by cone-plate viscometer using artificial mucin. The results are shown in **Figure 3.21**. A significant ($p < 0.05$) decrease in viscosity was found for AM-PCP-PAP nanoparticles in 6 hours as compared to unmodified formulation. This shows the high impact of enzyme in cleavage of mucus glycoproteins which reduced the viscosity. On the other hand, the viscosity increased 1.5 folds for AM-PCP-Cys nanoparticles

after 6 hours incubation with mucin showing the positive impact of thiomer on mucoadhesive behavior. The viscosity of unmodified formulation (AM-PCP) also increased to certain limit in 6 hours. The results for final formulation (AM-PCP-Cys-PAP) was between the values of AM-PCP-PAP and AM-PCP-Cys nanoparticles. The viscosity for AM-PCP-Cys-PAP was found to be 4.1 Pa.s that is exactly between AM-PCP-PAP and AM-PCP-Cys nanoparticles viscosity (0.1 and 6.0 Pa.s respectively). The results showed that AM-PCP-Cys-PAP nanoparticles improved the viscosity as compared to unmodified nanoformulation due to the presence of thiol moiety on PCP structure. Nevertheless, due to the presence of papain in AM-PCP-Cys-PAP nanoparticles the rheological parameter was not up to extent of AM-PCP-Cys nanoparticles. Therefore the AM-PCP-Cys-PAP nanoparticles can be categorized as mucoadhesive and mucopenetrating.
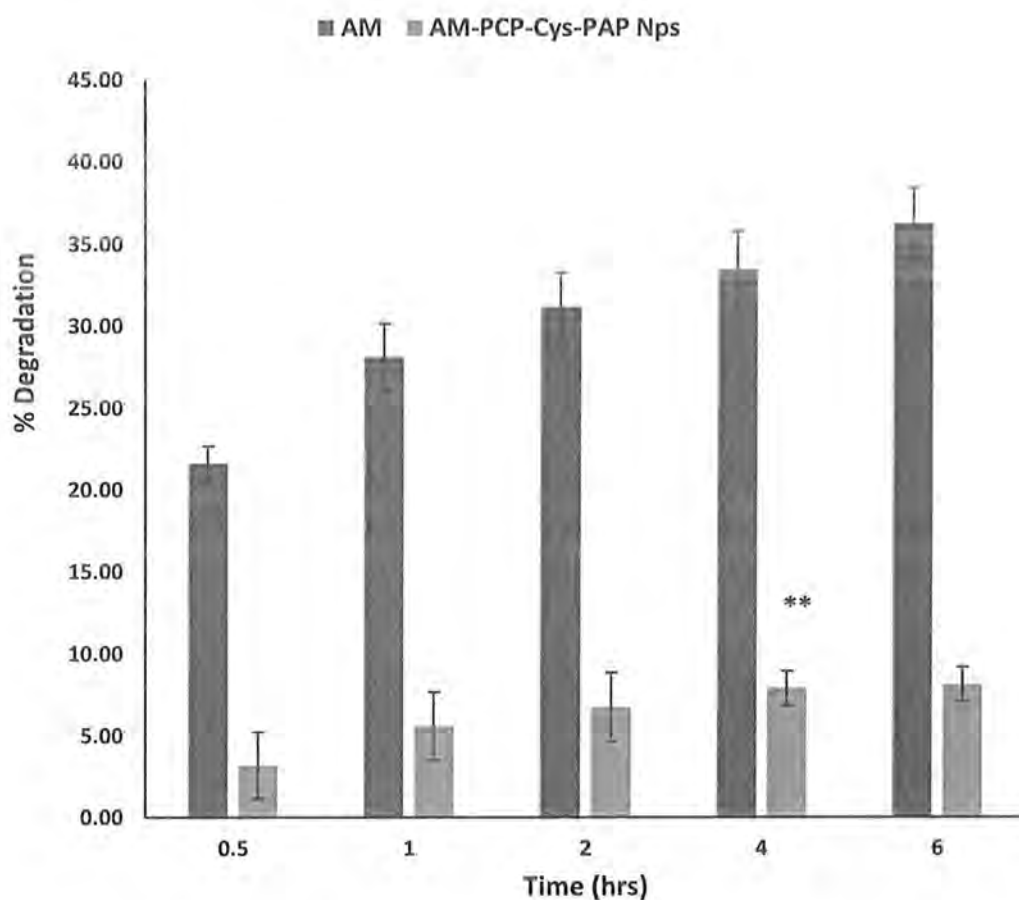
Figure 3.20. Stability comparison of pure amoxicillin vs amoxicillin loaded papain modified thiolated polycarbophil (AM-PCP-Cys-PAP) nanoparticles in 0.1 N HCl (pH 1.2) for 6 hours. Values are indicated as means ± standard deviation (n = 3).

AM-PCP-Cys-PAP: Amoxicillin loaded papain modified thiolated polycarbophil nanoparticles.
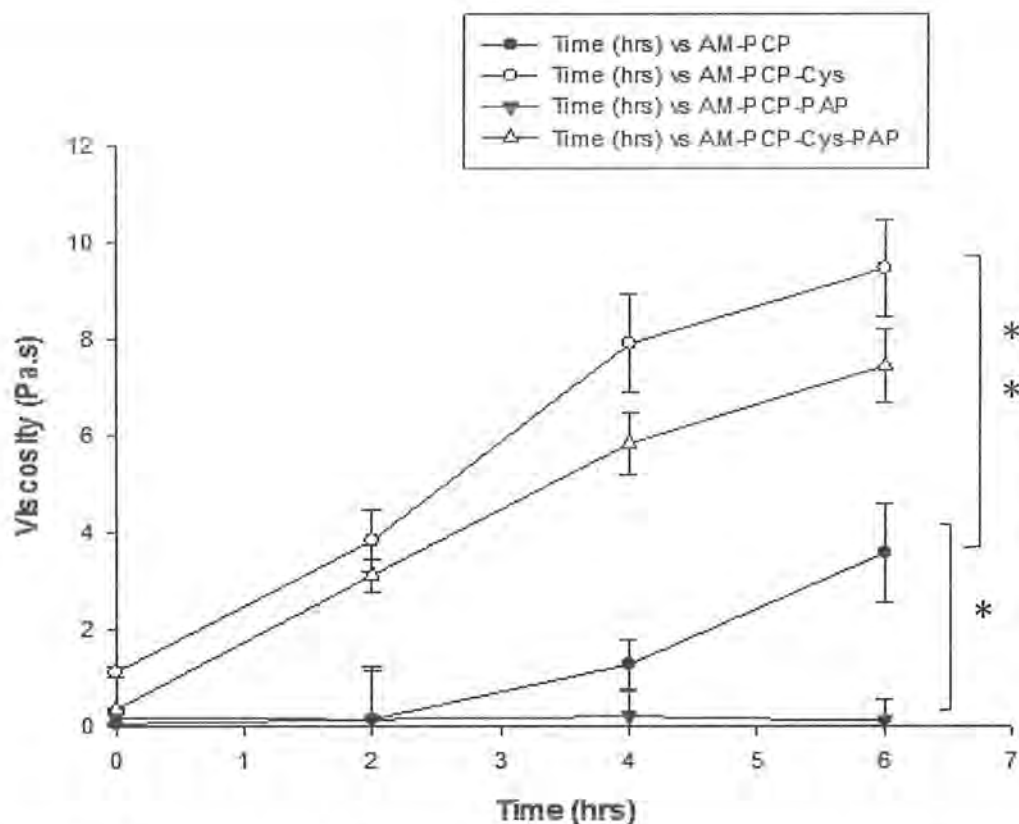
Figure 3.21. Rheological study of nanoparticles regarding mucopenetration and mucoadhesion activity. Values are indicated as means ± standard deviation (n = 3).

AM-PCP: Amoxicillin loaded polycarbophil nanoparticles, AM-PCP-Cys: Amoxicillin loaded thiolated polycarbophil nanoparticles, AM-PCP-PAP: Amoxicillin loaded papain modified polycarbophil nanoparticles, AM-PCP-Cys-PAP: Amoxicillin loaded papain modified thiolated polycarbophil nanoparticles.

* $p < 0.05$, ** $p < 0.01$

3.12. Exvivo Study

3.12.1. Calibration curve of fluorescein diacetate (FDA)

Calibration curve of FDA was prepared in acetone and NaOH using different concentrations. Concentrations of dilutions and their respective absorbance are given in **Table 3.7**. **Figure 3.23** shows the calibration curve of FDA at 490 nm wavelength.

3.12.2. Quantification of FDA in nanoparticles

Nanoparticles were labeled with FDA for diffusion/penetration study. It is a lipophilic dye. After incorporation, it retains in nanoparticles through temporary attachment. The FDA content was found to be 71% in AM-PCP, 52 % in AM-PCP-Cys, 49 % in AM-PCP-PAP and 45 % AM-PCP-Cys-PAP nanoparticles as shown in **Table 3.8.** This shows the dye was successfully loaded in nanoparticles.

Table 3.7. Concentrations of fluorescein diacetate (FDA) dilutions and their absorbance

Dilutions	Concentration (µg/ml)	Absorbance
1	0.6	0.005
2	2	0.009
3	6	0.021
4	10	0.037
5	14	0.051

$y = 0.0035x + 0.002$
$R^2 = 0.997$
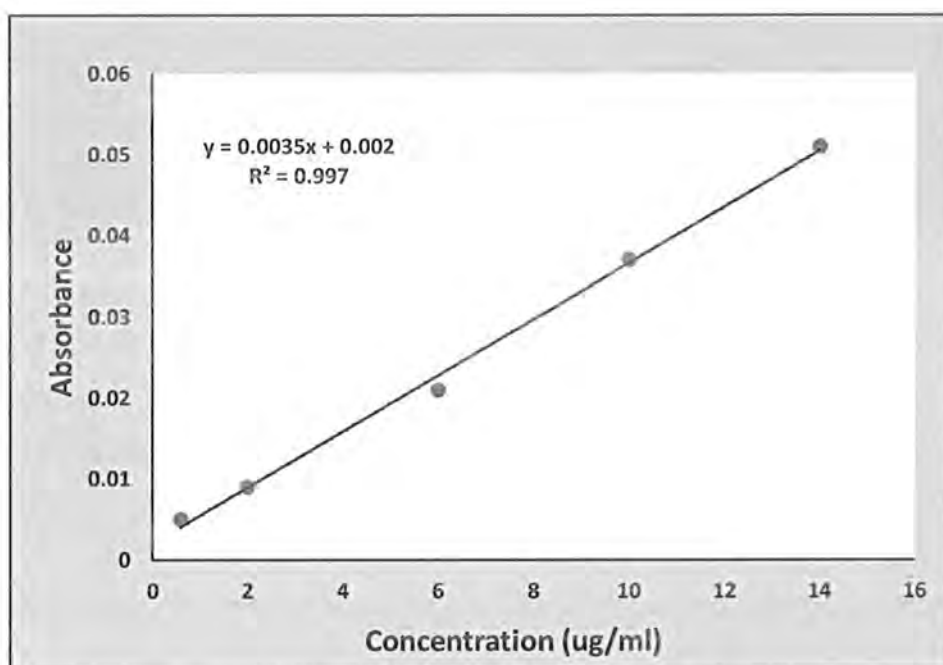
Figure 3.23. Calibration curve of fluorescein diacetate (FDA).

3.12.3. Permeation study via silicon tube method

Permeation studies were conducted on freshly isolated mucus using silicon tube method with little modification. The results for permeation studies are shown in **Figure 3.24**. AM-PCP-PAP nanoparticles showed deep mucus penetration up to the last segment 16 that is equal to 34 mm. The percent particle penetration for these nanoparticles was 11 % in the last segment. AM-PCP-Cys-PAP were found to have lower detection values in last segments 14-16 than AM-PCP-PAP nanoparticles. The reason for this can be the presence of thiol groups that reduced the penetration capacity of nanoparticles.

However, % particles penetration in 1-6 segments for AM-PCP-Cys-PAP nanoparticles was higher than AM-PCP-PAP. Very lower detection values in 11-16 segments were observed for AM-PCP-Cys and AM-PCP nanoparticles. This shows significant ($p <$ 0.01) influence of papain modification over permeation enhancement by cleavage of mucus glycoproteins.

Table 3.8. Comparison of optimized amoxicillin loaded nanoparticles for percent FDA load. Values represent ± standard deviation of means (n = 3)

AM loaded Formulations	Loaded FDA (%)
AM-PCP	71
AM-PCP-Cys	52
AM-PCP-PAP	49
AM-PCP-Cys-PAP	45

FDA: Fluorescein diacetate, AM: Amoxicillin, AM-PCP: Amoxicillin loaded polycarbophil nanoparticles, AM-PCP-Cys: Amoxicillin loaded thiolated polycarbophil nanoparticles, AM-PCP-PAP: Amoxicillin loaded papain modified polycarbophil nanoparticles, AM-PCP-Cys-PAP: Amoxicillin loaded papain modified thiolated polycarbophil nanoparticles.

Mucoglycoproteins cleavage activity is absent in AM-PCP-Cys and AM-PCP nanoparticles which resulted in lower diffusion to the deepest segments. Considering segment 2-8, higher detection values were observed for AM-PCP-Cys nanoparticles as compared to AM-PCP nanoparticles with 2 folds lower mucoadhesive property. Thus thiolated nanoparticles displayed significantly ($p < 0.001$) higher mucoadhesive behavior than non-thiolated nanoparticles. The results of AM-PCP-Cys and AM-PCP-Cys-PAP in segment 2-8 were close to each other regarding mucoadhesive properties. Thus AM-PCP-Cys-PAP nanoparticles are mucoadhesive as well as mucopermeating.

3.13. *In-vitro* Efficacy

3.13.1. Culture of *H.pylori* bacteria

The *H.pylori* strains taken from biopsy samples were successfully grown over chocolate agar by streaking method. Microaerophilic conditions were maintain during the growth of bacteria. The colonies were identified by morphology of bacteria. The successful growth of bacteria over chocolate agar medium was visually observed.
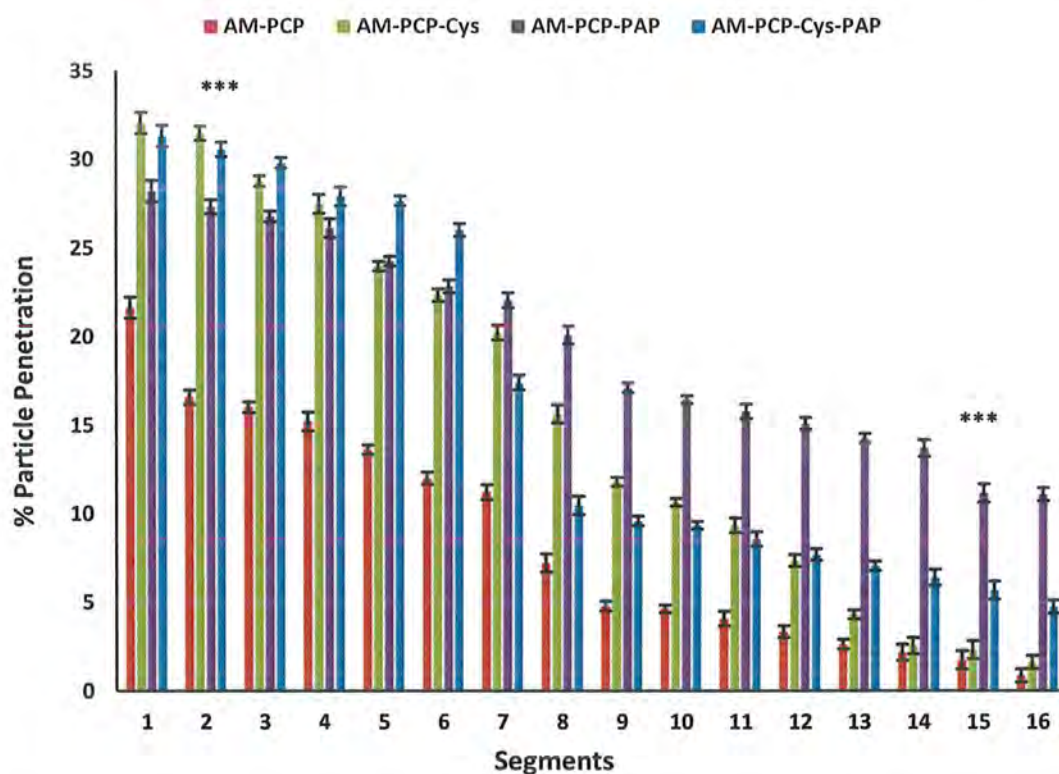
Figure 3.24. Permeation studies of FDA labeled amoxicillin loaded nanoparticles using silicon tube method at 37 °C. The results are indicated as ± standard deviation of mean (n = 3).

AM-PCP: Amoxicillin loaded polycarbophil nanoparticles, AM-PCP-Cys: Amoxicillin loaded thiolated polycarbophil nanoparticles, AM-PCP-PAP: Amoxicillin loaded papain modified polycarbophil nanoparticles, AM-PCP-Cys-PAP: Amoxicillin loaded papain modified thiolated polycarbophil nanoparticles. *** $p < 0.001$.

3.13.2. *In-vitro* growth inhibition study

The *in-vitro H.pylori* growth inhibition activity of AM-PCP-Cys-PAP nanoparticles and pure AM suspension was evaluated by colony count method. The amount of drug used was double of minimum inhibitory concentration value.

The results are shown in **Figure 3.25.** The percent growth inhibition increased with time. Pure amoxicillin showed nearly 100 % growth inhibition at 4 hours' time interval. While the results of AM-PCP-Cys-PAP nanoparticles displayed a gradual increase in % growth inhibition. The percent growth inhibition values were found to be 40 %, 71 % and 83 % at time interval of 2, 6 and 12 hours. AM-PCP-Cys-PAP nanoparticles showed complete growth inhibition of H.pylori after 24 hour incubation.
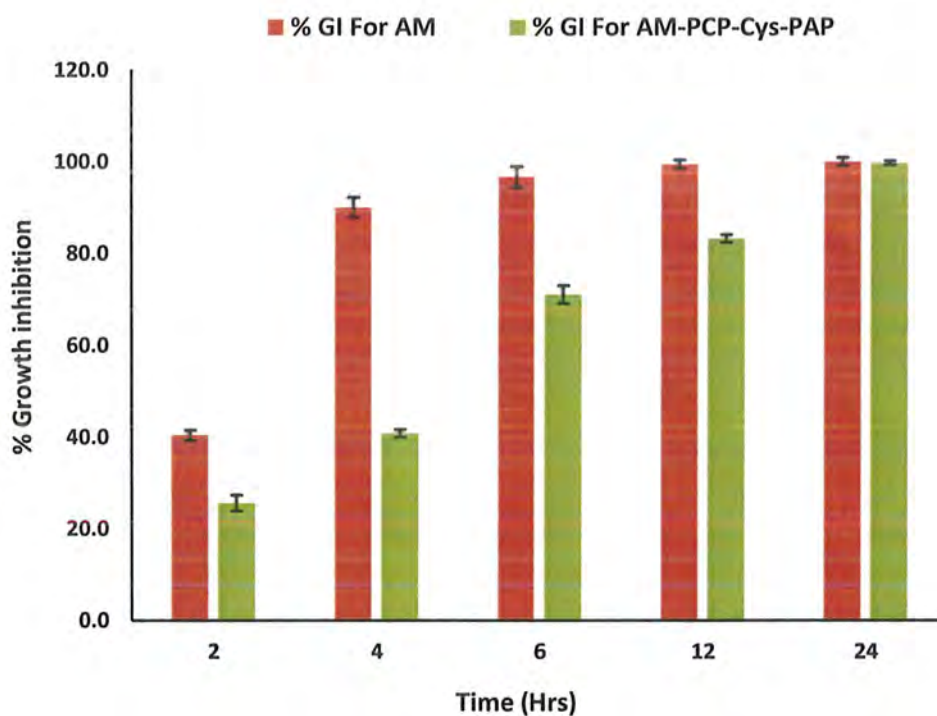
Figure 3.25. Evaluation of anti H.pylori activity. Comparison of percent growth inhibition of by pure amoxicillin suspension and amoxicillin loaded papain modified thiolated polycarbophil (AM-PCP-Cys-PAP) nanoparticles for 24 hours incubation period. Values are indicated as means ± SD (n = 3).

AM: Amoxicillin, AM-PCP-Cys-PAP: Amoxicillin loaded papain modified thiolated polycarbophil nanoparticles.

CHAPTER 4

DISCUSSION

4. DISCUSSION

Helicobacter pylori (*H.pylori*) has become the most common and widespread pathogens, affecting 50 percent of the world population. The current treatment strategies have come across high failure rates due to their poor stability, short retention time and bacterial resistance. The use of nanoparticulate drug delivery system is becoming common to eliminate all the mentioned problems (Zazo H *et al.*, 2016). The nanoparticles based on thiomers is a new method that prolongs the residence time at gastro-intestinal (GI) mucosal layer and ensuring optimal bioavailability (Bernkop-Schnürch A, 2005). These thiomer nanoparticles provide strong mucoadhesion by forming S-S bonding to the cysteine parts in GI mucosal layer. Mucus layer with a thickness of 15-600 µm (Sigurdsson HH *et al.*, 2013), is complex aqueous gel composed of glycoproteins that provide barrier properties to the underlying membranes (Cone RA, 2009). These properties together with the high mucus turnover rate, usually clear the nanoparticles from mucosa before the therapeutic concentration could reach the deep tissues where *H.pylori* resides (Arora S *et al.*, 2011). The thiomer nanoparticles must have the ability to penetrate the mucus and eradicate the bacteria from the target site. The most reliable technique is to use protease enzymes in the nanoparticulate system to cleave glycoproteins of mucus layer (Müller C *et al.*, 2013). Among these enzymes, papain has been found to significantly reduce the viscosity of mucus. Thus papain modified thiolated polycarbophil nanoparticles incorporating amoxicillin were prepared with the ability to use in anti *H.pylori* therapy.

Amoxicillin is synthetic, orally absorbed antibacterial with improved spectrum against gram-negative bacteria (Rossi A *et al.*, 2016). It has worldwide use in standard therapy against *H.pylori* eradication combined with another antibiotic and an antacid. A wide range of polymers are available to synthesize mucoadhesive drug delivery systems. Among these polymers, polyacrylic acid and their derivatives are in order of highly ranked mucoadhesive polymers (Bernkop-Schnürch A and Steininger S, 2000). Polycarbophil is a highly hydrophilic, mucoadhesive and negatively charged polymer (Asija R, 2014) that can be easily modified by carbodiimide chemistry thus facilitating its permeation through highly negative charged mucus layer due to sulfonic and sialic acid groups (Crater JS and Carrier RL, 2010). To improve the mucoadhesive and permeation properties of polycarbophil, the thiomer (PCP-Cys) was synthesized by conjugating the carboxylic groups of polycarbophil to the amino group of L-cysteine

covalently. The results from FTIR analysis **Figure 3.17** confirmed the successful thiolation of polycarbophil. Reportedly the thiol moieties attached to the polymer are critical for improvement of permeation and mucoadhesion effect. Polycarbophil is also reported to retain the mucolytic properties of papain (Vetter A *et al.*, 2010). Polycarbophil-papain (PCP-PAP) conjugate was prepared similarly by covalent attachment of papain the polymer backbone. This led to the formation of amide bond between amine group of enzyme and carboxylic groups of polymer. A study showed that covalent attachment of papain to the polymer increases the stability of enzyme as compared to free papain (Homaei AA *et al.*, 2010). It also improves the ease of handling of the enzyme. Furthermore, the polymeric conjugates of the enzyme have less sensitivity toward denaturation as mentioned by (Hanefeld U *et al.*, 2009).

Swelling study was carried out to demonstrate the influence of thiolation and papain modification on the swelling properties of polymer. The swelling property of polymers and their conjugates are reported to have a high impact on drug release, mucoadhesion and stability. Mucoadhesion has three stages: wetting, swelling and entanglement of polymer with mucus layer. When attached to the mucus layer the polymer take water from the surrounding layer, swell, get adsorbed and strengthen the mucoadhesion (Sohail MF *et al.*, 2016). Excess of water absorption also causes over swelling and as a result detaches the polymer from mucus layer. Thus for strong mucoadhesion, moderate water absorption property is necessary as mentioned previously (De Robertis S *et al.*, 2015). The thiolated polycarbophil was found to have moderate swelling property increasing at a constant rate. This favorable swelling is considered to have a remarkable impact on strong mucoadhesion and controlled release of drug from polymeric nanoparticles for an extended period of time. The surface thiol groups and disulfide linkages render the polymer more capable of water uptake at a constant rate. Papain conjugate of polymer was also observed to improve swelling property as compared to unmodified polymer. Thus these conjugates can be considered to have better influence over prolong retention and stability.

AM loaded PCP, PCP-Cys, PCP-PAP and PCP-Cys-PAP nanoparticles were produced by ionic gelation method. Ionic gelation method was selected for the preparation of modified and unmodified nanoparticles due to mild conditions of the process. Thus, harsh parameters like organic solvents, high temperature, sonication and extreme pH that can affect the enzymatic activity of papain modified nanoparticles were avoided.

Calcium chloride was used as crosslinker because of favorable effects on the activity of papain. Several metal ions inhibit the enzymatic activity, whereas Ca^{++} ions have been found to improve the activity of papain (Kaul P *et al.*, 2002). The polymer and crosslinker concentrations were optimized by design expert software version 7. The independent variables included polymer and cross-linker concentrations. The nanoparticles were optimized for entrapment efficiency, particle size and polydispersity index as response variables. To obtain lowest size AM-PCP-PAP nanoparticles and AM-PCP-Cys-PAP nanoparticles, a ratio of 1:2 was used for polymer to papain conjugate. Different pH values are reported to affect the particle size of nanoparticles, with lowest size at pH 8 (Greindl M and Bernkop-Schnürch A, 2006). Thus a pH value of 8 was kept constant throughout the development procedures of modified and unmodified nanoparticles. The results showed a significant effect of independent variables over response factors. As shown in **Figure 3.5 and 3.6**, Entrapment efficiency varied from 70 % - 88 % with varying concentrations of polymer and calcium chloride. It increased with the increase in concentration of PCP and $CaCl_2$. The reason for this was due to the formation of intact matrix of nanospheres by higher concentrations of polymer and cross linker that entrap more drug by dispersion in the matrix (Cohen-Sela E *et al.*, 2009). Also amoxicillin is a hydrophilic drug that was entrapped in a matrix formed by polycarbophil. Due to hydrophilic nature of polymer and cross linker, more drug diffused and attached to the polymer network. Thus higher concentrations of polymer and cross linker entrapped more drug and hindered its backward diffusion from the matrix surface. A similar positive impact was found in determining particles size by increasing concentration of independent variables as shown in **Figure 3.7 and 3.8**. Particle size varied from 95 nm to 182 nm. The particle size significantly increased with increase in polymer concentration because of the increase in consistency at higher concentrations (Sharma PR and Varma AJ, 2014). While crosslinker had mild positive impact on particle size. Other response variable was polydispersity index PDI that was analyzed by design expert software. The values of PDI were in range of 0.043 to 0.18. The independent variables had significant impact on PDI as shown in **Figure 3.9 and 3.10**. With the increase in polymer concentration, the PDI increased while it decreased with increase in crosslinker concentration. The increase polymer concentration usually causes hindrance in the passage of solvent due to which PDI was increased. While the higher concentration of crosslinker resulted in lower PDI due to more stabilizing effect on formation and movement of nanoparticles. Based on the impact of response

variables, a point at optimal area was chosen where % entrapment efficiency was maximum and particle size and polydispersity index were minimum. The selected optimized formulation was again developed and compared with the predicted results **Table 3.3**. The results indicated that both experimental analysis and predicted values were close to each other. The optimized nanoparticles were analyzed by SEM. SEM analysis confirmed the spherical shape of amoxicillin loaded polycarbophil, thiolated polycarbophil and papain modified nanoparticles with average particle size less than 400 nm. All the formulations were noted to have negative zeta potential due to carboxylic groups of polycarbophil. Unmodified nanoparticles displayed lowest particle size and highest negative zeta potential. Whereas thiolated and papain modified nanoparticles resulted in increased particle size. Also, the negative zeta potential was reduced with thiolation and papain modification due to occupation of most of the negatively charged groups. From FTIR analysis **Figure 3.17**, characteristics peaks of drug, PCP-Cys and papain were observed in final nanoparticle formulation (AM-PCP-Cys-PAP) showing the successful loading of drug in papain modified thiolated polycarbophil nanoparticles.

The *in-vitro* drug release profile from AM suspension, AM-PCP, AM-PCP-Cys, AM-PCP-PAP, AM-PCP-Cys-PAP nanoparticles was examined by dialysis tube process for 48 hours at pH 6.8. As shown in **Figure 3.19** nanoparticles indicated a sustained drug release behavior. The drug release from thiomer and papain modified nanoparticles was in order of AM-PCP-PAP > AM-PCP-Cys-PAP > AM-PCP-Cys. The papain modified nanoparticles (AM-PCP-PAP) displayed high cumulative drug release due to lack of modification with thiol moieties which attributed to the faster diffusion of drug from the nanoparticles. Upon modification with thiol groups, the release rate was slower and prolonged due to the formation of disulfide linkages within the polymer matrix. In case of AM-PCP-Cys-PAP nanoparticles, papain is also present along with thiol groups that reduce the disulfide linking within the thiolated polymer. As a results swelling improved thereby it increased the release rate as compared to AM-PCP-Cys nanoparticles. However, the release rate was found to be slower than AM-PCP-PAP nanoparticles with no disulfide linkages.

Stability of pure amoxicillin and newly developed amoxicillin loaded papain modified thiolated polycarbophil (PCP-Cys-PAP) nanoparticles was evaluated in 0.1 N HCl with a pH of 1.2. Reportedly 0.1 N HCl (pH 1.2) is equivalent to simulated gastric fluid

without enzymes (Marques MR *et al.*, 2011). In comparison to pure drug, AM-PCP-Cys-PAP nanoparticles showed significant stabilizing effect on loaded amoxicillin as shown in **Figure 3.20**. The increased protective efficiency can be due to matrix system of PCP-Cys nanocarriers. Previous studies reported high stability of thiolated polycarbophil at pH below 4 toward ionization and swelling. As a result, the nanocarriers hold the drug tightly in the inner matrix and protect from acidic degradation. Thus PCP-Cys-PAP nanoparticles can be used as an effective carrier for antibiotic to prolong its retention time and improve stability in acidic medium. Rheological investigation was also carried out to assess mucoadhesion properties of nanoparticles as shown in **Figure 3.21**. Rheology is reported to be an *in-vitro* parameter for the investigation of mucoadhesive behavior of polymeric nanoparticulate formulations. When nanoparticles interact with mucin, conformational changes and chemical or electrostatic interactions occurs that lead to changes in the rheological behavior of two agents. The change in viscosity of both nanoparticles and mucin is considered to affect the strength of mucoadhesion. Higher rheological parameter ($\Delta\eta$) reflects strong mucoadhesion to the mucus layer (Shahnaz G *et al.*, 2010). The presence of thiol groups on polycarbophil chain resulted in the formation of disulfide bond with the cysteine groups of mucin. These disulfide bonds aided in strengthening the mucoadhesive force between nanoparticles and mucus surface. Thus the viscosity significantly increased for AM-PCP-Cys nanoparticles as compared to AM-PCP nanoparticles. The mild increase in viscosity for AM-PCP nanoparticles could be the formation of other non-covalent bonds between PCP carboxyl groups and mucus surface. These bond include hydrogen bonding or electrostatic interactions. However, the mucoadhesive behavior was not pronounced as thiolated nanoparticles. The presence of papain in nanoparticles significantly reduced the rheological parameter showing the remarked effect of papain on mucin viscosity. In AM-PCP-Cys-PAP nanoparticles thiol groups were present which formed disulfide bond with the mucus thiol groups and increased the viscosity thus improved the mucoadhesive property. Furthermore, they also have papain functional group. Papain cleaved the bonds in mucus glycoproteins at specified positions which accounts for reduction in rheological parameter ($\Delta\eta$) and increased mucopenetration.

Nanoparticles were labeled with FDA for diffusion/penetration study. FDA is aqueous insoluble and lipophilic dye. It is freely soluble in acetonitrile and acetone. After

incorporation, it retained in nanoparticles through temporary attachment. Due to water insolubility and temporary attachment, FDA does not diffuse out in aqueous medium (Bernkop-Schnürch A *et al.*, 2006). To avoid precipitation problem during FDA labeling of nanoparticles, the FDA and polymer solution were first mixed thoroughly then crosslinker solution was added dropwise to form nanoparticles. The FDA content was found to be 45-71% as shown in **Table 3.7**. To determine any leakage of dye, the labeled nanoparticles were in redispersed in an aqueous medium for 4 hours and the quantity was calculated before and after incubation. The amount was determined as % weight of nanoparticles. If there was any leakage of FDA, the payload of dye would have reduced. The amount determined before and after incubation showed that there was no leakage of dye from nanoparticles. This suggests a better impact on diffusion studies.

Permeation studies were conducted on freshly isolated mucus using silicon tube method with little modification. This method is reported to have the advantage of direct contact of nanoparticles with the mucus (Köllner S *et al.*, 2015). On the basis of results of permeation study AM-PCP-Cys-PAP nanoparticulate drug delivery system presented both the strategies: mucopenetration as well as mucoadhesion. These properties were evaluated in AM-PCP-Cys-PAP nanoparticles to describe the influence of thiol and papain modification. The AM-PCP-Cys-PAP nanoparticles were compared to AM-PCP-PAP nanoparticles which exhibit mucus cleavage property. While the mucoadhesive properties of AM-PCP-Cys-PAP nanoparticles were compared with AM-PCP-Cys nanoparticles. Papain modified particles AM-PCP-PAP nanoparticles revealed improved permeation in comparison with the unmodified nanoparticles; AM-PCP and AM-PCP-Cys. Thiolated nanoparticles i.e. AM-PCP-Cys showed the lowest amount of percent penetration values. Whereas the results of AM-PCP-Cys-PAP were between the values of AM-PCP-Cys and AM-PCP-PAP, therefore AM-PCP-Cys-PAP nanoparticles exhibit improved permeation and mucoadhesion at the same time. These findings are based on the fact that papain modified thiolated PCP nanoparticles are more permeable through the highly negatively charged mucus layer (Crater JS and Carrier RL, 2010). Polycarbophil based nanoparticles bear negative zeta potential due to the carboxylic acid groups in the polymer backbone. Because of these negative charges, the nanoparticles were repelled by sialic acid and sulfonic acid groups of mucus membrane and facilitated their transportation to the deeper parts. Furthermore, the

human GIT mucus layer is composed of a linear peptide called mucin. This peptide forms a glycosidic linkage to different polysaccharides (Lai SK *et al.*, 2009). The mucus layer is highly protected from proteolytic activity and microbes because of these branched polysaccharides regions. In addition to polysaccharide chains which are hydrophilic, the mucus layer also possesses hydrophobic parts. This region is uncovered and sensitive to enzymatic lysis. Papain specifically cleaves these peptide domains composed of 110 amino acids with several cysteine groups (Cone RA, 2009). As a result of mucolytic activity for papain modified nanoparticles, the woven matrix of mucin broke down and penetration of nanoparticles was enhanced through the mucus.

The *in-vitro H.pylori* growth inhibition activity of AM-PCP-Cys-PAP nanoparticles and pure AM suspension was evaluated. AM-PCP-Cys-PAP nanoparticles showed better *in-vitro* efficacy based on high stability, prolong drug release and complete eradication as compared to pure amoxicillin. The usual transit time of pure amoxicillin in stomach is almost 2 hours (Narkar M *et al.*, 2010). Whereas as in case of AM-PCP-Cys-PAP nanoparticles, AM was dispersed inside the polymeric matrix which retarded its diffusion. Furthermore due to the presence of thiol groups, the drug formed hydrophilic interactions with the polymer. Thus the drug was held tightly inside the matrix and diffuse out slowly. Overall the results showed that AM-PCP-Cys-PAP nanoparticles have prolong drug release pattern. The transit time was also greater than pure amoxicillin. Based on high stability and long residence time, AM-PCP-Cys-PAP nanoparticles displayed a better in vitro efficacy as compared to pure amoxicillin.

CONCLUSION

- AM-PCP-Cys-PAP nanoparticles were successfully prepared and evaluated for enhanced mucoadhesion, mucopermeation, drug stability and prolong retention.

- AM-PCP-Cys-PAP nanoparticles were capable of cleaving mucoglycoproteins because of the presence of papain.

- The nanoparticulate system also displayed higher mucoadhesive behavior and sustained drug release profile.

- The results of in vitro *H.pylori* growth inhibition activity indicated that AM-PCP-Cys-PAP nanoparticles effectively inhibit the complete growth of H.pylori with prolong retention as compared to pure amoxicillin.

- Overall the newly developed AM-PCP-Cys-PAP nanoparticles can be an effective nanocarrier for anti H.pylori therapy because of the potential of enhanced mucopermeation and mucoadhesion property with better stability and prolong drug release.

FUTURE PROSPECTS

Mucosal delivery is more effective for H.pylori eradication than systemic administration. Thus further studies with animal models can be conducted to confirm the localized delivery and prolong retention of the drug at the target site. Combination of antibacterial can be used to ascertain the eradication of bacteria. Capsules and tablet dosage forms can be made of nanoparticles to further enhance the stability and ease of administration.

REFERENCES

A El-Zahaby S, A Kassem A and H El-Kamel A (2014). Helicobacter pylori: An overview on antimicrobials and drug delivery systems for its eradication. Curr Drug Deliv, 11(3): 306-312.

Adam G and Duncan H (2001). Development of a sensitive and rapid method for the measurement of total microbial activity using fluorescein diacetate (fda) in a range of soils. Soil Biol Biochem, 33(7-8): 943-951.

Arora S, Gupta S, Narang RK and Budhiraja RD (2011). Amoxicillin loaded chitosan–alginate polyelectrolyte complex nanoparticles as mucopenetrating delivery system for h. Pylori. Sci Pharm, 79(3): 673-694.

Asija R (2014). Gastrointestinal mucoadhesive drug delivery system: An overview. JDDT, 2(20): 213-219.

Bernkop-Schnürch A (2005). Thiomers: A new generation of mucoadhesive polymers. Advanced drug delivery reviews, 57(11): 1569-1582.

Bernkop-Schnürch A, Hornof M and Zoidl T (2003). Thiolated polymers—thiomers: Synthesis and in vitro evaluation of chitosan–2-iminothiolane conjugates. Int J Pharm, 260(2): 229-237.

Bernkop-Schnürch A, Scholler S and Biebel RG (2000). Development of controlled drug release systems based on thiolated polymers. J Control Release, 66(1): 39-48.

Bernkop-Schnürch A and Steininger S (2000). Synthesis and characterisation of mucoadhesive thiolated polymers. Int J Pharm, 194(2): 239-247.

Bernkop-Schnürch A, Weithaler A, Albrecht K and Greimel A (2006). Thiomers: Preparation and in vitro evaluation of a mucoadhesive nanoparticulate drug delivery system. Int J Pharm, 317(1): 76-81.

Cai J, Huang H, Song W, Hu H, Chen J, Zhang L, Li P, Wu R and Wu C (2015). Preparation and evaluation of lipid polymer nanoparticles for eradicating h. Pylori biofilm and impairing antibacterial resistance in vitro. Int J Pharm, 495(2): 728-737.

Callens C, Ceulemans J, Ludwig A, Foreman P and Remon JP (2003). Rheological study on mucoadhesivity of some nasal powder formulations. Eur J Pharm Biopharm, 55(3): 323-328.

Cammarota G, Sanguinetti M, Gallo A and Posteraro B (2012). Biofilm formation by helicobacter pylori as a target for eradication of resistant infection. Alimentary pharmacology & therapeutics, 36(3): 222-230.

Cevher E, Sensoy D, Taha MA and Araman A (2008). Effect of thiolated polymers to textural and mucoadhesive properties of vaginal gel formulations prepared with polycarbophil and chitosan. Aaps Pharmscitech, 9(3): 953-965.

Chowdary K, Reddy KG and Bhaskar P (2001). Mucoadhesive polymers-promising excipients for controlled release. Int. J. Pharma Excip, 2(5): 33-38.

Clausen AE and Bernkop-Schnürch A (2000). In vitro evaluation of the permeation-enhancing effect of thiolated polycarbophil. J Pharm Sci Exp Pharmacol, 89(10): 1253-1261.

Cohen-Sela E, Chorny M, Koroukhov N, Danenberg HD and Golomb G (2009). A new double emulsion solvent diffusion technique for encapsulating hydrophilic molecules in plga nanoparticles. J Control Release, 133(2): 90-95.

Cone RA (2009). Barrier properties of mucus. Advanced drug delivery reviews, 61(2): 75-85.

Crater JS and Carrier RL (2010). Barrier properties of gastrointestinal mucus to nanoparticle transport. Macromol Biosci, 10(12): 1473-1483.

Cu Y and Saltzman WM (2009). Mathematical modeling of molecular diffusion through mucus. Advanced drug delivery reviews, 61(2): 101-114.

De Robertis S, Bonferoni MC, Elviri L, Sandri G, Caramella C and Bettini R (2015). Advances in oral controlled drug delivery: The role of drug–polymer and interpolymer non-covalent interactions. Expert Opin Drug Deliv, 12(3): 441-453.

De Sousa IP, Steiner C, Schmutzler M, Wilcox MD, Veldhuis GJ, Pearson JP, Huck CW, Salvenmoser W and Bernkop-Schnürch A (2015). Mucus permeating carriers: Formulation and characterization of highly densely charged nanoparticles. Eur J Pharm Biopharm, 97(4): 273-279.

Dubreuil JD, Del Giudice G and Rappuoli R (2002). Helicobacter pylori interactions with host serum and extracellular matrix proteins: Potential role in the infectious process. Microbiol Mol Biol Rev, 66(4): 617-629.

Dünnhaupt S, Barthelmes J, Hombach J, Sakloetsakun D, Arkhipova V and Bernkop-Schnürch A (2011). Distribution of thiolated mucoadhesive nanoparticles on intestinal mucosa. Int J Pharm, 408(1): 191-199.

Engstrand L, Graham D, Scheynius A, Genta R and El-Zaatari F (1997). Is the sanctuary where helicobacter pylori avoids antibacterial treatment intracellular? Amer jour of clini path, 108(5): 504-509.

Fedwick JP, Lapointe TK, Meddings JB, Sherman PM and Buret AG (2005). Helicobacter pylori activates myosin light-chain kinase to disrupt claudin-4 and claudin-5 and increase epithelial permeability. Infect Immun, 73(12): 7844-7852.

Greindl M and Bernkop-Schnürch A (2006). Development of a novel method for the preparation of thiolated polyacrylic acid nanoparticles. Pharm Res, 23(9): 2183-2189.

Hanefeld U, Gardossi L and Magner E (2009). Understanding enzyme immobilisation. Chem Soc Rev, 38(2): 453-468.

Homaei AA, Sajedi RH, Sariri R, Seyfzadeh S and Stevanato R (2010). Cysteine enhances activity and stability of immobilized papain. Amino acids, 38(3): 937-942.

Hunt R, Xiao S, Megraud F, Leon-Barua R, Bazzoli F, Van der Merwe S, Vaz Coelho L, Fock M, Fedail S and Cohen H (2011). Helicobacter pylori in developing countries. World gastroenterology organisation global guideline. J Gastrointestin Liver Dis, 20(3): 299-304.

Iqbal J, Shahnaz G, Perera G, Hintzen F, Sarti F and Bernkop-Schnürch A (2012). Thiolated chitosan: Development and in vivo evaluation of an oral delivery system for leuprolide. Eur J Pharm Biopharm, 80(1): 95-102.

Josenhans C, Eaton KA, Thevenot T and Suerbaum S (2000). Switching of flagellar motility in helicobacter pyloriby reversible length variation of a short homopolymeric sequence repeat in flip, a gene encoding a basal body protein. Infect Immun, 68(8): 4598-4603.

Kaul P, Sathish H and Prakash V (2002). Effect of metal ions on structure and activity of papain from carica papaya. Mol Nutr Food Res, 46(1): 2-6.

Kharia AA and Singhai AK (2013). Stomach-specific mucoadhesive nanoparticles as a controlled release drug delivery system. MJPMS, 2(3): 12-24.

Köllner S, Dünnhaupt S, Waldner C, Hauptstein S, de Sousa IP and Bernkop-Schnürch A (2015). Mucus permeating thiomer nanoparticles. Eur J Pharm Biopharm, 97(265-272.

Konturek J (2003). Discovery by jaworski of helicobacter pylori. J Physiol Pharmacol, 54(3): 23-41.

Kumari A, Yadav SK and Yadav SC (2010). Biodegradable polymeric nanoparticles based drug delivery systems. Colloids Surf B Biointerfaces, 75(1): 1-18.

Lai SK, Wang Y-Y and Hanes J (2009). Mucus-penetrating nanoparticles for drug and gene delivery to mucosal tissues. Advanced drug delivery reviews, 61(2): 158-171.

Lamont JT (1992). Mucus: The front line of intestinal mucosal defense. Annals of the New York Academy of Sciences, 664(1): 190-201.

Lehr C-M (2000). Lectin-mediated drug delivery: The second generation of bioadhesives. J Control Release, 65(2): 19-29.

Lele B and Hoffman A (2000). Mucoadhesive drug carriers based on complexes of poly (acrylic acid) and pegylated drugs having hydrolysable peg–anhydride–drug linkages. J Control Release, 69(2): 237-248.

Lin Y-H, Chiou S-F, Lai C-H, Tsai S-C, Chou C-W, Peng S-F and He Z-S (2012). Formulation and evaluation of water-in-oil amoxicillin-loaded nanoemulsions using for helicobacter pylori eradication. Process Biochem, 47(10): 1469-1478.

Lin Y-H, Feng C-L, Lai C-H, Lin J-H and Chen H-Y (2014). Preparation of epigallocatechin gallate-loaded nanoparticles and characterization of their inhibitory effects on helicobacter pylori growth in vitro and in vivo. Sci Technol Adv Mater, 15(4): 45-51.

MacAdam A (1993). The effect of gastro-intestinal mucus on drug absorption. Advanced drug delivery reviews, 11(3): 201-220.

Mamboya EAF (2012). Papain, a plant enzyme of biological importance: A review. American Journal of Biochemistry and Biotechnology, 8(2): 99-104.

Marques MR, Loebenberg R and Almukainzi M (2011). Simulated biological fluids with possible application in dissolution testing. Dissolu Technol, 18(3): 15-28.

Marshall B and Warren JR (1984). Unidentified curved bacilli in the stomach of patients with gastritis and peptic ulceration. Lancet, 323(83): 1311-1315.

McColl KE (2012). Pathophysiology of duodenal ulcer disease. Eur J Gastroenterol Hepatol, 9(2): 9-12.

McNulty CA, Lehours P and Mégraud F (2011). Diagnosis of helicobacter pylori infection. Helicobacter, 16(1): 10-18.

Metin AÜ and Alver E (2016). Fibrous polymer-grafted chitosan/clay composite beads as a carrier for immobilization of papain and its usability for mercury elimination. Bioroc Biosys Eng, 39(7): 1137-1149.

Müller C, Leithner K, Hauptstein S, Hintzen F, Salvenmoser W and Bernkop-Schnürch A (2013). Preparation and characterization of mucus-penetrating papain/poly (acrylic acid) nanoparticles for oral drug delivery applications. J Nanopart Res, 15(1): 1353-1357.

Müller C, Leithner K, Hauptstein S, Hintzen F, Salvenmoser W and Bernkop-Schnürch A (2013). Preparation and characterization of mucus-penetrating papain/poly (acrylic acid) nanoparticles for oral drug delivery applications. J Nanopart Res, 15(1): 13-19.

Müller C, Perera G, König V and Bernkop-Schnürch A (2014). Development and in vivo evaluation of papain-functionalized nanoparticles. Eur J Pharm Biopharm, 87(1): 125-131.

Narkar M, Sher P and Pawar A (2010). Stomach-specific controlled release gellan beads of acid-soluble drug prepared by ionotropic gelation method. AAPS PharmSciTech, 11(1): 267-277.

Netsomboon K and Bernkop-Schnürch A (2016). Mucoadhesive vs. Mucopenetrating particulate drug delivery. Eur J Pharm Biopharm, 98(3): 76-89.

Novelli F, De Santis S, Punzi P, Giordano C, Scipioni A and Masci G (2017). Self-assembly and drug release study of linear l, d-oligopeptide-poly (ethylene glycol) conjugates. New Biotechnol, 37(5): 99-107.

Ohta T, Shibata H, Kawamori T, Iimuro M, Sugimura T and Wakabayashi K (2001). Marked reduction of helicobacter pylori-induced gastritis by urease inhibitors, acetohydroxamic acid and flurofamide, in mongolian gerbils. Biochem Biophys Res Commun, 285(3): 728-733.

Otero Regino W, Trespalacios AA and Otero E (2009). Helicobacter pylori: Current treatment an important challenge for gastroenterology. Rev Colomb Gastroenterol, 24(3): 279-292.

Pan-In P, Tachapruetinun A, Chaichanawongsaroj N, Banlunara W, Suksamrarn S and Wanichwecharungruang S (2014). Combating helicobacter pylori infections with mucoadhesive nanoparticles loaded with garcinia mangostana extract. Nanomedicine, 9(3): 457-468.

Patel P, Varshney P and Rohit M (2014). Analytical method development and validation for simultaneous estimation of metronidazole and amoxicillin in synthetic mixture by uv-visible spectroscopy. Int J Pharm Pharm Sci, 6(4): 317-319.

Perioli L, Ambrogi V, Pagano C, Massetti E and Rossi C (2011). New solid mucoadhesive systems for benzydamine vaginal administration. Colloids Surf B Biointerfaces, 84(2): 413-420.

Persson C (2009). Roles of helicobacter pylori infection, host genetic variation, and other environmental exposures in gastric carcinogenesis (PhD Thesis). Karolinska

Institute, Stockholm, Sweden. Prego C, Garcia M, Torres D and Alonso M (2005). Transmucosal macromolecular drug delivery. J Control Release, 101(1): 151-162.

Proctor MJ and Deans C (2014). Complications of peptic ulcers. Surgery, 32(11): 599-607.

Rathee P, Jain M, Garg A, Nanda A and Hooda A (2011). Gastrointestinal mucoadhesive drug delivery system: A review. J Pharm Res, 4(5): 1448-1453.

Rossi A, Conti C, Colombo G, Castrati L, Scarpignato C, Barata P, Sandri G, Caramella C, Bettini R and Buttini F (2016). Floating modular drug delivery systems with buoyancy independent of release mechanisms to sustain amoxicillin and clarithromycin intra-gastric concentrations. Drug Dev. Ind. Pharm, 42(2): 332-339.

Saha P, Goyal AK and Rath G (2010). Formulation and evaluation of chitosan-based ampicillin trihydrate nanoparticles. Trop J Pharm Res, 9(5): 112-118.

Samaridou E, Karidi K, de Sousa IP, Cattoz B, Griffiths P, Kammona O, Bernkop-Schnürch A and Kiparissides C (2014). Enzyme-functionalized plga nanoparticles with enhanced mucus permeation rate. Nano Life, 4(04): 144-149.

Sayın B, Somavarapu S, Li X, Thanou M, Sesardic D, Alpar H and Şenel S (2008). Mono-n-carboxymethyl chitosan (mcc) and n-trimethyl chitosan (tmc) nanoparticles for non-invasive vaccine delivery. Int J Pharm, 363(1-2): 139-148.

Shahnaz G, Perera G, Sakloetsakun D, Rahmat D and Bernkop-Schnürch A (2010). Synthesis, characterization, mucoadhesion and biocompatibility of thiolated carboxymethyl dextran–cysteine conjugate. J Control Release, 144(1): 32-38.

Sharma PR and Varma AJ (2014). Thermal stability of cellulose and their nanoparticles: Effect of incremental increases in carboxyl and aldehyde groups. Carbohydr Polym, 114(5): 339-343.

Sigurdsson HH, Kirch J and Lehr C-M (2013). Mucus as a barrier to lipophilic drugs. Int J Pharm, 453(1): 56-64.

Sohail MF, Javed I, Hussain SZ, Sarwar S, Akhtar S, Nadhman A, Batool S, Bukhari NI, Saleem RSZ and Hussain I (2016). Folate grafted thiolated chitosan enveloped nanoliposomes with enhanced oral bioavailability and anticancer activity of docetaxel. J Mater Chem, 4(37): 6240-6248.

Sostres C, Gargallo CJ, Arroyo MT and Lanas A (2010). Adverse effects of non-steroidal anti-inflammatory drugs (nsaids, aspirin and coxibs) on upper gastrointestinal tract. Best prac & res Clinl gastroenterol, 24(2): 121-132.

Suerbaum S and Michetti P (2002). Helicobacter pylori infection. N Engl J Med, 347(15): 1175-1186.

Tsang KW and Lam SK (1999). Helicobacter pylori and extra-digestive diseases. J Gastroenterol Hepatol, 14(9): 844-850.

Umamaheshwari R, Ramteke S and Jain NK (2004). Anti-helicobacter pylori effect of mucoadhesive nanoparticles bearing amoxicillin in experimental gerbils model. Aaps Pharmscitech, 5(2): 60-68.

Vetter A, Martien R and Bernkop-Schnürch A (2010). Thiolated polycarbophil as an adjuvant for permeation enhancement in nasal delivery of antisense oligonucleotides. J Pharm Sci Exp Pharmacol, 99(3): 1427-1439.

Viji Chandran S, Amritha TS, Rajalekshmi G and Pandimadevi M (2015). A preliminary in vitro study on the bovine collagen film incorporated with azadirachta indica plant extract as a potential wound dressing material. Drug Dev. Ind. Pharm, 42(2): 242-256.

Wu H, Shi X, Wang H and Liu J (2000). Resistance of helicobacter pylori to metronidazole, tetracycline and amoxycillin. J Antimicrob Chemother, 46(1): 121-123.

Yamamoto Y, Fujisaki J, Omae M, Hirasawa T and Igarashi M (2015). Helicobacter pylori-negative gastric cancer: Characteristics and endoscopic findings. Digest Endosc, 27(5): 551-561.

Zazo H, Colino CI and Lanao JM (2016). Current applications of nanoparticles in infectious diseases. J Control Release, 224(14): 86-102.

Amoxicillin Loaded Mucoadhesive Thiomer Based Nanoparticles for H.pylori Infection Therapy

by Hajra Zafar